Deltares

Enabling Delta Life

Towards guidelines for effective plastic removal from rivers

phase 1

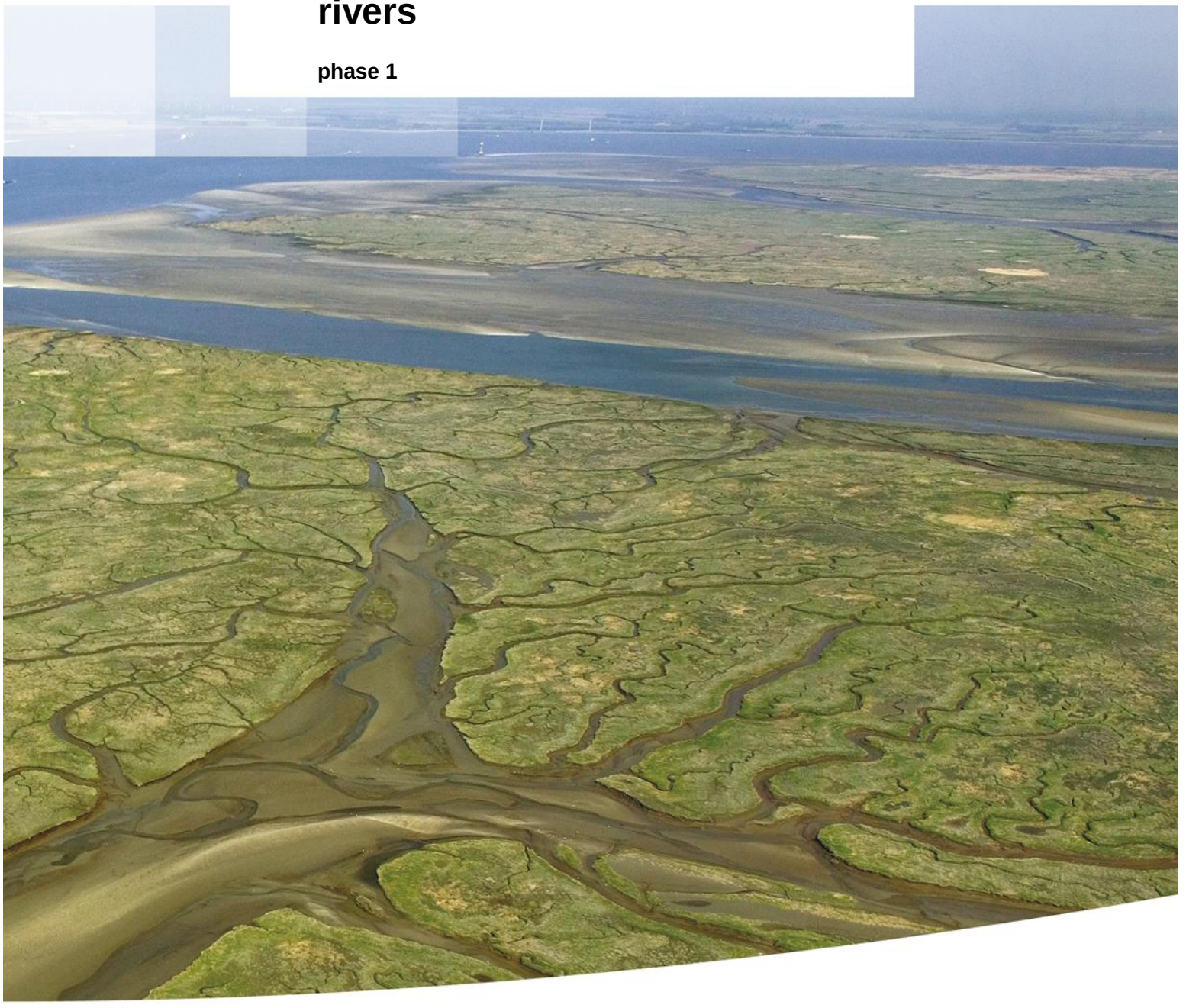

Deltares

Towards guidelines for effective plastic removal from rivers

phase 1

Frans Buschman
Frank Kleissen
Arjen Markus
Joana Mira Veiga
Dick Vethaak and Mohamed Yossef

Title
Towards guidelines for effective plastic removal from rivers

Client	Project	Attribute	Pages
Allseas Engineering BV, DELFT	11203036-000	11203036-000-ZWS-0006	132

Keywords
Modelling, plastic flux, macroplastic items, microplastic particles, estuaries and rivers.

Summary
Rivers and estuaries transport plastic particles towards the sea. Within the river the concentration of different types of plastic particles and the flow velocity varies both spatially and temporally. It is the product of the local concentration and the local flow velocity, which is the plastic flux, that determines how effective a system to collect plastic particles is at a location. The objective of phase 1 was to increase the understanding of the transport of plastic particles in rivers by model case studies and by reviewing literature. Typical characteristics of macroplastic items and microplastic particles are detailed, and a selection has been made which types of plastic particles are most relevant in a river. The rising (or falling) velocity was determined from observed rising velocities for the macroplastic items and for microplastics from a recently published paper. These characteristics per type were used for a pilot modelling exercise on the plastic transport in the Rhine-Meuse delta, including the Nieuwe Maas. The two software modules that were used showed reasonable results, although a verification with observations was not possible. Trends observed in observations by Allseas in the Nieuwe Maas and trends from the pilot modelling exercise showed similarities. From the similarities and results of software verifications, we conclude that the two software modules are suitable to model the transport of plastic particles, although some limitations apply. Results of the modelling and the literature survey gave rise to draft guidelines where in a river the plastic flux is relatively high. Optimal locations for plastic collection in rivers are within the reach where both ebb and flood flow occur, since absolute flow velocities are on average relatively high in this zone and thus the flux of plastics is high as well. The optimal location to collect falling macroplastic items (e,g. PET drink bottles) is somewhere in the deeper part of the cross section of the river, whereas the optimal location to collect rising plastic particles (e.g. bottle caps) is where the flow is highest. Wind can play a prominent role in the distribution of plastic particles that float or that have the tendency to rise. The flux of these plastic particles may be much higher near the downwind river bank.

References
Contract 710339-AEBV-ENG-001

Status
final

Contents

1 Introduction

1.1 Background

Since the 1950's worldwide plastic production has been increasing, because the material is relatively cheap and durable. With the increased production, the amount of wasted plastic items has been increasing as well. Plastic items wasted on land often end up in waterways and may be transported to the ocean via rivers. It is estimated that globally each year about 1.5-2.4 million metric tonnes of plastic litter enter the ocean via rivers (Lebreton et al., 2017). Van der Wal et al. (2015) estimated that 20-31 tonnes of plastic litter are transported to the North Sea via the river Rhine. Since its degradation is very slow, plastics are persistent in the environment and are continuously accumulating. Plastic particles that are transported via rivers to the ocean either accumulate near the ocean surface in great "garbage patches" driven by the largescale circulations (LeBreton et al., 2018) or sink and accumulate to the ocean bed.

In general, plastic litter is a threat to ecosystems, especially to animals higher in the food chain. The impact of plastic debris on marine life includes entanglement, ingestion and contamination of the food chain by persistent pollutants (Derraik, 2002). For birds and mammals, entanglement can lead to suffocation, whereas ingestion can lead to reduced fitness, starvation and even death. For human health, especially small plastic particles are a risk, since they may be taken up in our bodies, but potential negative impacts are still poorly understood. A potential risk that has recently been found is the consumption of sea food contaminated with small plastic particles (Barboza et al., 2018). Other possible risks of aquatic plastics are related to hazardous chemicals that could lead from plastics to the water and food chain, and the spread of pathogens and anti-bacterial resistance (GESAMP, 2016).

Figure 1.1 A dead whale was found in the Philippines with 88 pounds of plastic bags and other disposable plastic products in its stomach (New York Times, March 2019)

\

Allseas has decided to take an active stance in supporting the global effort to eliminate plastics from our seas. Allseas' approach is oriented towards the development of a cost-effective and sustainable system to remove plastic litter from rivers, as these are considered major pathways of plastic waste from land into the sea. Targeted are both large plastic items (macroplastic items) and small plastic items (microplastics) that are present within the water column. **We define macroplastic items as plastic items with a size of 5 mm and larger**, which is a common definition. Fragmentation of macroplastic items results in microplastics. Microplastics are also produced in the industry; e.g. pellets and microbeads. For microplastics various definitions are used in literature. **We define microplastics in this report as plastic particles with a size in the range 1 to 5 mm**. The lower bound of 1 mm is used in this report, because particles smaller than 1 mm are unlikely to be caught with the system that Allseas is preparing to remove plastics.

1.2 Problem statement

Allseas decided to contribute to prevent plastics entering the ocean worldwide by means of developing, and deploying, a system to remove plastic litter from rivers before the plastics reach the ocean (Allseas, 2018). Currently, Allseas is designing the system, aiming at removing plastics in a cost-effective and sustainable manner. We understand that the system, once deployed, removes plastics that are passing through a selected part of the river cross section, collecting both the larger (macroplastic items) and smaller fractions (microplastics) that are transported within the watercolumn. The system has a fixed width and is intended to collect the plastic particles larger than 1 mm from the river bed to the water surface. To be cost-effective, the amount of plastic transported through this particular cross-sectional area should be as high as possible.

The amount of plastic transported through a particular cross-sectional area is the plastic flux.
The plastics flux through the area covered by the system is calculated as the product of flow velocity and the concentration of the plastics, summed for each part of the cross-sectional area. The flux is highest, when both a high flow velocity and a high plastic concentration occur. The spatial variation of flow velocity and plastic concentration within the particular cross-sectional area is taken into account in the flux.

The problem is that general knowledge on the spatial distribution of plastics concentration and its variation in time with conditions is limited. This problem can be translated into the following general question:

> *"Can we develop guidelines to identify the locations, in a river, with a high probability of finding a relatively high plastics flux?"*

There is a knowledge gap that makes it difficult to give a direct answer to this question. Therefore, research is needed. We can identify the following direct research questions:

1. What are **characteristics** of plastic litter in rivers?
2. What are the **dominant processes** that govern transport of plastics in rivers?
3. What are the **river planform features (geometry)** affecting transport of plastics?
4. What are the **forcings** contributing to the transport of plastics?

The river planform features at large scale include a straight reach and bend curvature. At smaller scale it includes obstacles, groynes and patches of vegetation. Examples of forcings are river discharge, wind, waves and tides.

Preferred locations to deploy a system to remove plastics from the water column cost-effectively should show a high plastics flux. Besides, operational limitations are also relevant for the selection of a preferred location; e.g. the system should not hamper navigation. Another operational limitation is a high concentration of organic material is or floating debris. The operational limitations are not considered in this study. This study focusses on identifying potential locations in a river, where a system to remove plastics could be placed cost-effectively, based on understanding the plastics flux solely.

An additional objective of Allseas, is to optimise the design of the system to remove plastics from the river. This question is outside the scope of this study. However, the knowledge of processes governing the plastics flux and the characterization of the plastic particles larger than 1 mm may also contribute to improve the design of the system.

1.3 Objectives

This study covers (part of) the knowledge gaps and attempts to answer the four research questions identified above. The general objective of this study can be defined as to:

> *"Develop guidelines to identify the locations, in a river, with high probability of finding a relatively high flux of plastics"*

Based on this general objective, the direct objectives of this study are:

1. Increase the understanding of how macroplastic items with various characteristics are transported.
2. Increase the understanding of how microplastic particles with various characteristics are transported.
3. Take steps towards the preparation of guidelines for identification of zones with elevated plastics flux in rivers.

1.4 Overall Approach

1.4.1 Phases

We follow a two-step approach to reach the direct objectives. In phase 1, we carry out a literature survey, numerical simulations and a desktop assessment. Phase 1 aims to reach a level of understanding that allows us to identify the range of conditions that needs to be addressed, in more detail, in the second phase. Phase 1 includes a detailed setup of phase 2. In phase 1 we give draft guidelines for locations in rivers with high probability of high transport of plastics. In phase 2 we aim to test and extend the guidelines by means of a dedicated analysis (desktop/model-based) of a large number of numerical modelling cases. The present report is the report of phase 1 only.

1.4.2 Phase 1

Phase 1 aims to reach a level of understanding that allows us to identify the range of processes, river planform features, and forcings that needs to be addressed for the most relevant characteristics of plastic particles larger than 1 mm. From a literature survey, a selection of processes, river planform features, and forcings is made. These will be evaluated to identify locations with high probability of relatively high transport rates of different types of plastics. To better understand the effects of processes, planform features and forcings on the plastic transport, we carry out two different modelling exercises using two software modules of Delft3D: Delft3D-PART (D-PART in short) and D-water quality (WAQ in short) in phase 1. The aim is to verify that the models are suitable (fit for purpose) to identify areas with high probability of high plastic flux. In other words, the aim is to verify that uncertainties in the results of plastic transport are sufficiently small.

Over the past decades, both modules WAQ and D-PART have been tested intensively by simulating transport of a substance for cases with an outcome that is quantitatively known. They have been also used in numerous projects. The tests and applications have been successful. However, these tests were usually not specifically aimed at the transport of plastics. Therefore, Allseas proposed to perform additional tests to verify the software modules (minutes of meeting at the 29th August 2018). The software verifications aim at the transport and fate of plastics in rivers. Several software verifications are carried out for both D-PART and WAQ using simple cases. The modelling comprises the use of a suitable flow model in combination with the designated module to track the transport of plastics. The plastic particles in the model have characteristics based on plastics selected based on the literature review and expert judgement.

As the second modelling exercise, we model plastics transport in the Rhine-Meuse system using both WAQ and D-PART as a pilot of modelling the transport of plastics for a realistic river. For this purpose, *Havenbedrijf Rotterdam* allowed to use their detailed 3D hydrodynamic model of the region (*Operationeel Stromingsmodel Rotterdam,* in short OSR model). The Rhine branch the *Nieuwe Maas,* where Allseas performed sampling of plastic items (Section 1.6), is situated within this model domain. Because of the necessary assumptions (for example using one upstream source and no emissions of plastic within the model) a direct comparison of observed and simulated time series of the plastic concentrations cannot be made. Instead, trends are compared. Based on the literature survey, the software verifications and the pilot realistic river modelling, we prepare expert-opinion-based draft guidelines and we formulate the detailed scope of phase 2.

1.4.3 Software: WAQ and D-PART

For the transport of plastics, we use two software modules: WAQ and D-PART, in combination with a hydrodynamic model to simulate transport processes of plastics. A general description of these modules is given in the textbox.

For microplastics, it is important to capture the aggregation of a plastic particle to a sediment particle. The combined particle has different settling characteristics. For macroplastic items aggregation is usually not a leading process, because the behaviour does generally not change much after aggregation. Currently, aggregation is only available in WAQ. Apart from this, both modules include the relevant physical processes to sufficiently capture the behaviour of plastics in waterbodies. Therefore, we use WAQ for microplastic particles and D-PART for modelling the macroplastic items.

Still, we need to verify that a sufficiently accurate answer can be reached in the problem at hand for both software modules. In the next paragraph we describe what spatial scales are aimed to be resolved in the numerical modelling.

WAQ
This programme simulates the far and mid-field water and sediment quality due to a variety of transport and water quality processes. To accommodate these, it includes several advection diffusion solvers and an extensive library of standardised process formulations with the user-selected substances. Default processes allow you to simulate for instance nitrification, elementary growth of algae and nutrient cycling, exchange of substances with the atmosphere, adsorption and desorption of contaminant substances and the deposition and resuspension of particles and adsorbed substances to and from the bed. Deltares' knowledge in the field of water quality is made available to the professional world by means of this module.

D-PART
This short-term, near-field water quality programme estimates the dynamic, spatial (on a sub-grid scale) concentration distribution of individual particles by following their tracks in time. The waste substances may be conservative or subject to a process of simple, first order decay; a typical application is oil spill modelling. The programme is also used for near-field fate simulations of dredging spillage.

1.4.4 Scale of the problem and modelling options

The problem at hand is to identify locations with a high probability of finding an elevated plastics flux. This problem may be categorised into a number of spatial scales, from the largest to the smallest, as follows:

1) **Mega scale**: on this scale, the emission of plastics from a catchment, via point or distributed sources, to a river system is perhaps the most relevant component. This scale can be modelled using large-scale hydrological models and one-dimensional hydrodynamic and transport models. This scale, including the modelling of plastics emissions, is outside the scope of this study.
2) **medium to large-scale**: on this scale, the distribution of plastics along the river, and the formation/existence of higher concentration and transport zones in certain reaches can be discussed. This scale is best modelled by depth averaged models, and in some cases we can also revert to width averaging as well (1D-longitudinal models).
3) **small to medium scale**: on this scale the accumulation of plastic in a certain part of the cross-section can be discussed. This scale is better studied using 3D models. In some cases, we may revert to depth averaged models, only for models that include the proper parameterisation of the relevant physics of 3D flow and transport of plastics.
4) **micro to small scale**: this scale is relevant when dealing with the optimisation of the plastic collection technique and equipment. This scale requires the use of detailed 3D models and laboratory experiments using physical scale models. This scale is outside the scope of this study.

In this study, we focus on the **medium to large** and the **small to medium scales** (2nd and 3rd scales). The hydrodynamics of these scales can be modelled using the Delft3D modelling suite, or similar packages such as Simona (2D: WAQUA and 3D: TRIWAQ). Regarding time-scale, we focus on time-scales corresponding to the travel time of plastics for the considered spatial-scale. The long-term accumulation of plastics is not part of the scope of this study, since longer time scales are needed for this.

1.5 Detailed approach phase 1

1.5.1 Literature survey

The approach for the literature survey is to summarize available publications and reported observations on three topics.

The first topic is to identify the typical characteristics of plastic items/particles to be considered in this study. Accordingly, we carry out a literature survey aiming to reach the following:

A) Make a selection for the **size** of plastic particles which we will consider in this study. The sizes that occur most often are selected.
B) Identify the polymer types most frequently found in riverine litter and make a selection of the characteristic **density** of the types that will be used in this study.
C) Make a selection of the **shape** of plastic particles that are prevailing.

The second topic is to identify typical river planform features and forcing considered in this study. We evaluate the contribution of two main components:

A) We make a selection of the **river planform** features, which are dominant in affecting plastics transport world-wide. Based on the sensitivities and ranges of the features that occur in rivers, we select several features for further analysis in phase 2.

B) We make a selection of the typical **forcing** variables that determine plastics transport. The sensitivity of the different forcing variables is summarized based on existing literature.

The third topic is to identify dominant processes that control the transport of plastics. The following is considered:

A) We identify and describe the most relevant **processes** that determine plastics transport. For the processes the sensitivity is summarized based on existing literature for both macroplastic items and microplastic particles. For the most relevant processes the relation to the selected river planform features and forcings is indicated by expert judgement.
B) In addition to the **river planform features**, smaller scale effects are discussed. Examples are the effect of groynes and the effect of vegetation types near river banks on plastic flux.

1.5.2 Verification software modules

The tests to verify the two software modules consist of a simulation of a simple case with an expected outcome, which can be a qualitative expectation or if available an outcome based on an analytic formula. For each of the software modules, at least five tests are conducted on simplified test cases. The selection of these cases is based on progress meetings with Allseas and Deltares. The results are evaluated based on expert judgement.

1.5.3 Pilot realistic river modelling

The pilot realistic modelling offers a twofold benefit. Firstly, we verify if a realistic model can handle the problem of transport and accumulation of plastics. Secondly, this pilot case study enables building experience and forming an opinion on the behaviour of plastics under different conditions for different plastic characteristics. The Pilot realistic river modelling is a test for the combination of the software and the other components of a model (e.g. schematisation of the river bed, roughness, initial condition and boundary conditions). Both for D-PART and WAQ the 3D hydrodynamic results from the OSR model are used.

The pilot realistic modelling for transport of microplastic particles (using WAQ) and macroplastic items (using D-PART) includes a discussion to what extent the software modules can represent the processes most relevant for plastics transport. If any, we describe what processes need to be added or improved in the software to represent the most relevant processes.

1.5.4 Desktop assessment

Based on the knowledge gained from literature as well as the preliminary results of the modelling of the realistic river case, we formulate a set of draft guidelines for identification of potential plastic collection locations in rivers. These draft guidelines are related to river planform, dominant forcings, existence of certain features (e.g. vegetation, groynes, obstacles), and categorised based on the selected typical plastic characteristics.

1.6 Allseas surveys in the Nieuwe Maas

1.6.1 Summary

In preparation for removing plastic litter from rivers, using their system, Allseas has started a test campaign to investigate the distribution of plastic litter both horizontally and vertically in a river cross-section. Tests are currently being conducted in the Nieuwe Maas during various conditions of river discharge and tide.

Allseas has conducted field surveys to monitor different types of litter in the Nieuwe Maas near the Brienenoordbrug in Rotterdam (Figure 1.2, Allseas (2018)). The objective of these field tests is to monitor the concentration of different types of litter, as well as the distribution within the river cross

section. Within the period between 30 January and 10 July 2018 in total 28 surveys were conducted. The surveys were carried out either in the inner bend or in the outer bend. For half of the surveys static sampling was used, mooring the sampler in one location. Dynamic sampling was used for the other half of the surveys by pushing the sampler with a boat in an 8-shaped trajectory (Figure 1.2 right). The duration of an observation was in between 0.25 and 2.5 hours, depending on the filling rates of the net. The surveys were carried out either at established (at least an hour before and after slack tide) flood tide or at established ebb tide. Hence, the litter concentrations are representative for either ebb or flood tide.

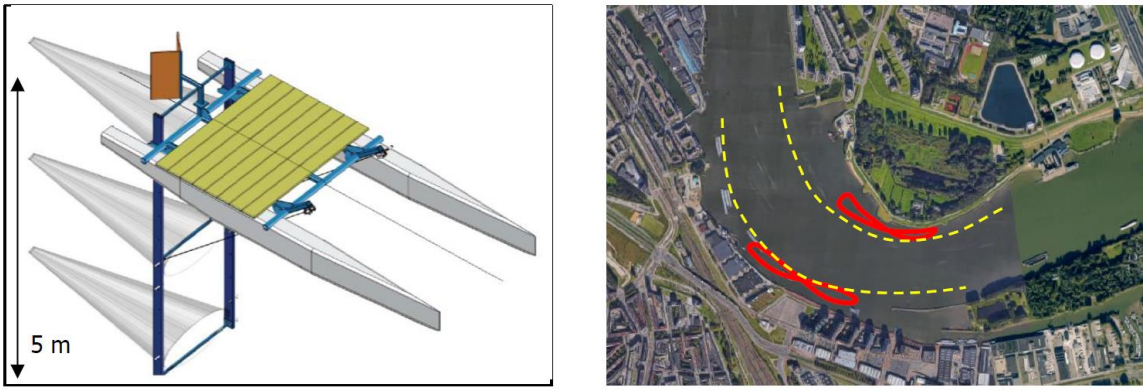

Figure 1.2 Left: the litter sampler used for the field surveys; Right: the trajectories for the dynamic surveys (red) in the inner and outer bend in the Nieuwe Maas, which are located just out of the traffic zone (yellow lines). Figure reproduced from Allseas (2018).

For each of the surveys three nets were deployed on the sampler: a surface net that skimmed the water surface, a middle net with the central position at 2.5 m below the water surface and a deep net at 5 m below the water surface. The nets had a mesh size of 3 x 4 mm, aiming to capture macroplastic items. For each of the nets the filtered residue was analysed. Almost 90 % of the litter weight was organic. Plastic litter is the largest share of non-organic material. The concentration of all plastic litter was typically 0.5 mg/m^3, ranging from 0 to 39 mg/m^3. The size fraction mostly found was 5-25 mm, and second most 25-500 mm. Although small microplastics can pass the nets, the third size fraction was <5 mm. The type of plastic litter mostly found was soft plastic (68%), then hard plastics (25%) and the last type of plastic that was determined was foam (7%). These are results of lumping all 28 surveys in the three nets together.

1.6.2 Trends

By analysing the differences in plastic and organic litter concentration per net, per location and per flow direction trends were determined from the surveys (Allseas, 2018). Trends that are supported by the graphs in Allseas (2018) are listed:

1) Soft plastic litter was found both at the water surface and at depths 2.5 and 5 m below the surface.
2) Hard plastic litter was mostly found at the surface and at 5 under the water surface, not at 2.5 m below the water surface. The organic litter showed the same distribution.
3) Foam was mostly found at the water surface.
4) During established ebb tide plastic concentrations are higher than during established flood tide for all three depths.
5) More organic and plastic litter is found at the inner bend than at the outer bend.
6) Wind enhances the concentration of floating plastic litter at the downwind side of the river.

1.7 Report outline

This report of phase 1 is structured as follows:

- The literature survey is summarized in chapter 2.
  - Identification of typical characteristics of plastics in rivers (sections 2.1 to 2.6);
  - Identification of typical river planform features and forcings (section 2.7 and 2.8);
  - Identification of dominant processes for plastic transport (section 2.9);
  - Overview of studies on modelling plastic transport in rivers (section 2.10);
- The results of the software verification for D-PART (macroplastic items) is described in chapter 3 and for WAQ (microplastic particles) in chapter 4.
- Results of the Pilot realistic river modelling of the Nieuwe Maas for D-PART are described in chapter 5, and for WAQ in chapter 6.
- In the synthesis (chapter 7) model results, trends from the surveys and the software verifications are put in perspective. This general discussion results in draft guidelines.
- The report ends with the conclusions and recommendations from phase 1 and details the proposed approach for phase 2.

1.8 Project team

The project team and the main role of each person is given in Table 1.1.

Table 1.1 The whole project team of Deltares and the main activity of each team member

Frans Buschman	Project leader
Frank Kleissen	Modelling
Marc Weeber	Modelling
Myra van der Meulen	Literature survey
Mohamed Yossef	Advisor river hydrodynamics
Dick Vethaak	Quality assurance plastics
Joana Mira Veiga	Literature survey
Arjen Markus	Modelling
Carlijn Bak	Modelling
Remco Pliegert	Modelling
Jos van Gils	Reviewer

2 Literature survey

2.1 Most relevant studies for plastics characteristics

We conducted a literature review on reports and papers on riverine litter to understand what is known about the characteristics of plastics found in European rivers and in particular Dutch rivers. As riverine litter is only recently gaining attention, there are still a limited number of publications available on the subject. Nevertheless, **24** publications were considered the most relevant, **9** of which focused on Dutch rivers (Table 2.1). Out of these 9 studies, only 5 studies presented in some way results on the variation of plastic items in the water column (Table 2.1). For studies where only plastic items at the water surface were monitored, the observations may not be representative for the entire water column. Heavier plastics may be closer to the river bed. Due to the limited amount of observations available, we have not corrected for this bias.

Table 2.1 Studies of riverine litter relevant for the Netherlands

Author(s)	Title	Year	River(s)	Compartment
Van der Wal et al.	Identification and Assessment of Riverine Input of (Marine) Litter (Service Contract for DG ENV)	2015	Rhine (NL)	Water surface/column
Urgert	Microplastics in the rivers Meuse and Rhine-Developing guidance for a possible future monitoring program (MSc Thesis)	2015	Maas & Rhine (NL)	Water surface/column
Mani et al.	Microplastics profile along the Rhine River	2015	Rhine (DE)	Water surface/ subsurface
Klein et al.	Occurrence and Spatial Distribution of Microplastics in River Shore Sediments of the Rhine-Main Area in Germany	2015	Rhine (DE)	Shoreline sediments
Leslie et al.	Microplastics en route: Field measurements in the Dutch river delta and Amsterdam canals, wastewater treatment plants, North Sea sediments and biota	2017	Maas, Reine (NL)	Water column
Plastic Soup Foundation, North Sea Foundation	*Schone Rivieren* (report from monitoring of 2017 and preliminary results from 2018)	2018	Waal, Maas (NL)	River banks
Allseas	Plastic sampling in the Nieuwe Maas	2018	Maas (NL)	Water surface/column
Gonzalez-Fernandez et al.	Floating Macro Litter in European Rivers - Top Items	2018	EU Rivers	Water surface

From the literature, we tried to draw conclusions on those characteristics that may affect their transport along the river, namely:

a) the most abundant microplastic particles (<5 mm) and macroplastic items (=>5 mm) recorded in riverine studies and surveys
b) the type of polymers that compose them
c) their shape and size
d) The rising and fall velocity of the items

2.2 Macroplastic items

2.2.1 Key plastic items

Most of the existing studies, which focused on macroplastic sampled in riverine environments, classified the litter into categories of items that are in line with the category list used for beach litter (standardised list adopted by OSPAR and the TGML[1]). This classification enables comparison of occurrence of items in these different environments.

In order to select the most important plastic items, we listed the Top 10 items and their ranking position across the different studies (Figure 2.1). Consistently, unidentifiable pieces of plastic of variable sizes are the most abundant type of litter, not only in riverine surveys but also on aggregated beach litter data for Europe (Figure 2.1 – EU Beach, JRC – Addamo et al., 2017). This was also seen in the samples collected and analysed by Allseas. Other items with high incidence include cigarette butts, plastic bottles, bottle caps, packets of sweets and crisps and food containers. Nevertheless, although some litter items are recurring, their ranking in the TOP 10 is variable across locations. In addition, it is important to note that for riverine litter, the compartments surveyed and methodologies used can be distinct: recording of litter items found on river banks (e.g. *Schone Rivieren*) or visual observation of floating items from bridges (e.g. JRC – Gonzalez-Fernandez, 2018).

2.2.2 Characteristics of macroplastic items

For identifiable plastic items equal or larger than 5 mm, polymer type, size and shape were obtained from known objects' physical characteristics, since these are typically not described or analysed in the studies. Based on desk research and available information from plastic producers, for each plastic item, we attempted to describe the polymer type(s) that these items are usually made of and their typical size (length, as the higher dimension). Densities were obtained from published sources, based on the polymer type (e.g. Polymers: A Property Database, 2009).

Disposable drink cups, for example, can be made of PS, PP, EPS or PET and have slightly different sizes. On the other hand, there are hundreds of variations of polymers, often with additives which change slightly their mechanical properties. We used intervals of sizes and densities for each item, to accommodate for these variations.

The category of "plastic fragments" (=>5mm, <500mm)", tends to be the category of plastic items recorded with higher frequency, not only in riverine litter but also in beach litter. However, additional differentiation regarding shape and polymer type is very limited and when the OSPAR/TGML standardised list of items is used, the plastic fragments are attributed to only two broad categories of sizes (2,5 – 50cm; > 50cm). In Allseas campaigns, distribution of plastic fragments was roughly 70% between 5-25mm and 30% between 25-50mm.
When defining attributes of plastic fragments, we considered that these can be made of different polymer types and present different sizes and shapes. A similar approach was taken for the "string and cord" items category, since the size frequency is not specified nor the polymer type that these items are made of.

[1] *OSPAR – Regional Sea Convention for the North East Atlantic, which has in place a beach litter monitoring programme since 2001*

TGML – Technical Group on Marine Litter, an expert group set up under the Marine Strategy Framework Directive to provide guidance to European Member States on monitoring of Marine Litter

In Figure 2.2 and Figure 2.3 we map the main items of plastic across a range of sizes and densities, to help determine the values that need to be modelled. The interval of densities is smaller around the density of freshwater (about 1000 kg/m^3), since the behaviour of vertical movement is sensitive to the difference between the polymer density and the water density.

The items with a density smaller than the density of water may float at the water surface. When an item is floating, we assume that the wind force has a major influence in its transport, whereas for items that tend to remain near but below the water surface the wind only has indirect effect on its transport by generating a near surface flow velocity.

	EU Beach (JRC, 2017)	NEAtlantic (JRC, 2017)	MED (JRC, 2017)	Baltic Sea (JRC, 2017)	Black Sea (JRC, 2017)	Adour, FR (Bruge et al)	Schone Rivieren (2018)	Schone Rivieren (2017)	Rhine (van der Wal, 2015)	NE Atlantic (JRC, 2018)	EU rivers (JRC, 2018)	Adour, FR (Bruge et al)	Thames, UK (Morrite et al)	Tiber, IT (Crosti et al)	MED (JRC, 2018)	Baltic (JRC, 2018)	Black (JRC, 2018)	Po (van der Wal, 2015)	Danube (van der Wal, 2015)	Dalålven (van der Wal, 2015)
MACRO Litter types							NL	NL	NL	NL	inc NL									
Plastic pieces 2,5 - 50 cm	1						1	1		1	1			1	1	9	2			
Plastic pieces 0 - 2,5 cm	2						1	1		1	1			1	1	9	2			
String and cord	3	1		6		3		7								3				
Cigarette butts	4	5	1	2	2	2		6				9								
Plastic caps/lids	5	2	2	4	1	6		4				4								
Cotton-bud sticks	6	3	3			9	7	8												
Wax/paraffin	7			1																
Crisp packets/sweet wrappers	8	4			7	7	3	2		2	3	1		4	4		3			
Other (identifiable)	9	6											2,6							
Plastic bags (inc. small)	10		6	3	4		9			4	4			4	3	5	4			
Plastic bottles			4		3	1	4	4		6	2			2	2	1	1			
Foam			5			8				7	9	2		5	9					
Cups and cup lids						10	10						5	4						
Food containers				5	6	4	6	10		2	3	3	1	4	4		3			
Toys and party poppers					5															
Sanitary towel components							8						3							
Tobacco packing												6	4							
Agricultural tarpaulin												5								
Industrial, plastic sheeting										5		7								
Polystyrene pieces							2			3	5			3	5		9			
Crates/containers/baskets																	5			

Figure 2.1 Position of items of litter found in riverine (headings in blue) and coastal environments (headings in yellow) within the TOP 10 recorded items from key studies in Europe and in the Netherlands.

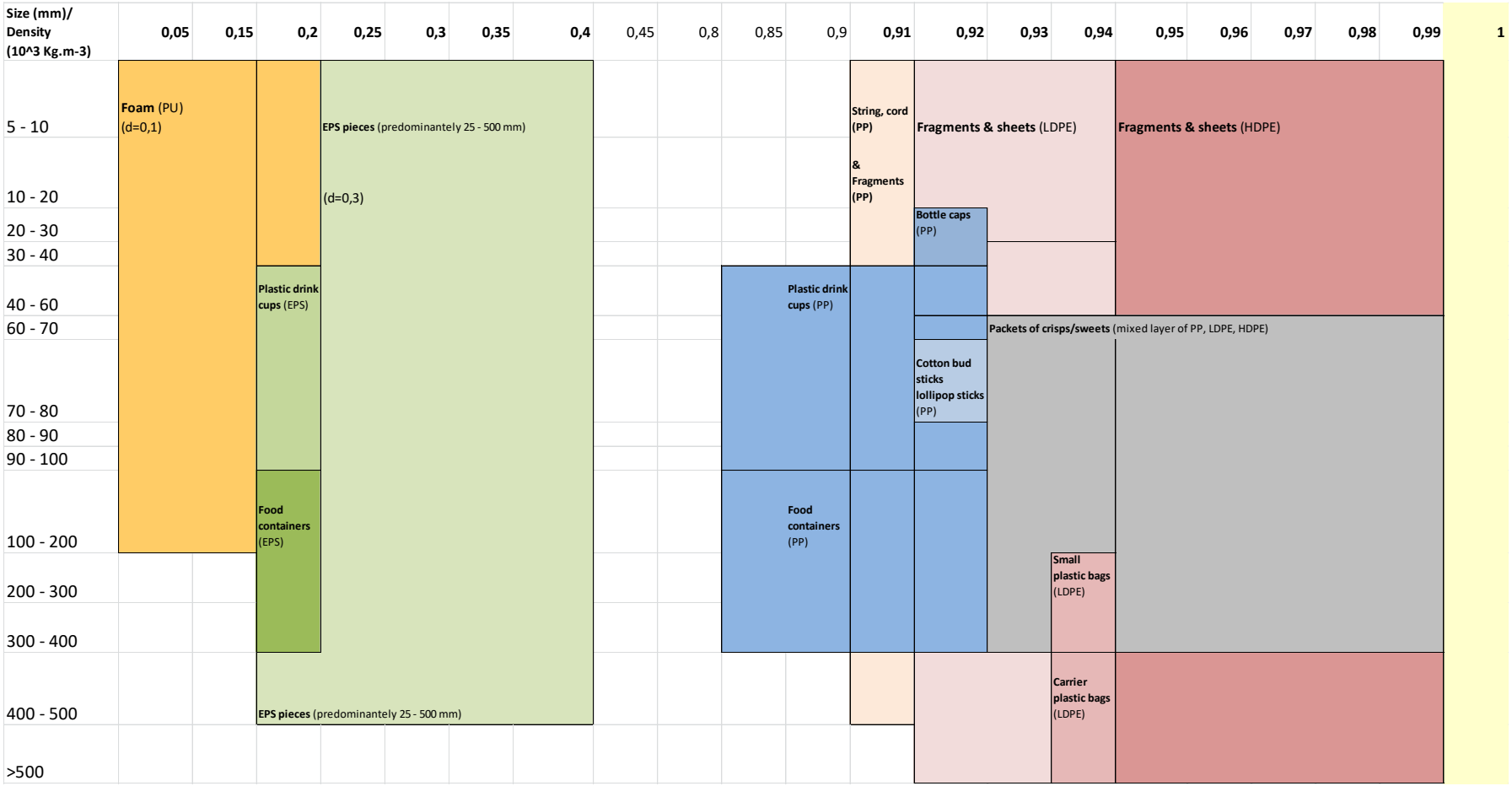

Figure 2.2 Mapping of most common plastic items found on rivers and beaches across densities (horizontal axis - 1x 10^3 Kg.m-3) and range of sizes (vertical axis - mm). Water density (ρ=1) is shown in pale yellow and figure includes those items made of polymers with density > 1).

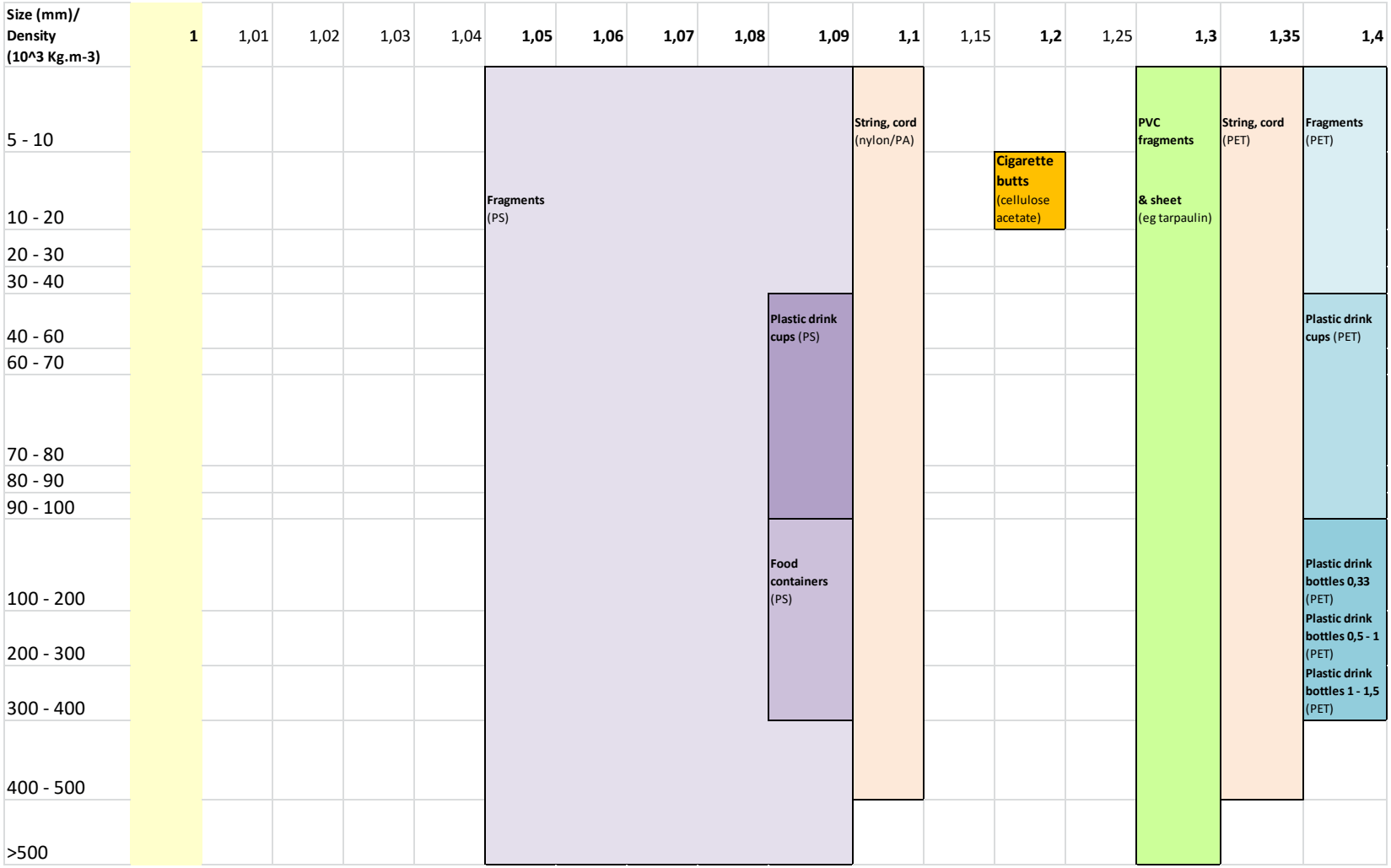

Figure 2.3 Mapping of most common plastic items found on rivers and beaches across densities (horizontal axis - 1x 10^3 Kg.m-3) and range of sizes (vertical axis - mm). Water density (ρ=1) is shown in pale yellow and figure includes those items made of polymers with density > 1).

2.2.3 Variability

In studies of macrolitter, a high temporal and spatial variability is found (e.g. van der Wal et al, 2015; Urgert, 2015; Allseas, 2018). The composition of plastic litter in rivers will be affected by the sampling location in relation to nearby point sources (e.g. nearby industries or recreational areas), the variation in the river discharge and other forcing factors such as the wind. According to the *Schone Rivieren* report (based on data from 2017), litter recorded in the river banks of the Waal and the Maas, varied between 41-556 and 46-357 items per 100 m stretch along the river, respectively. A high variability is also seen in types and amounts of items measured recorded in monitoring programmes of beach litter in Europe.

Dominant macroplastic items identified in rivers include plastic fragments, plastic packaging, such as bottles, food containers, wrapping of sweets/crisps, pieces of EPS and foam.

2.3 Microplastics

2.3.1 Microplastics characteristics

As for the macroplastic items, we found for the size fractions of plastic litter smaller than 5 mm that studies use different approaches for sampling and classifying plastic particles larger than 1 mm. Some studies sampled only the surface and subsurface (e.g. van der Wal et al, 2015; Mani et al, 2015), while others attempted to sample a larger portion of the riverine water column (e.g. Morrit et al, 2014; Sadri & Thompson, 2014).

Except for resin pellets, the microplastics fraction corresponds to unrecognisable fragmented pieces of larger items. Thus, the characterisation of these particles is usually done based on analysis of polymer type and/or classification of size and/or shape (Figure 2.5). Due to the lack of standardised methodologies, different classifications of the shape are used (e.g. “pellets”, “spherules”, “flakes”, “fibres”, fragments”, “sheet”, “foam”), which makes it difficult to compare and integrate results. Nevertheless, either spherical particles or fragments tend to be the dominant shape in microplastics particles.

For the different classifications of shape used in the literature we attributed one of four 4 main types of shape: *spherical, sheet-like*, *cuboid* and *elongated,* to which a shape-factor was defined. If we take as an example Figure 2.4, type A and B would be classified as *cuboid*, type C (pellets) and F as *spherical*, type D as *sheet-like* and type E as *elongated*.

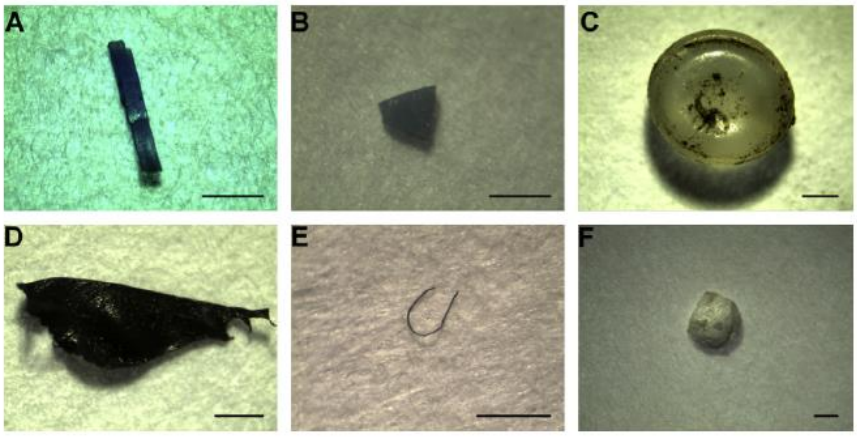

Figure 2.4 Examples of microplastics in different shapes found on Tamar Estuary, Southwest England. Scale bars represent 1mm (source: Sadri & Thompson, 2014)

In terms of size distribution, particles within the size class of 1-3 mm seem to be the most abundant in the Thames (e.g. Morrit et al, 2014) and marine waters surrounding the United Kingdom (microplastics collected at and near surface with manta-trawl, Maes et al, 2017). Other studies reporting the size distribution of microplastics have not been found. Several studies have reported that the dominant polymer type that microplastics consist of is polyethylene (PE, Figure 2.5).

Similar as for the macroplastic items, the microplastics were mapped by size and density to have an overview of the microplastics sizes and densities found (Figure 2.6). This overview has been used to determine the microplastics characteristics to be modelled.

Microplastics found in rivers tend to be dominated by PE and fragments between 1-3 mm tend to be the most represented.

	Thames, UK (Morrit et al)	Danube 2010 (Lechner et al)	Danube 2012 (Lechner et al)	Antua, PT (Rodrigues et al 2018)	Rhine (Mani et al)	Rhine (van der Wal, 2015)	Po (van der Wal, 2015)	Danube (van der Wal, 2015)	Dalålven (van der Wal, 2015)
microplastics POLYMER					300 µm - 5mm				
PE - polyethylene	40%				20%	43-78%	75%	62%	30%
PP - polypropylene	19%				17%	12%	17%	4%	3%
PS - polystyrene	25%				30%	6-11%	4%	15%	6%
PVC - polyvinyl chloride	7%				2%				
Polyester	6%				5%				
Nylon	3%							8%	15%
Acrylate					9%				
Other					14%	1 - 25%		5%	40%
microplastics SIZE									
300–1000 µm	NA								
< 1mm									
1-3 mm									
3-5 mm									
>5 mm									
microplastics SHAPE									
Pellets									
Flakes									
Spherules					68%				
Fibers					3%				
Fragments					38%				
Sheet									
Foams									

Figure 2.5 Relative frequency of different polymers, size classes and shape of microplastics sampled and analysed in key studies in rivers in Europe and in the Netherlands.

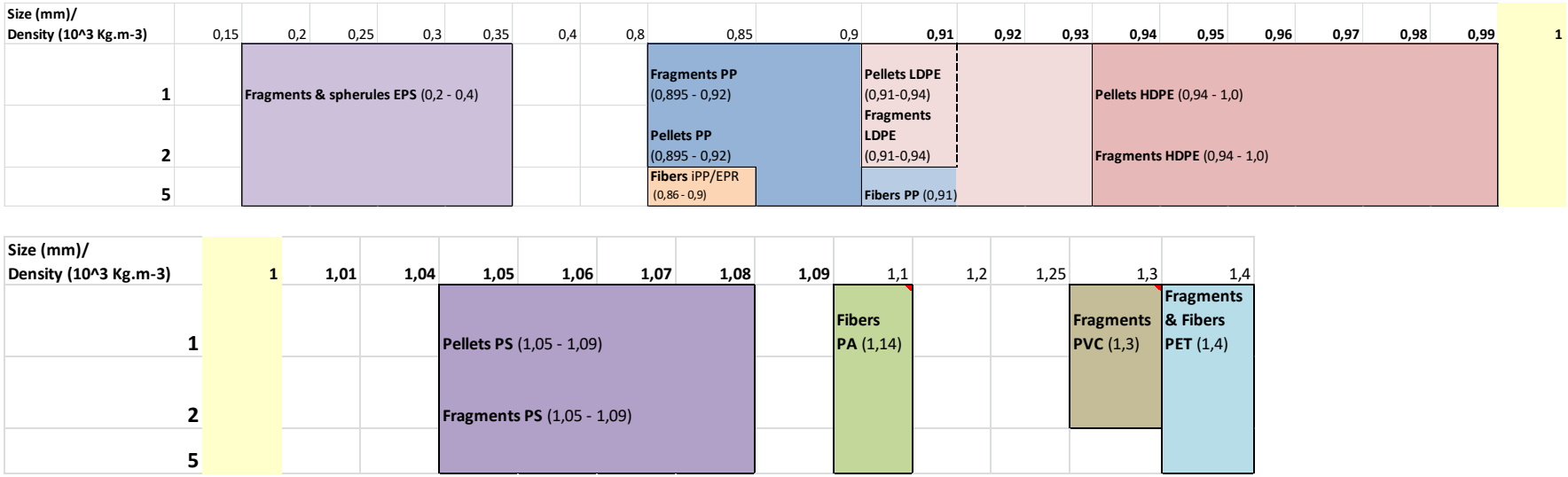

Figure 2.6 Mapping of main polymers and shapes of microplastics across densities (horizontal axis - 1x 1000 kg/m^3) and size classes (vertical axis - mm). Water density (ρ=1000 kg/m^3) is shown in pale yellow. Top: floating particles (density < 1000 kg/m^3); Bottom: sinking particles (density > 1000 kg/m^3).

2.3.2 Variability

A key conclusion from the literature reviews is that the spatial and temporal variability between results from the studies considered is high. Not only the concentration (number per volume) varied, but also the polymer type of the microplastics particles. Take for example the analysis done by Mani et al (2015) of the samples obtained from different stations along the Rhine (Figure 2.7): both the number and the relative composition of microplastics varied greatly along the river Rhine.

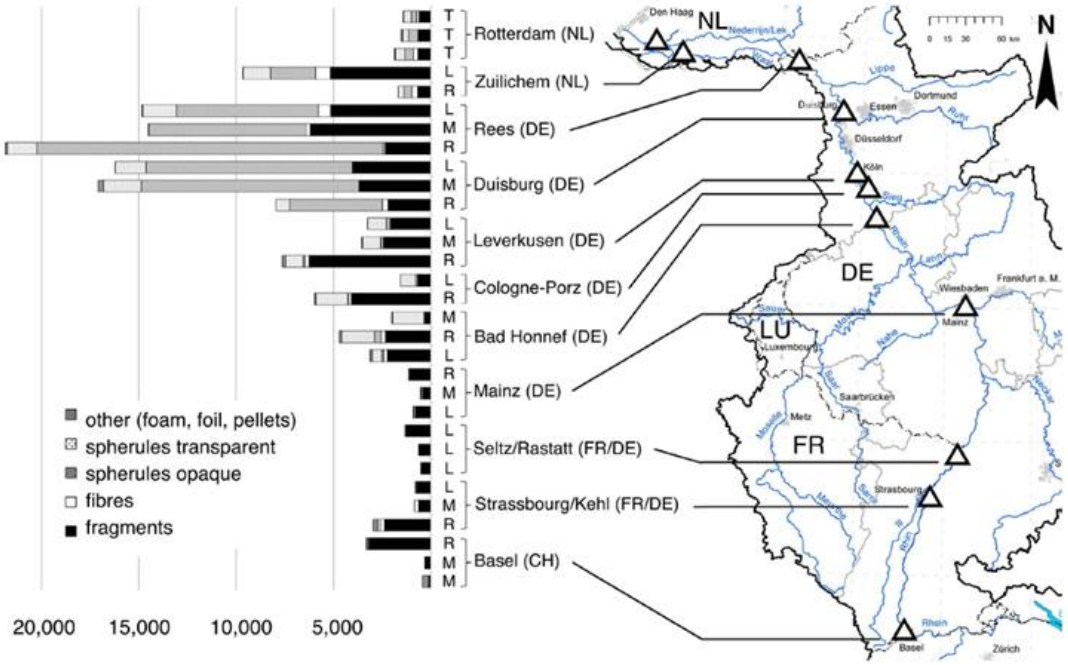

Figure 2.7 Number of microplastic particles (300µm-5 mm) 1000m^{-3} in categories of shapes sampled in sites along the Rhine (after Mani et al, 2015)

2.4 Full matrix of plastic items

2.4.1 Density, size and shape

Based on the mapping of the densities and sizes of plastic items found in rivers (Figure 2.2, Figure 2.3 and Figure 2.6), we defined a large set of combinations of values for densities, values for sizes and characterizations of the shape (Appendix A). Within this matrix of plastic combinations, the shape varies from spherical particles to elongated fibres for microplastics. We classified the shape of macroplastic items with an approximated shape-type, e.g.: string/cords, cotton-bud sticks – *elongated*; drink bottles, cigarette butts – *cylindrical*; food containers – *cuboid*; tarpaulin – *sheet-like*. For the "fragments", as this is a very general category, we considered these can have multiple shapes (*cuboid, sheet*).

For microplastics particles shape is an important characteristic for their transport. We have chosen to sort the full matrix of microplastics by shape (appendix A.2). For macroplastic items, however, the ratio of volume and surface area is higher than for microplastics particles. The density is more likely to be dominant for its transport. Since density relates to the polymer type of which an item dominantly consists, we grouped the macroplastic items by polymer type (appendix A.1) as for the mapping in Figure 2.2 and Figure 2.3.

We limited the number of densities and sizes to reduce the number of combinations, while defining class size intervals that can still capture the range of sizes of specific items. The most critical item types are those made of high-density polyethylene (HDPE), which has densities between 940 and 1000 kg/m^3 close to the freshwater density. Plastic items within this density range may have a substantially different fall velocity, since the density for this commonly found polymer is so close to that of water. To select combinations to be modelled, we included in the list a level of "**occurrence**" (*low, medium, high*) documented in the literature (Appendix A). For the modelling we selected only combinations with *high* occurrence.

2.4.2 Level of occurrence

The level of occurrence was attributed based on the reported field results (
Figure 2.1 and Figure 2.5). For microplastics, literature indicates that pellets can have high abundance in riverine samples, in particular the ones made of Polyethylene (PE), while fragments made of polystyrene can be as low as 0-5% for microplastics. In fact, PE tends to be the dominate type of polymer in the samples. In terms of size classes, plastic fragments between 1-3 mm tend to be the most represented.

For larger plastic items, we attributed *high* to those items that tend to be ranked in the first 5 positions of TOP 10 (e.g. bottle caps, drink bottles) *medium* within position 6-10 (e.g. plastic bags, food containers) and *low* when they tend not to be part of this list. As plastic fragments between 2,5 and 50 cm tend to be the most abundant category of items recorded but is encompasses a large range of sizes, we considered a *high occurrence* for multiple shapes and polymers of smaller ranges of size (5-25 mm) but *medium* to 25-100 mm and *low* to 100-500 mm, assuming that this would reflect the distribution of sizes resulting from the process of fragmentation in the Tiber River (Crosti et al, 2018; Figure 2.8).

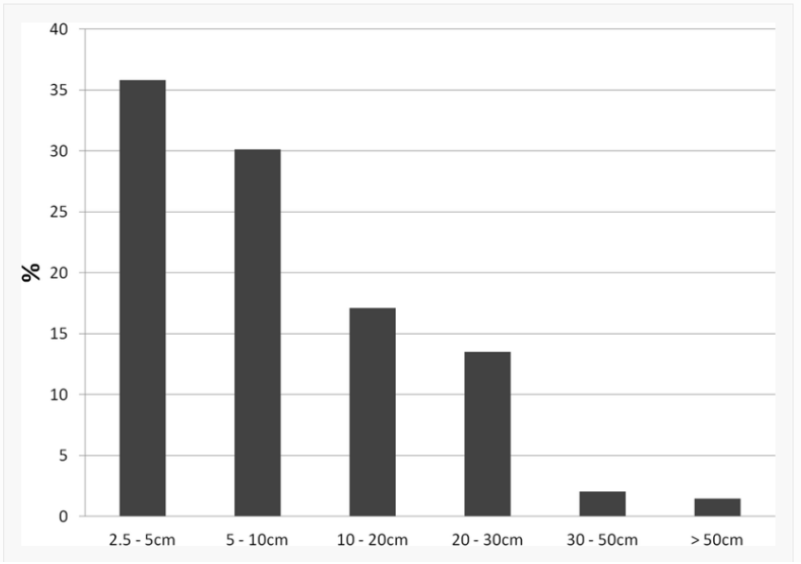

Figure 2.8 Percentage of recorded items in different class sizes observed in the Tiber River (Italy) (Source: Crosti et al, 2018)

2.5 Falling velocities of plastic particles

2.5.1 Theory

The characteristics of plastic items determine its fall velocity, which is sometimes also referred to as the fall velocity. The fall velocity is the characteristic of a particle that determines its vertical displacement with respect to the water.

The fall velocity of a plastic item makes that the item behaves differently from a neutrally buoyant tracer that is transported with the flow.

The fall velocity of a particle is constant when the gravitational force on the particle equals the drag force on the particle. This fall velocity can be derived for spherical particles with the Stokes' law (Lamb, 1994):

$$w_s = \frac{2}{9}\frac{(\rho_p - \rho_f)}{\mu} gR^2 \qquad (2.1)$$

where:
w_s – fall velocity (m/s); It is directed downwards if the density of the particle is larger than the surrounding water
g – gravitational acceleration (m/s^2)
ρ_p – particle density (kg/m^3)
ρ_f – fluid density (kg/m^3)
μ – dynamic viscosity of the fluid (kg/ms)
R – radius (m)

Stokes' fall velocity is valid for spheres and in laminar flow around the particle. The fall velocity increases quadratically with its size. The fall velocity of a particle can change when the density of the water changes, due to temperature of salinity changes. We note that for negative values of the fall velocity (when the density of a particle is smaller than the density of the fluid), the particle will move upwards towards the water surface. Hence, a rising velocity is a negative fall velocity.

To consider the effect of the different shapes of particles found in the field, varieties of shape factors have been introduced. Usually the so-called Corey Shape Factor is used, resulting in a lower fall velocity depending on the shape of the particle. It is defined as:

$$S = \frac{c}{\sqrt{ab}} \qquad (2.2)$$

Where:
S – Corey shape factor [m]
c – shortest length of a particle (thickness) [m]
b – intermediate length [m]
a – longest length [m]

For a spherical particle S equals one. Particles shaped as fibres are have among the lowest values for S. When S is added to the righthand side of the Stokes' law (2.1), the fall velocity of different shapes of a particle can be estimated theoretically. However, Waldschläger and Schüttrumpf (2019) found large differences in observed fall velocities from 468 tests for microplastics and fall velocities calculated by implementing the particle properties in (2.1) with S (2.2) added. For larger particles falling in water, the flow around the particle is usually not laminar. Therefore, the Stokes' law (2.1) does not give accurate results for the fall velocity of macroplastic items (LeBreton et al. 2018). Additionally, plastic items often have irregular shapes, making it difficult to estimate a representative shape factor (2.2). Alternative approaches were followed to obtain this vital characteristic of plastic items for both microplastic particles and macroplastic items.

2.5.2 Microplastics

Waldschläger and Schüttrumpf (2019) published empirical relations for fall and rising velocities. The resulting empirical relation for the fall/rising velocity was used in this study. The shape of the plastic particles is accounted for by the Corey shape factor (S; equation 2.2). For rod-like particles (not included in this study) the diameter of the rod is used instead of an equivalent

diameter based on *S*. The relations for the more spherical particles provided by Waldschläger and Schüttrumpf (2019) read:

$$D_* = S \cdot d \cdot \sqrt[3]{\left(\frac{\rho_p - \rho_w}{\rho_w}\right)\frac{g}{\nu^2}} \quad (2.3)$$

$$w_s = 0.0025\, D_* \quad (2.4)$$

where:
D_* – the dimensionless diameter
S – the shape factor and
d – the equivalent diameter of the particle
ρ_p – the density of the particle and ρ_w is the density of water.
g – the gravitational acceleration, v the kinematic viscosity of water.
w_s – the fall or rising velocity (depending on whether the density of the particle is larger or smaller than that of water.

The deposition of particles heavier than water is controlled via the Krone formula (Deltares, 2018d). This way a fraction of the particles that are in the lowest layer will be incorporated in the water bottom (in the model this means that part of the plastics in the water phase is turned into plastics in the bottom, a different substance).

2.5.3 Macroplastic items

As an alternative for calculating the fall velocity of macroplastic items from the size, density and shape using the Stokes' law, fall velocities were estimated from a list of plastic items that LeBreton et al. (2018) collected near the sea surface in the Pacific Ocean around the Great Pacific Garbage Belt. As the particles are collected near the surface and sources of plastic are far away, the particles must have been transported to this location near the water surface and the listed must be buoyant (Ryan, 2015). For each of the plastic items captured in surface nets or trawls, LeBreton et al. (2018) listed size and type of plastic. Furthermore, they determined rising velocity for the particles. For each of the four types of plastics the rising velocity is plotted against the size of the particles (Figure 2.9).

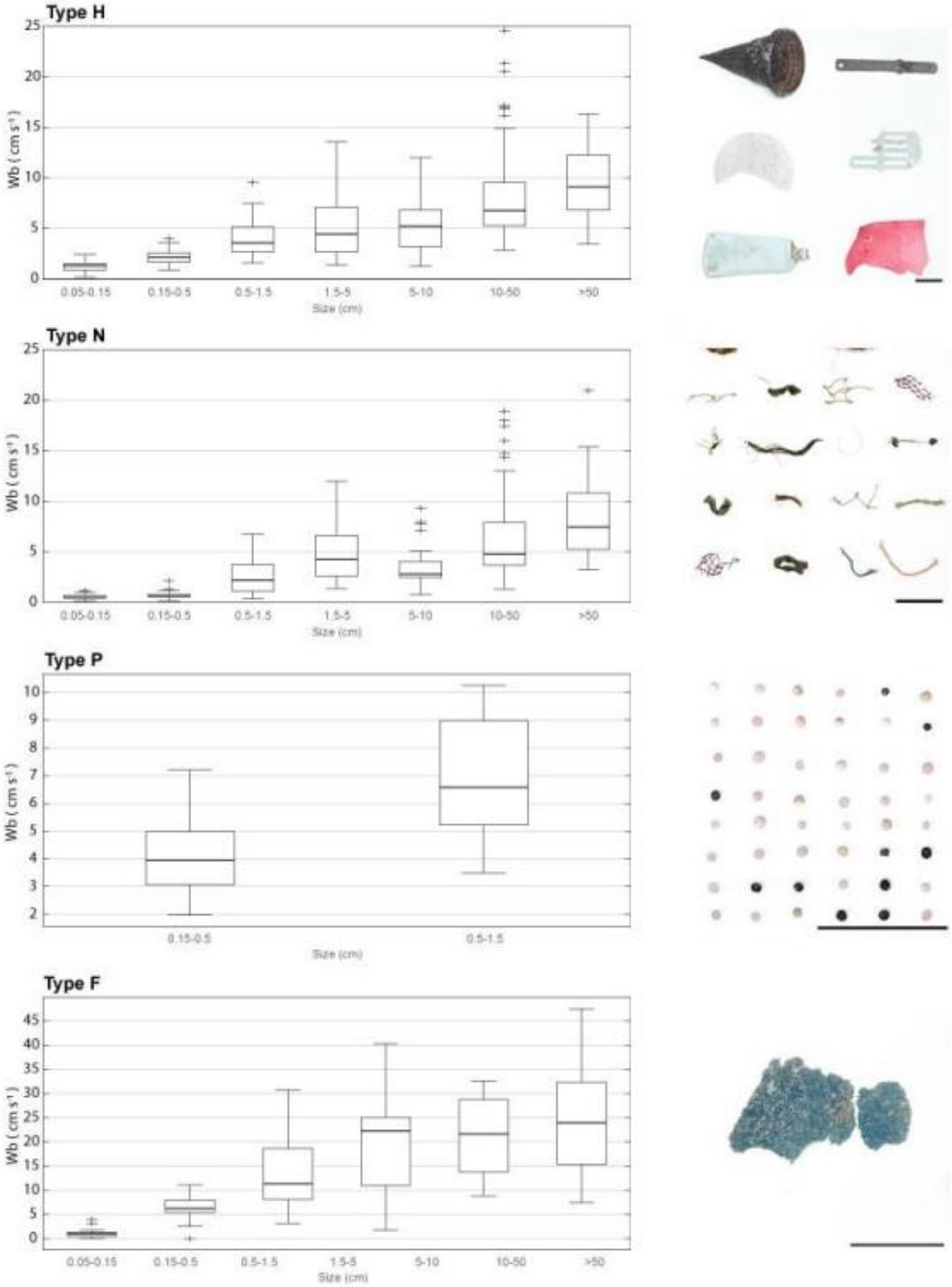

Figure 2.9 After supplementary method 1 of LeBreton et al. (2018); Terminal rising velocities (Wb) of plastics in sea water within different size classes for four plastic types. Photographs provide examples of ocean plastic within each type class. Plastic type H include 101 pieces of hard plastic, plastic sheet and film, type N encompasses plastic lines, ropes and fishing nets, type P are pre-production plastic pellets, and type F are pieces made of foamed material. The black scale bar within each photograph is 5 cm long. Median Wb are represented as bold lines, boxes range from 25th to 75th percentiles and whiskers extend from minimum to maximum values not considering outliers which are plotted as crosses. Two outliers are not shown in the 'Type H' graph: 35.6 and 37.4 cm s-1 for the 10 - 50 cm size class.

For each of the buoyant items in the full matrix with high occurrence (appendix A.1) the rising velocity was estimated from Figure 2.9. Density was estimated based on the most common polymer type. Because shape was not determined for the list of plastics found near the surface of the Pacific Ocean, several items of the matrix were clustered together resulting in the combinations in Table 2.2. The shape of the macroplastic items collected at sea was assumed to have a similar shape factor as plastic items in a river. Besides shape, density is not available in the list of LeBreton et al. (2018). We assumed that the items listed in the full matrix with a density more than 5% different than the density of sea water (around 1023 kg/m^3) are enough buoyant to be transported to the sample locations in the Pacific Ocean. Hence, we assume that the list of LeBreton et al. (2018) does not include items with a density close to or higher than sea water (indicated as 'not available' in Table 2.2).

Table 2.2 Rising velocity for macroplastic items of the full matrix with high occurrence estimated from Figure 2.9 for foam and for hard plastics; NA = Not Available

Item	**Size (mm)**	**Assumed density (kg/m^3)**	**Rising velocity (mm/s)**
Fragments of EPS foam	5	300	120
Fragments of EPS foam	25	300	220
Bottle caps (PP)	20	910	20
Bottle caps (PP)	40	910	20
Fragments of PP / Fragments of LDPE / Fragments of HDPE	5	910-940	10
Fragments of PP / Fragments of LDPE / Fragments of HDPE	25	910-940	20
Packets of crisps/sweets	60	930-970	50
Packets of crisps/sweets	400	930-970	70
Packets of crisps/sweets	60	1000	NA
Packets of crisps/sweets	400	1000	NA
Fragments of HDPE	5	970-1000	NA
Fragments of HDPE	25	970-1000	NA

To estimate the rising velocity in Table 2.2, we further assumed that the rising velocity in freshwater was similar to the rising velocity for that type of plastics with the same size in sea water. This assumption was necessary, since detailed information for fall velocities of macroplastic items in freshwater has not been found. The error made by using this assumption can be estimated, because for some items the rising velocity was determined both in sea water and in freshwater (supplementary material of LeBreton et al. 2018). The rising velocity in sea water was found to be 1.02 to 2.52 times higher than for freshwater. Since this is such a wide range and salt water may intrude up to Rotterdam, the rising velocity has not been corrected for salinity. Without having detailed information for the items heavier than water, the fall velocity was chosen to be the same but with opposite sign as the rising velocities.

2.6 Selection of combinations in matrix to model

2.6.1 Macroplastic items

For macroplastic items in rivers detailed information on the fall velocity has not been found. Therefore, we estimated the rising velocity for the items in the full matrix with high occurrence based on LeBreton et al. (2018) in Table 2.2, which is based on the density, size and shape of these items found in the ocean. To determine the rising velocity of particles modelled with D-PART, we selected a range of rising velocities covering the rising velocities in Table 2.2. The rising velocities for these items are in between 10 and 220 mm/s. Based on these values we chose to simulate items with a rising velocity of 10 and of 200 mm/s. Since items with a density within 5% of the density of sea water are most likely not collected in the Pacific Ocean, we added a rising velocity of 0.1 mm/s. Using these three rising velocities, gives a first indication of the behaviour of macroplastic items. The macroplastic fall and rising velocities used for the modelling in phase 1 of this project are summarized in Table 2.3.

Table 2.3 Selected fall velocities for macroplastic items based on Table 2.2 and assumptions

Item	Density (kg/m^3)	Fall velocity (mm/s)	Fall velocity (m/d)
Fragments of EPS foam	300	-200	-17,280
Fragments of PP / Fragments of LDPE / Fragments of HDPE	910-970	-10	-864
e.g. Sheet fragments high density PE (density 950-1000 kg/m^3)	930-1000	-0.1	-9
Fragments of PET/ drink bottle	1400	200	17,280
Fragments of polystyrene	1090	10	864
e.g. Sheet fragments of PS	1000-1050	0.1	9

2.6.2 Microplastic particles

For microplastic particles the fall velocity is determined by its the size, density and shape factor of the particle, using equation 2.3. From the list of microplastic particles (appendix A.2) we selected the items with high occurrence and from these items we selected the items with characteristics that cover the variety found for microplastic particles. The selection of items, which is also used for the pilot realistic modelling using WAQ, is given in Table 2.4

Table 2.4 Selected microplastics particles that are typical for rivers, including their characteristics size, density, shape factor and fall velocity (rising when negative)

No.	Size (mm)	Density (kg/m^3)	Shape factor	Fall velocity (m/day)
1	1	1050	1	170
2	2	1050	1	341
3	5	1050	1	852
4	1	970	0.01	-1.4
5	2	970	0.01	-2.9
6	5	970	0.01	-7.2
7	1	1000	0.01	0
8	2	1000	0.01	0
9	5	1000	0.01	0
10	1	970	1	-144

No.	Size (mm)	Density (kg/m^3)	Shape factor	Fall velocity (m/day)
11	2	970	1	-287
12	5	970	1	-719
13	1	1000	1	0
14	2	1000	1	0
15	5	1000	1	0
16	1	1050	1	170
17	2	1050	0.01	3.4
18	5	1050	0.01	8.5
19	1	1300	0.01	3.1
20	2	1300	0.01	6.2
21	5	1300	0.01	15.5
22	1	1050	0.1	17
23	2	1050	0.1	34
24	5	1050	0.1	85

2.7 River planform features

2.7.1 Classification of natural rivers

To find locations with high probability of relatively high flux of plastics world-wide, we attempt to classify natural rivers by their geometry. Besides this larger scale planform feature of rivers, we also discuss external factors that could be important at smaller scale for the spatial distribution of plastic items. Literature directly linking the spatial distribution of plastic particles larger than 1 mm to zones in rivers have not been found.

At largest scale, a classification of river deltas is relevant. The formation of a delta determines its current geometry. The formation is controlled by the dominant forcing (Figure 2.10). Deltas dominated by river discharge build out into the sea with the sediment transported by the flow in the river, making the river elongated. The Mississippi river is a typical example of this type of river delta. When tides are dominating the delta formation, several channels connect the river to the sea and these distributaries widen towards the sea having a trumpet shape. The plastics transported in such a river can follow several pathways to the sea. Furthermore, salt water can intrude in far into these deltas. The part of the river where salt intrudes is an estuary. When waves are the dominant variable forming a delta, the river consists typically of one distributary channel that flows out at a smooth coastline.

Figure 2.10 Classification of deltas by the forcing dominant in forming the delta (Seybold et al. 2007)

Since we attempt to find locations with high probability of relatively high flux of plastics, we look for a classification of a river reach. A reach is typically defined as a length of river with consistent valley and channel geometry. In a reach channel planform as well as other characteristics of rivers are similar. On a large river, a reach can be 10^2–10^4 m long. On a smaller river, individual reaches of consistent geometry might be only 10^1–10^2 m long. Because river systems commonly exhibit substantial downstream variability in geometry, reach-scale classifications are widely used to understand the river process (Wohl, 2015).

Several, complementary classification systems are used to differentiate aspects of reach-scale valley and channel geometry. Channel geometry can be classified based on planform into straight, meandering, braided, and anastomosing (Figure 2.11). Channels can also be classified based on predominant bed substrate into bedrock, gravel-bed, sand-bed, and fine cohesive, bed channels. The bed sediment size determines how sediment is transport dominantly: as suspended load, as bed load or as a mix of the two. For relative coarse bed sediment, bed load transport is likely to be dominant and the river planform is more likely to be straight. On the other hand, for relatively small sediment size, suspended load will be dominant, and this usually leads to stable meandering channels (Figure 2.11). The longer the meander bends are, i.e. the higher the sinuosity, the larger the bars in the inner bend where the water depth is reduced (grey shading in Figure 2.11).

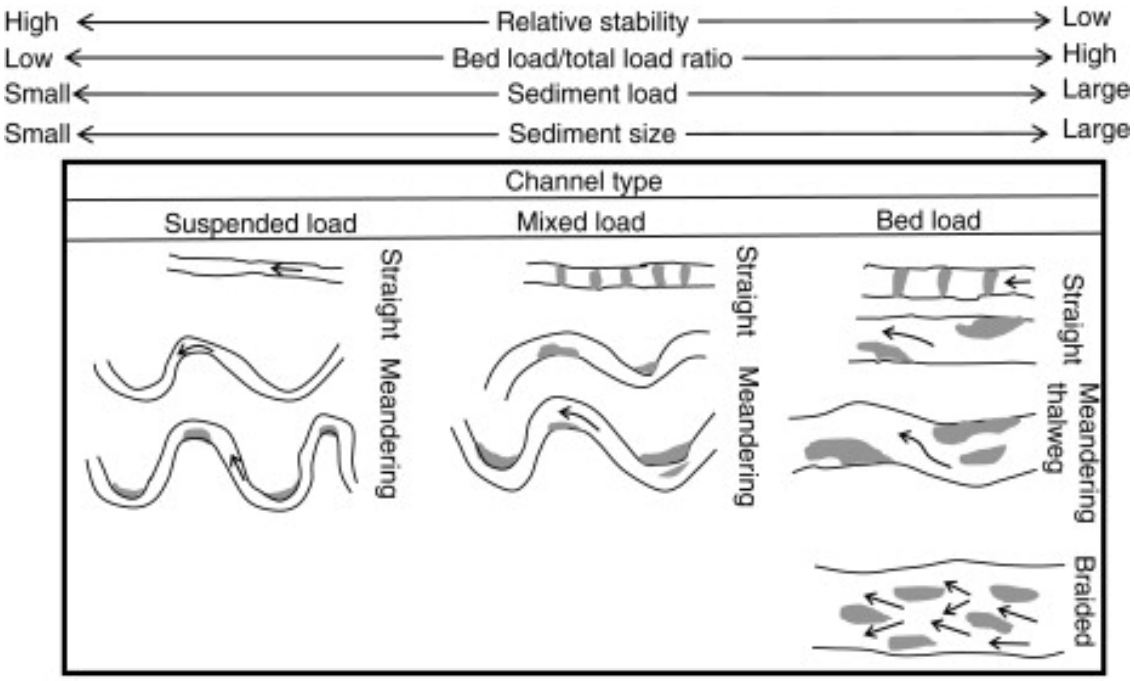

Figure 2.11 Simple classification of channel planform into straight (single flow path, sinuosity < 1.5), meandering (single flow path, sinuosity > 1.5) or braided (multiple flow paths). Relative levels of channel stability, the ratio of bed load to total sediment load, the amount of sediment transported, and the grain size of the sediment in transport are shown along the upper horizontal axis. Grey shading within plan view drawing of each channel segment indicates riffles and bars; arrows indicate flow paths. After Schumm (1981).

Since several mechanisms may result in spatial distribution of particles transported with the flow in a river bend, we zoom in into a river bend. For that reason, we elaborate on the mechanisms in a river bend. The geometry of the channel having a deep part in the outer bend (pool) from which the bed level increases gradually to the bar at the inner bend is shown in Figure 2.12. For falling particles, the pool in the outer bend may lead to particles being trapped in this deeper main channel of the river, since a falling particle is not easily transported upwards towards the shallow inner or outer bank.

The channel planform is largely determined by the helical flow in a meandering river. In Figure 2.12 the realistic helical flow is shown and also the secondary flow, which is the component of the flow in the transverse direction of the channel. This transverse flow transports particles with a tendency to rise to the outer bend, and particles with a tendency to fall towards the inner bend. This helical flow can explain why Bruge et al. (2018) found highest litter deposition in a French river on the outer bank. The macroplastic items had a tendency to rise and were thus transported to the outer bend.

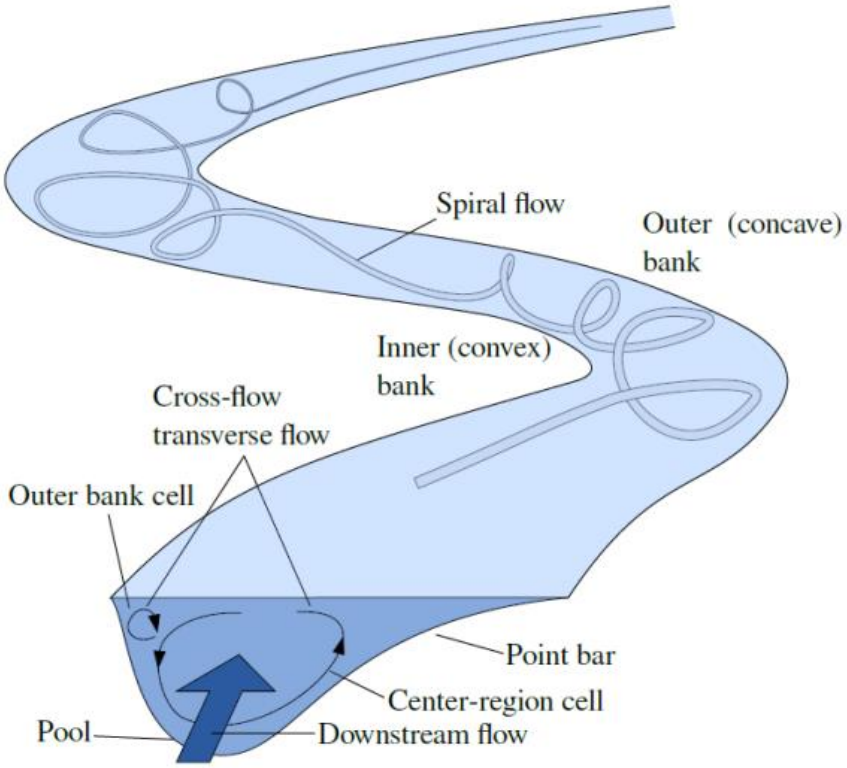

Figure 2.12 A schematic of the helical flow and the channel planform of a typical river bend (Vermeulen, 2014).

2.7.2 External factors

Besides the planform features found in natural rivers, external factors such as man-made structures may influence the distribution of plastic particles larger than 1 mm. A first example is the effect of groynes on the flow (Figure 2.13). In the main channel the flow accelerates at the groyne and decelerates again in between groynes. A circulating flow, i.e. primary eddy, occurs with flow in the downstream direction close to the main channel and returning flow close to the river bank (at the top in Figure 2.13). The circulating flow pattern on the water level and the submergence of the groyne. For any condition, it could enhance deposition of particles that are trapped in the circulating flow. Furthermore, groynes are also an obstacle for plastic particles and plastic particles larger than 1 mm may be trapped within the groyne.

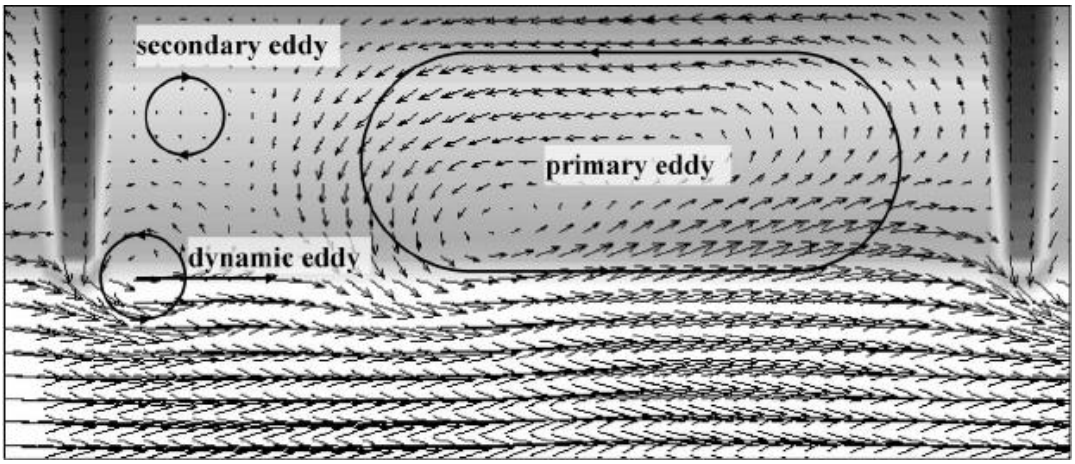

Figure 2.13 Typical depth averaged flow velocity in between two river groynes with circulation cells indicated (Yossef, 2005).

At weirs, the flow velocity is limited when the weir is closed. Under these conditions plastic particles larger than 1 mm with a tendency to fall may deposit to the bed. Rising particles may be trapped at the weir, when the weir is blocking the upper part of the water column, but not the lower part.

Bridge piles can result in accumulation of plastic particles larger than 1 mm, when they get stuck in there. In extreme cases, this can lead to blockage of a river with flooding as a result. At smaller scale, fences in floodplains may lead to accumulation of plastic particles larger than 1 mm. Any roughness increasing elements, e.g. fences, vegetation that has relatively high roughness for the flow, vegetated embankments, dunes in the main channel or smaller bedforms such as ripples have a local effect on the flow and can have an effect on the distribution of plastic particles larger than 1 mm. Trapping of plastics within the feature is only likely to occur for vegetation patches and at small scale within groynes.

Special man-made features are harbours. Especially for floating plastic particles larger than 1 mm that are directly forced by the wind, the harbours act as a trap. Depending on the wind direction, they may be blown out of a harbour, but after a longer period of time with changing wind direction the floating particles tend to accumulate in harbours. This wind effect is apparent for a simulation result where plastic particles were released at the three indicated sources in the *Noordzeekanaal* (Figure 2.14). This accumulation of plastics may occur in any side channel.

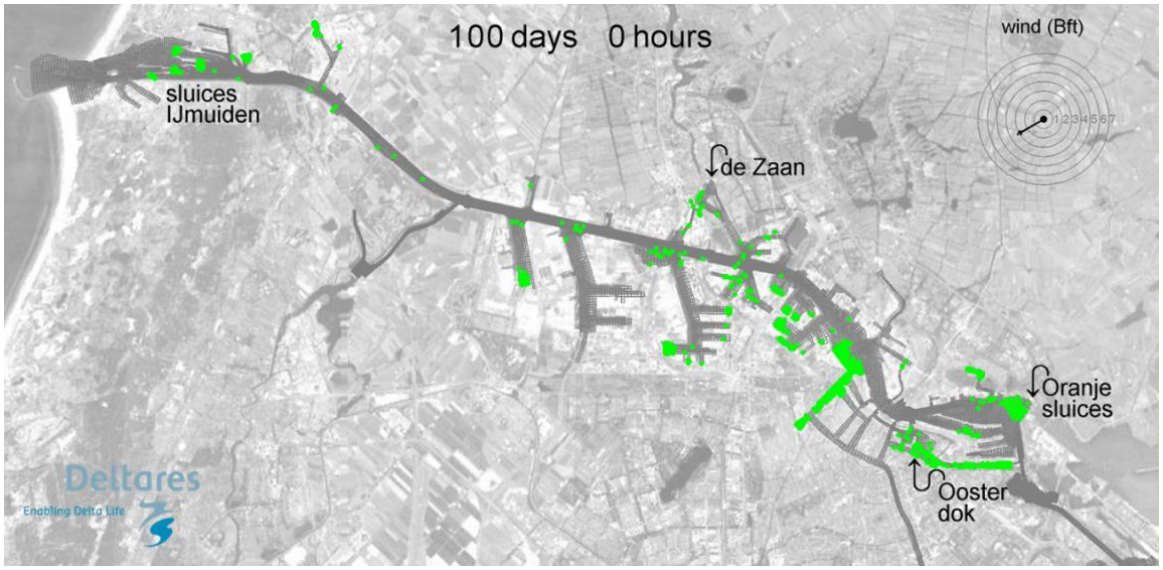

Figure 2.14 Numerical model result of floating particles in the Noordzeekanaal, showing their accumulation in harbours

2.7.3 Selection

The described planform features may have an effect on the distribution of plastics. The most direct effect is expected for bends, due to spiral flow affecting rising and falling particles in the water column.

At constructions such as weirs and groynes in the river and in harbours, plastic items may accumulate. The effect of a floodplain on the distribution of plastics can be substantial, especially when the floodplain starts to inundate and material including plastic litter is transported from the floodplain to the river. The other planform features may temporarily have a large effect on the distribution of either rising of falling plastic particles larger than 1 mm.

However, we expect that they have a smaller effect than river planform features mentioned earlier in this paragraph.

2.8 Forcings

2.8.1 General

The large-scale planform geometry and smaller scale external factors determine the bed level within a river reach. The forcings on a river reach determine the water level and flow velocity and their spatial and temporal distribution, which control for example deposition and resuspension of plastic particles larger than 1 mm, and there with plastic fluxes within the cross section and plastic transport through a cross section. In turn, the planform geometry can influence the flow, for example in a river bend.

As for the planform features, we attempt to give an overview of the forcings relevant for the plastic fluxes within a river reach. At the end of the section, we select the forcings that may generally be the most important for determining the plastic flux.

2.8.2 River discharge

The first relevant forcing is the river discharge. At low river discharge, flow velocities are small and falling particles may deposit. At increasing river discharge, resuspension of deposited particles may occur. Also, plastic items stranded in the river bank and floodplains may be resuspended again at increasing river discharge.

The highest microplastic concentrations were found during the rising limb (Figure 2.15), before the discharge peak occurred for observations in the main channel of the Po river (van der Wal et al., 2015). In the other three rivers they monitored, a discharge peak did not occur during the observations. The concentration increase occurred when the floodplains of the Po river started to be inundated. It is likely that plastics deposited in the floodplain are resuspended and transported towards the main channel, from the moment onwards when water starts to flow in the floodplain. This is an explanation for the high concentration of microplastics observed the main channel during the rising limb.

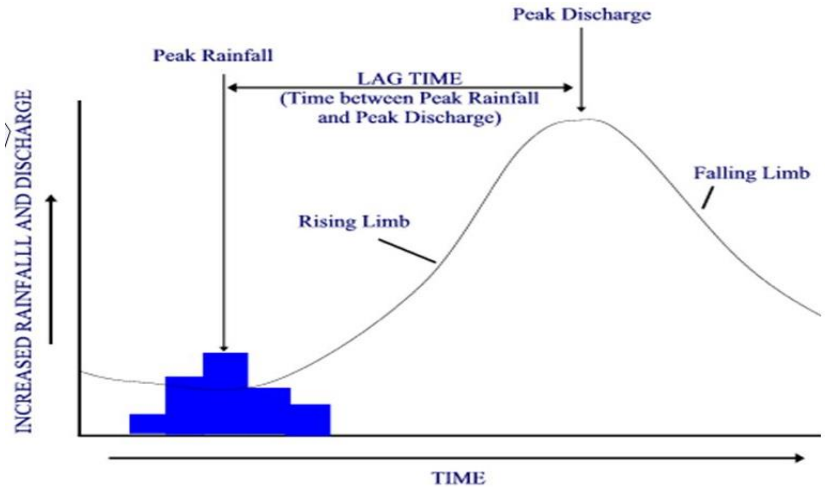

Figure 2.15 Schematic of temporal discharge variation as a result of a peak in rainfall, showing the rising limb.

During the discharge peak, most of the plastic particles that easily resuspend have already been transported from the floodplains to the main channel. In addition, assuming that the amount of plastic items discharged to the river is constant, the concentration will decrease at increasing river discharge due to dilution. Only when the number of plastic items transported to the river increases with the same factor as the river discharge, the concentration of plastic items remains the same on the longer term. Temporarily, resuspension of plastic items from the bed or bank is a source of plastic items for the water column, but this only occurs in the beginning of the river flood (the rising limb). This temporal variation during a discharge peak is expected to occur not only for microplastic particles, but also for macroplastic items.

2.8.3 Tides, wind and waves

The plastic flux in a river may vary in time and space by tides, wind and waves. Due to water level variations at sea with the tide, the flow in a river or estuary may vary with a semidiurnal of diurnal period. Within a day, flow velocity may vary. It may be landward directed for some time, which is a flood tide. During such a flood tide, plastic particles larger than 1 mm are transported landwards. This variation within a day is most pronounced during spring tide, and weakest about one week later during neap tide.

The effects of tides on the plastics concentration can be numerous. For the Rhine river, Mani et al. (2015) found that the concentration of microplastics reduced going from the non-tidal river to the tidal limit at *Zuilichem* in the *Waal*. The tidal limit is the first location as seen from the sea where the water level does not rise within a tidal period (Figure 2.16). The flood limit is situated seawards from this location. Macroplastic items transported into the tidally affected parts of a river are expected to travel seawards and landwards (during flood). As for the river water, the net movement of the items is slowly seaward directed. At a location seaward of the flood limit, a rising plastic particle is likely to pass a cross section several times before it is transported towards the sea.

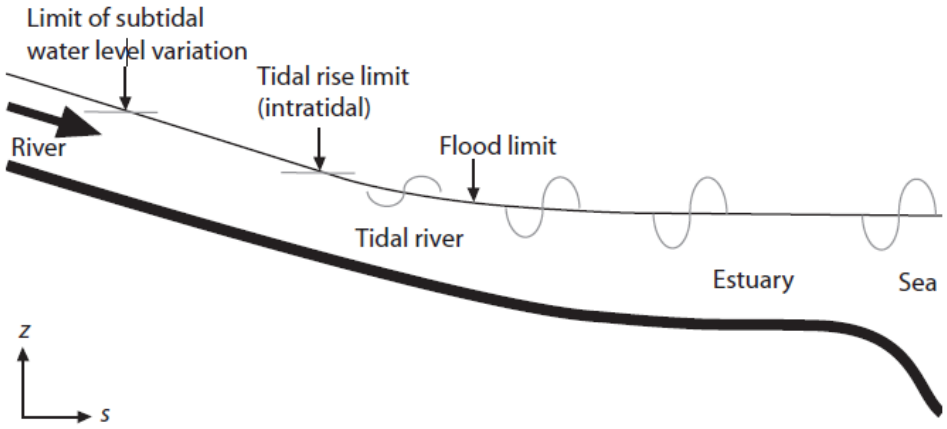

Figure 2.16 Schematic of the tidal influence in a channel that connects a river to sea (Buschman, 2011)

A landward directed wind generates a water level set up at the river channel mouth, which may temporarily reduce the net discharge to the sea. When the wind is blowing over the river, it generates a flow velocity at the surface in the direction of the wind. These effects lead to spatial variations of the flow within a river reach, which affects the plastic flux of plastic particles larger than 1 mm near the water surface. Furthermore, wind can have a direct effect on floating particles. The wind drag directly forces these particles in the downwind direction.

Another effect of the wind is that is can generate wind waves at the water surface. Wind waves tend to mix the water column and can play a role in mixing plastic particles larger than 1 mm from the top layer into the water column. Waves near the water surface can be particularly large in the mouth of a river or estuary, although waves in a river may be temporally substantial when a strong wind is directed along the channel such that the fetch covers a large part of a river reach.

2.8.4 Non-hydrodynamic

Besides the hydrodynamic forcings mentioned so far, the salinity and suspended sediment concentration are relevant, as they may interact with plastic particles larger than 1 mm. Suspended sediments may aggregate with plastic particles larger than 1 mm. An aggregated particle is likely to have a higher density than the plastic particle alone. Aggregation is most relevant for microplastics, because they have a large surface to volume ratio. This aggregation may also be affected by the salinity.

Furthermore, salinity has an effect on the vertical flow velocity profile (Figure 2.17). Whereas the flow velocity profile within a river is normally logarithmic, the net landward directed flow near the bed generated additional shear within the flow velocity profile in a reach. This gravitational circulation results in seawards flow near the surface, which enhances the flow only due to the river discharge. The strength of this gravitational circulation depends on the salt concentration at the upstream and downstream side of the estuary reach. Another consequence is that due to the density stratification mixing of the water column (e.g. by wind or bed-generated turbulence) is reduced. For rising plastic particles, the gravitational circulation enhances their seaward flow. On the contrary, particles with the tendency to fall may be transported landward to a location where the gravitational circulation has weakened. Furthermore, the fall velocity may change somewhat when the density of the surrounding water changes, due to the salinity gradients in an estuary.

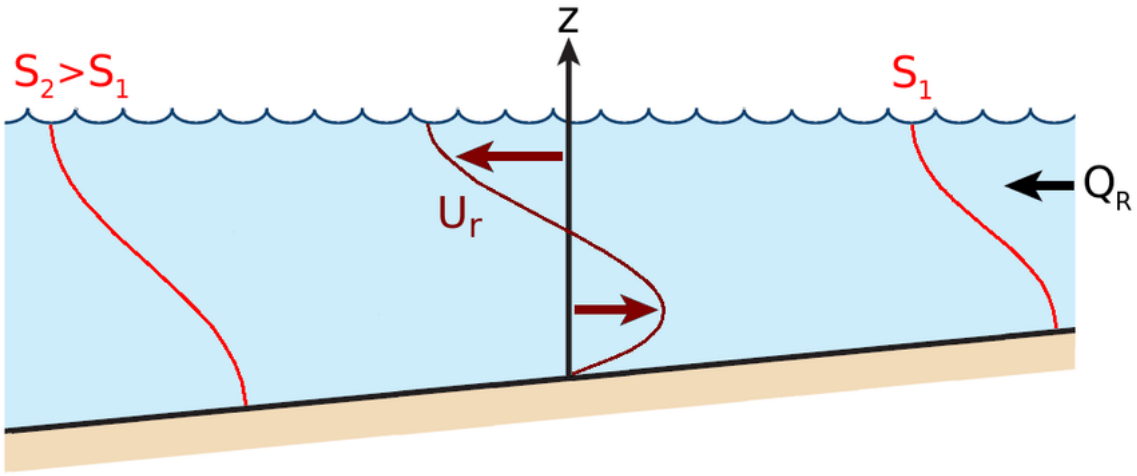

Figure 2.17 Schematic of the effect of an along channel density gradient on the flow in an estuary with the sea on the left-hand side.

2.8.5 Selection

Although all the mentioned forcings can be of importance for a river reach, river discharge and tides are considered to be dominant usually. Wind can be important for plastic particles larger than 1 mm in the top layer. Since reaches largely affected by tides are usually under the influence of salt water, selecting tides implicitly includes the salt concentration at the upstream and downstream end of the reach as well. For microplastics aggregation to sediment can be important, which is a reason to select the suspended sediment concentration of especially the finer sediment fractions. However, for the considered microplastics in between 1 and 5 mm, hetero-aggregation is not as important as for smaller particles smaller than 1 mm.

Because tides generate high flow velocity magnitudes and plastic particles may pass a location in an estuary or tidal river several times, a system to collect plastics is likely to be particularly effective in such a reach. Moreover, the sources of plastic litter are limited on the sea side of such a location.

2.9 Physical, chemical and biological processes

2.9.1 Overview

Plastic particles are transported with the flow of the water. This physical process is ‘advection’. In rivers, advection is likely to be the dominant process. Several processes (e.g. deposition and resuspension and trapping) have already been introduced in this chapter. These and other relevant physical, chemical or biological processes are defined in Table 2.5, which is based on Kooi et al. (2018) and Buschman et al. (2018).

Table 2.5 Definition of physical, chemical and biological processes that determine plastics transport

Process	**Definition**
Advection	Transport of a substance with the main flow of the water.
Mixing	Mixing of plastic particles within the water column due to turbulence, which is generated at the bed or at planform features. Turbulent mixing is modelled in WAQ and D-PART as dispersion of the plastic particles.
Fall	The falling or rising of a plastic particle, due to density differences with the surrounding water
Wind drag	Transport of floating plastic particles by wind force. Note that transport of particles with the tendency to rise (but not float) are only transported by advection with the near surface flow generated by wind.
Hetero-aggregation	Merging of plastic particles with other particles (usually sediment), which affects the density of the combined particle.
Homo-aggregation	Merging of plastic particles with other plastic particles, which affects the density of the particle.
De-aggregation	Splitting up of aggregated particles into the separate particles.
Deposition	Falling of plastic particles from the water column into the shallow sediment layer.
Stranding	Particles are left behind on the bed, when the water level is reduced, e.g. when a floodplain is drying out.
Resuspension	Release of plastics from the shallow sediment layer to the water column (e.g., due to erosion by water or wind, movement of the sediment)
Entangling	Capture of plastic particles in features that stand out into the water column (e.g. vegetation, groynes or river dunes/ripples). The plastic particles may be temporarily trapped within the feature.
Trapping by elevated roughness	Capture of plastic particles caused by increased roughness. This process reduces the flow velocity near the increased roughness, by which it has an indirect effect

Process	Definition
	on the plastic particles. Due to the low flow deposition may occur, which can be seen as trapping due to elevated roughness.
Ingestion	The take up of plastics by aquatic organisms (e.g. fish). This biological process does not represent bioaccumulation as these particles can still be excreted.
Excretion	The release of plastics by aquatic organisms to the shallow sediment layer (e.g. fish after ingestion).
Bioturbation	Disturbance of the river bed due to plants and animals (e.g., pelagic fish bottom feeding, benthic macroinvertebrates), moving plastic particles from the shallow bed layer to deeper sediment layers, and vice versa.
Burial	Disturbance of the river bed due to physical effects (e.g., dune formation, sedimentation of sand, erosion), moving plastic particles from the shallow bed layer to deeper sediment layers, and vice versa.
Biofouling	Collection of a bacterial / algal based film on plastic particle, which affects the density of the particle.
Degradation	Chemical process of mineralization of plastic particles. The overall quantity of plastic decreases due to this process.
Fragmentation	Separation of the plastic particle in smaller pieces. The overall quantity of plastic does not decrease with this process.
Anthropogenic disturbance	Disturbance and release of plastics from the shallow and deeper sediment layer due to dredging activities.

2.9.2 Macroplastic items

The processes that are relevant for the transport of macroplastic items is a subset of Table 2.5. With an effect chain model, we indicate the general importance of the processes within that subset. The effect chain model is a drastic simplification of the real-world processes found in rivers and estuaries. We chose to set the concentration of macroplastic items within the entire water column central and come back to the processes within the water column. Processes mentioned in Table 2.5, but not in the effect chain model were considered generally unimportant with respect to the processes included.

The source of macroplastic items can be either from point sources or from non-point sources such as plastic litter from an entire river bank (Figure 2.18). The variables most relevant for this concentration in the water column are the macroplastic concentrations in two sediment layers (mobile sediment layer and the deeper immobile layer), the submerged vegetation and a reservoir of biota. As can be seen from the thickness of the arrows, dominant processes are advection, wind drag (directly on the particle only for floating particles and wind drag that generates a flow in the top layer of the water column) and the net effect of resuspension and deposition of macroplastic items to the mobile sediment layer (Buschman et al., 2018). These processes have an orange colour, meaning that they are somewhat uncertain. The current literature does not provide a fully quantitative description for each of these processes. For example, it is unknown what exactly the wind drag on a floating particle with specific characteristics is.

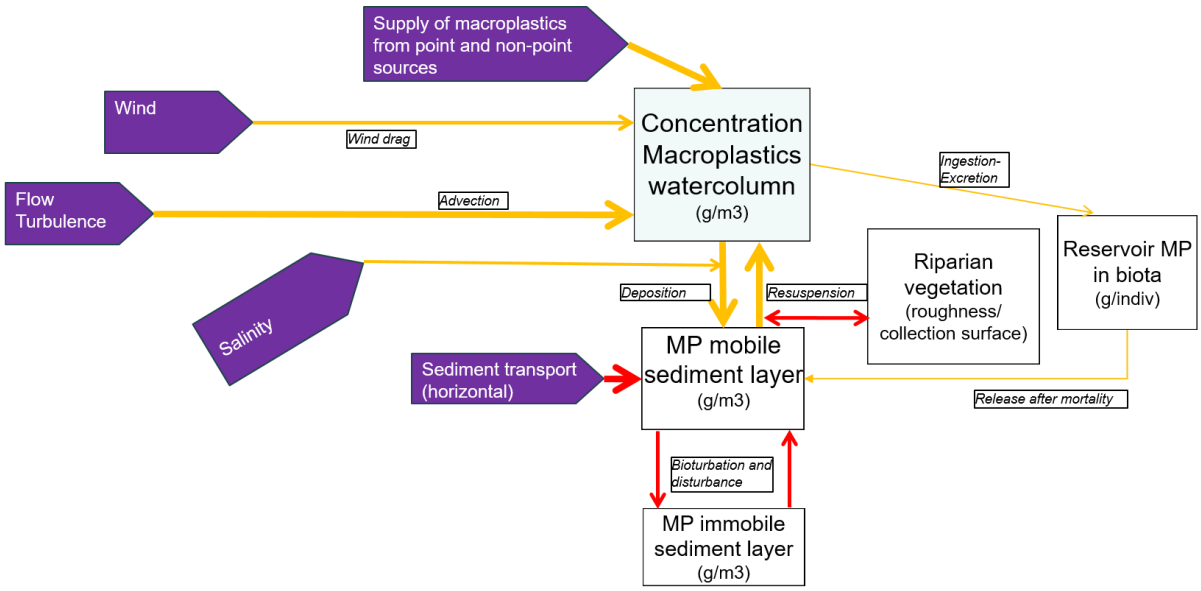

Figure 2.18 An effect chain of the forces (purple), relevant variables (boxes) and processes (arrows) affecting the concentration of macroplastic items (MP here) within the entire water column in an estuary or river; The thickness of the arrows depicts the importance of a process generally. Black arrows are reasonably certain, orange arrows are somewhat uncertain and red arrows are uncertain.

Figure 2.18 also shows the effect of salinity on deposition and resuspension by changing density. This effect of increasing buoyancy when going seawards in an estuary, is considered small. The effect of vegetation (entanglement and trapping by elevated roughness) on the resuspension and deposition of macroplastic items is not well understood. We gave it an intermediate thickness, since it may be important in some rivers. The data collected by Allseas (2018) suggests that vegetation plays a role in trapping or entangling of plastic items in vegetation and that plastic transport is elevated when vegetation is released for some reason from the river bed or river bank. The role of ingestion by biota is unimportant for macroplastic items.

The effect chain does not include the processes that determine the variation of macroplastic item concentration within the water column. Advection with the mean flow velocity profile is usually dominant. As flow velocities are usually largest near the water surface in the deepest part of the river, advection of items with the tendency to rise leads to the highest plastic flow rate. The density of particles determines whether it tends to fall or rise. Furthermore, the mixing by turbulence within the water column has an effect. The shape is important for this process of mixing. A sheet-shaped item is more likely to be mixed by turbulence than a spherical item with the same density and size. However, knowledge on the effect of shape on mixing is limited and could therefore not be considered in the modelling.

2.9.3 Microplastic particles

For microplastic particles the processes for the vertical distribution are the same as for macroplastic items, described in the previous paragraph. Advection with the mean flow is usually dominant together with the falling of the particles. Turbulent mixing plays a role in maintaining a concentration profile of microplastics vertically. In addition to the processes for macroplastic items, hetero-aggregation can be important when sediment is suspended. When a plastic particle merges with a or several sediment particles (hetero-aggregation, Table 2.5), the combined density is usually larger than the density of the plastic particle, which enhances deposition of the aggregated particle.

The effect chain for microplastic particles averaged over the entire water column (Figure 2.19) is somewhat more complex than the effect chain for the macroplastic items. Microplastic particles can be supplied to a river directly or from fragmentation of macroplastic items. Suspended sediment is added as a variable, since it is important for the hetero-aggregation. Salinity, in turn, can have the effect to enhance the hetero-aggregation in estuaries. De-aggregation by the flow is also shown, although it is generally assumed that aggregated particles remain aggregated (Buschman et al., 2018). For the rest of the effect chain, the processes and their effects on the concentration of microplastic particles are the same and have the same importance as for the macroplastic items (Figure 2.18). Biofouling can have effects on the density of a particle and may enhance aggregation by its stickiness. Because of a large surface to volume ratio, the effect of biofouling increases quickly with reducing size of plastics. Its effect and time scales for which biofouling is important are uncertain (Kooi et al., 2018). However, for the time scales that plastic particles larger than 1 mm are transported in the water column of rivers, the effect of biofouling is assumed to be limited. Therefore, biofouling is not included in the effect chain models.

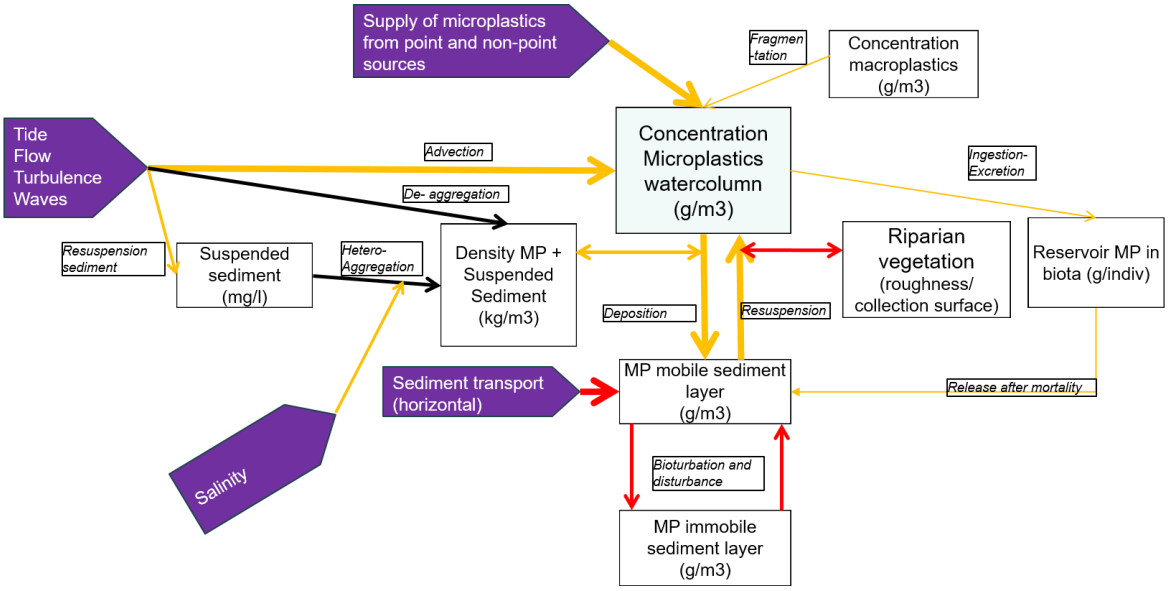

Figure 2.19 An effect chain of the forces (purple), relevant variables (boxes) and processes (arrows) affecting the concentration of microplastic particles (MP here) within the entire water column in an estuary or river; The thickness of the arrows depicts the importance of a process generally. Black arrows are reasonably certain, orange arrows are somewhat uncertain and red arrows are uncertain.

2.9.4 Selection

The dominant processes in rivers and estuaries for the transport of both macroplastic items and microplastic particles are advection, falling of the particles, mixing by turbulence, entangling within vegetation and resuspension and deposition. Only for microplastic particles, hetero-aggregation can play a role in changing the density. Only for floating macroplastic items wind drag can play a role.

2.10 Other studies modelling the transport of plastics

While plastics as a pollutant have been studied by many researchers, modelling the transport has been mainly restricted to the marine environment and to rivers as a source of plastics. A classical article on the oceanic transport patterns followed by plastic debris was published by Maximenko et al. (2011). The approach they took was that of tracing particles due to ocean currents. This led to the idea of conversion areas, gigantic gyres in several locations of the world oceans. For the purposes of this research, however, the scale is far too large to be of interest.

Recently the group Science Advice for Policy by European Academies (SAPEA, 2019) put all the knowledge together in a report, including various modelling studies. From the overview they provide several styles of modelling can be distinguished:

1. Source level studies like Schmidt et al. (2017) where the emphasis is on estimating the various sources in the region of interest. While this may not give much insight in where the plastic particles end up, such information is important for any type of realistic modelling of plastic pollution.
2. Material flow analysis and multimedia modelling: this style of modelling is characterized by attention to large scales with as little details as possible to physical, chemical or biological processes or to geographical features. The purpose is to describe the system as a whole. The approach works well for chartering the amounts of pollution and where the mass flows end up. The article by Kawecki et al. (2018) is an example. Nizzetto et al. (2016) present a spatially resolved model for the Thames river where a number of hydrological processes have been explicitly included.
3. Modelling of, notably, physical processes like hetero-aggregation and deposition can be found in Besseling et al. (2017). These researchers specifically include nanoplastics in their study, whereas Unice et al. (2019) concentrate on tyre and road wear particles (particle of comparable sizes as nanoplastics but of a different origin, even though they are all considered plastics). Critchwell and Lambrechts (2016) pay attention to the beaching of plastics via an oceanic model. Such modelling may in fact be of relevance for the beaching of plastic debris in rivers, although there the effect of wind will in general be more restricted (short fetch lengths).

The environment that is being studied also varies widely – some authors focus on the rivers themselves, though mostly as a source of plastics to the sea, whereas others focus on the seas and oceans. Rivers as water bodies of interest by themselves are seldom considered. It is also clear that microplastics (and nanoplastics) receive much more attention with respect to modelling transport and fate than do macroplastic items.

3 Verification software module D-PART

3.1 Introduction

The particle tracking model that is used in this study is based on the Delft3D-PART module, in short D-PART. D-PART simulates transport by means of a particle tracking method using the (2 or 3-dimensional) flow data from the FLOW module (Deltares, 2018b). Particle tracking allows the spatial distribution of substances to be described in a detailed spatial pattern, resolving sub-grid concentration distributions.

D-PART is considered best suited for studies over the mid-field range (200 m -- 15 km) of instantaneous or continuous releases, simulation of a plume (for example oil-spill), and modelling of the transport of substances such as salt, bacteria, rhodamine dye, oil, BOD, or other conservative or decaying chemical substances (following first-order kinetics). For this reason, the D-PART module is often referred to as the Mid-field Water Quality module. Details of the particle tracking module D-PART can be found in the relevant manual (Deltares, 2018).

The particles are followed in three dimensions over time, resulting in tracks. From the tracks, a concentration in each model cell can be obtained by calculating the mass of particles and the volume of the in a cell.

The processes are assumed to be deterministic, except for a random displacement of the particle at each time step which represents the dispersion. The particle tracking method is based on a random-walk method since the simulated behaviour is stochastic and the number of particles is limited.

The processes solved in D-PART have been verified generally, before releasing the software. In this study, a number of additional verifications were carried out to check the transport processes taken into account in D-PART for plastic particles. The general objective is to show that D-PART gives results for plastic particles as expected. The first five checks can be verified by a comparison to analytical solutions, whereas the two last verifications can only be verified by expert judgement.

PART includes the following processes, which are tested in this study:

- Advection and dispersion;
- Rising and falling;
- Deposition and erosion;
- Stranding of floating particles;
- Transport due to wind (wind friction).

3.2 Verify advection and falling/rising velocity

3.2.1 Objectives

The objective of this verification is to show that the combination of advection due to transport with the flow and falling/rising of particles is calculated correctly.

Rising and falling can be specified in the model by using a constant fall velocity, but it can also be calculated using the Stokes velocity (equation 2.1; see also Section 5.2.1). Both implementations are verified.

3.2.2 Falling and rising particles

3.2.2.1 Hydrodynamic model setup

The particle tracking model is driven by a flow model (Delft3D-FLOW) of a straight channel of 20km long and 400m wide, based on a computational grid with a horizontal resolution of 20 m (longitudinal) by 5 m (across). A constant depth is assumed of 8m and the model is set up with 10 equidistant layers. One layer has therefore a thickness of 0.8 m.

The discharge through the channel is forced at 1200 m^3/s. The flow velocity is forced to be constant over the cross section and vertical. Suppressing the usual logarithmic profile enables that the transport of the particles can be checked analytically. With the given cross section and discharge, this gives a flow velocity of 0.375 m/s.

3.2.2.2 Implementation of advection in D-PART and model setup

A schematic overview of the particle tracking model setup is shown in Figure 3.1.

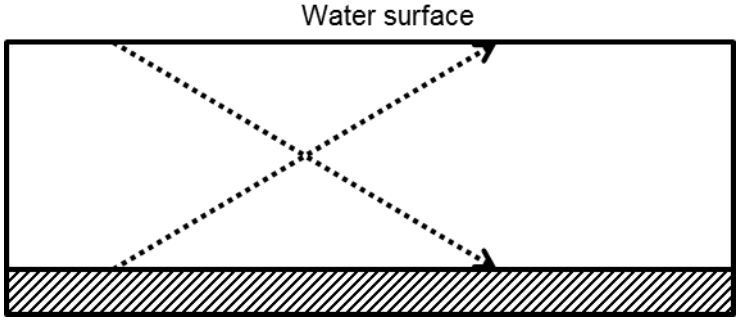

Figure 3.1 Schematic overview of the combined effect of advection due to flow velocities and falling/rising of particles in D-PART (side view along the river)

Two sets of particles are used, one with a falling and the second with a rising velocity. The falling particles are introduced in the surface layer and the rising particles are introduced in the layer near the bed. The introduction of particles in the model consists of a continuous discharge. For this verification, the horizontal and vertical dispersion coefficients are set to 0. The transport of the particles is a combination of current and falling speed and should therefore be a straight line, without deviations.

The constant falling and rising speed was arbitrarily set at 0.001 m/s. Other values for the falling and rising speed were not investigate since it is assumed that such a validation against theoretical derived values will hold for all values of settling and rising and that the transport due to settling has been implemented correctly and agrees with the theory.

3.2.2.3 Results for particles with constant fall velocity

The particle tracks of the verifications using falling particles are shown in Figure 3.2.

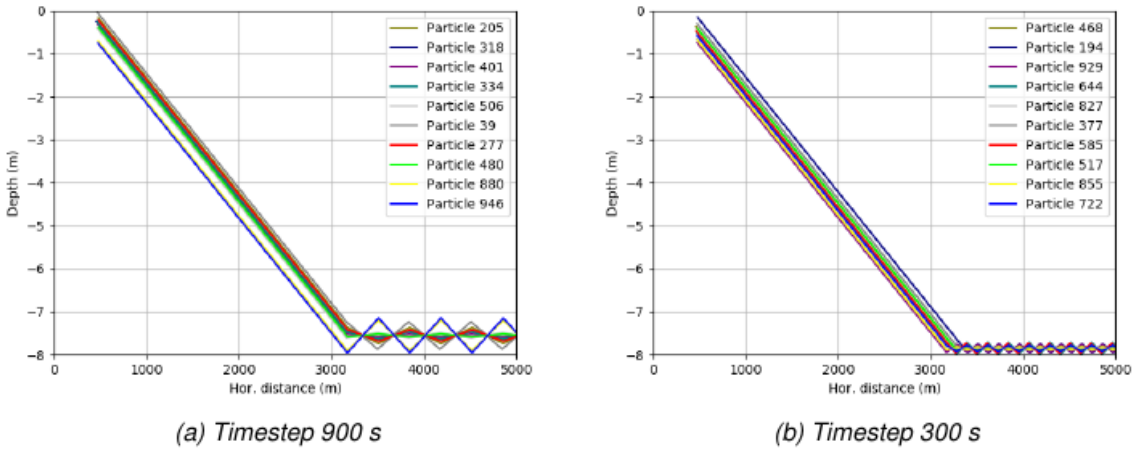

(a) Timestep 900 s (b) Timestep 300 s

Figure 3.2 Tracks of falling particles with a constant falling speed

The figure shows that the model particles settle about 6.75 m vertically over a distance of 2500 m in the horizontal. With a flow velocity of 0.375 m/s and a fall velocity of 0.001 m/s a vertical distance of 6.75 m is covered in 6750 s. In the horizontal this means a distance of 6750 * 0.375 = 2500 m, which is the horizontal distance that the particles need to cover 6.75 m in the vertical, as shown in Figure 3.2.

Figure 3.2 also shows the effect of the timestep on the movement of the particle near the bed. What can be seen is the so-called bouncing of the particle when it hits the bed. This means that when the particle's vertical velocity is such that it will hit the bed within one timestep, then it will bounce so that the total distance covered is as expected. Since the deposition process is switched off (i.e. particles will not settle on the bed, but remain in suspension to allow continuation of the horizontal transport along the bed) the bouncing is required for numerical reasons. With a larger time step, the distance travelled will be larger. The vertical distance travelled for a timestep of 300s is 3 times as small as for 900s, and this factor of 3 is also seen in the two figures (a) and (b) of Figure 3.2. If a bouncing particle remains with the same layer then the timestep is not an issue, but if the particle bounces into another layer, then essentially the timestep should be reduced. When dealing with macro-plastics then it may be argued that bouncing should not occur, in particular for larger settling or rising velocities. In that case the option of 'no bouncing' can be used. Vertical dispersion will still be active, but near the bed will only point upwards. With small settling speeds, compared to the vertical dispersion, a concentration gradient should develop with the highest concentrations near the bed. Without bouncing the concentrations near the bed (for falling particles) will be higher than with bouncing switched off.

What also can be noted in Figure 3.2 is that the release point of the particles varies in the vertical. This is because the particle in the model is released in layer one, which is the surface layer, but the actual vertical position within layer one is determined randomly over that layer. For each particle a random number between 0 and 1 will determine the relative vertical position of that particle. Since the model has 10 vertical layers, each layer is 0.8 m thick, which means that the particles are release between 0 and 0.8 m below the surface. This is also confirmed in the figures.

3.2.2.4 *Result for particles with a constant rising velocity*

When the fall velocity is negative (in this verification -0.001 m/s) the figure should show the same characteristics and the same velocity as with the sinking particles. With buoyant particles, they move away from near the bed towards the surface with the same reflection from the surface boundary. This is confirmed in Figure 3.3.

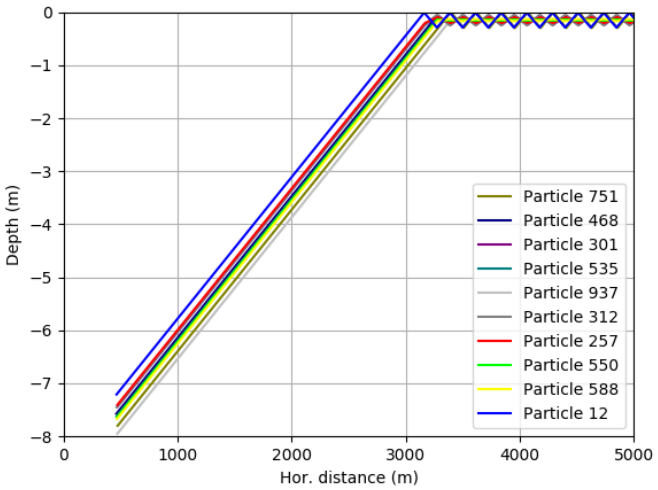

Figure 3.3 Rising of buoyant particles

3.2.2.5 *Results for fall velocity derived from Stokes law*

The D-PART model can also calculate falling velocities from Stokes law and the verification here is to verify the implementation of this calculation. The actual falling velocities that are used in the model are based on the Stokes' fall velocity. Stokes fall velocity is a simple description of falling. In the turbulent region, the linear relationship between the velocity and the density difference and the projected surface area no longer holds, and these relationships become non-linear.

Using Stokes and the Corey Shape Factor (equation 2.2) lead to examples of varying falling velocities as shown in Table 3.1 for a range of sizes, densities and shape factors.

Table 3.1 Fall velocity as a function of density, size and shape factor, assuming a water density of 1000 kg/m^3

Size (m)	Density (kg/m^3)	Fall velocity (S=1) (m/s)	Fall velocity (S=0.05) (m/s)
0.001	920	-0.04	-0.002
0.001	980	-0.01	-0.0005
0.001	1040	0.02	0.001
0.001	1100	0.05	0.003
0.002	920	-0.17	-0.009
0.002	980	-0.04	-0.002
0.002	1040	0.09	0.004
0.002	1100	0.22	0.011
0.005	920	-1	-0.05
0.005	980	-0.27	-0.014
0.005	1040	0.54	0.003
0.005	1100	1.36	0.068
0.025	920	-27.3	-1.37

0.025	980	-6.81	-0.341
0.025	1040	13.6	0.681
0.025	1100	34.1	1.7
0.500	920	-11000	-545
0.500	980	-2725	-136.3
0.500	1040	5450	272.5
0.500	1100	14000	700

A fall velocity of 0.01 m/s (10 mm/s) will result in falling over a depth of 8 m (similar to the depths in the Nieuwe Maas; Figure 5.3) in less than 30 minutes and can therefore be considered high. The falling velocities of Table 3.1 are very high, particularly for particles larger than a few mm, indicating that the shape value will be crucial, and for the software module verification the shape factor will also need to be shown to have been implemented correctly, hence a shape factor of 0.1 will also be used in the verifications.

When applying the Stokes' law to calculate the falling velocity, characteristics of the particle is used as well as the fluid density. To verify that the Stokes velocity has been implemented correctly, a settling velocity can be calculated theoretically and checked against the model.

For this verification an example was used with particles with characteristics given in Table 3.2.

Table 3.2 Particle parameters for software module verification - Stokes velocity

Description	Value
Density (kg/m^3	999.0
Shape factor	0.1
Diameter (mm)	0.001
Stokes velocity (m/s)	0.00005

The fluid density was set at 1000kg/m^3. The result of this simulation is shown in Figure 3.4. The figure shows a limited amount of randomly selected particles and dispersion was switched off to allow direct comparison.

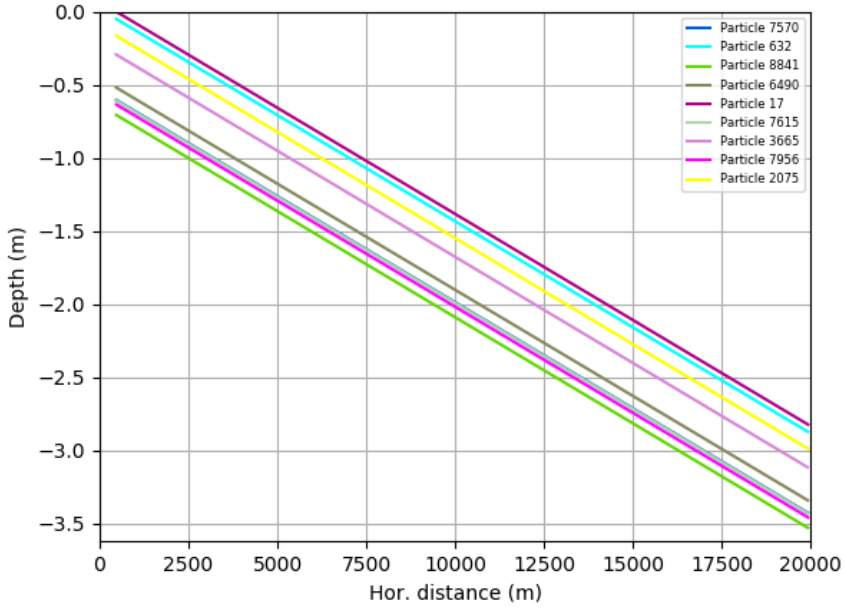

Figure 3.4 Falling with Stokes velocity

The derived Stokes velocity (including the shape factor of 0.1 and assuming a dynamic viscosity of water of $1.002 \cdot 10^{-3}$ Pa·s) is $5.44 \cdot 10^{-5}$ m/s. The model output generates a falling speed of $5.44 \cdot 10^{-5}$ m/s, equal to theoretical derived falling. With this falling speed, a vertical falling of 2 m takes 36800 sec. In the horizontal, with a current speed of 0.375 m/s, this equates to approximately 13700 m, which is the distance that can also be derived from Figure 3.4.

3.2.3 Conclusion of falling and rising

From the verifications in this section, it can be concluded that advection and falling/rising has been implemented correctly in D-PART. For high rising/settling velocities bouncing will limit the timestep. For macro plastics bouncing can be switched off to allow accumulation of plastics near the bed (or surface).

3.3 Verify effect of wind friction at surface on transport

3.3.1 Objectives

In D-PART, particles can float and when they float the transport is subject to both advection by flow and by wind drag directly on the particle. This verification is to verify the implementation of the effect of the wind friction on the transport of the particles.

3.3.2 Implementation of advection in D-PART and model setup

The effect of the wind friction on the advection of floating particles is based on a linear dependency of the speed of the particle on the wind. This is implemented in D-PART according to equation:

$$\overrightarrow{u_p} = C_{wd} \cdot (\overrightarrow{V_w} - \overrightarrow{V_f}) \tag{3.1}$$

With $\overrightarrow{u_p}$ the resulting particle velocity due to the wind. The friction factor (C_{wd}) acts on the vector difference between the wind ($\overrightarrow{V_w}$) and the flow velocity ($\overrightarrow{V_f}$). In the special case that

flow velocity and wind have the same velocity in the same direction then the particle will be advected with exactly that velocity. When the water is still, a particle will get a resulting horizontal velocity in the direction of the wind at a speed controlled by the wind and the friction factor. When the water is flowing, the particle velocity is the sum of both the flow velocity vector and the particle velocity due to the wind.

For this verification the same hydrodynamic model was used as in Section 3.2 and the wind friction was set at 3%. A current of 0.375 m/s can be counteracted by a wind speed from the opposing direction of (12.5-0.375) = 12.125 m/s at which point the floating particle will remain stagnant.

3.3.3 Results

Figure 3.5 shows the starting position of the particles and the final position 2 days after release.

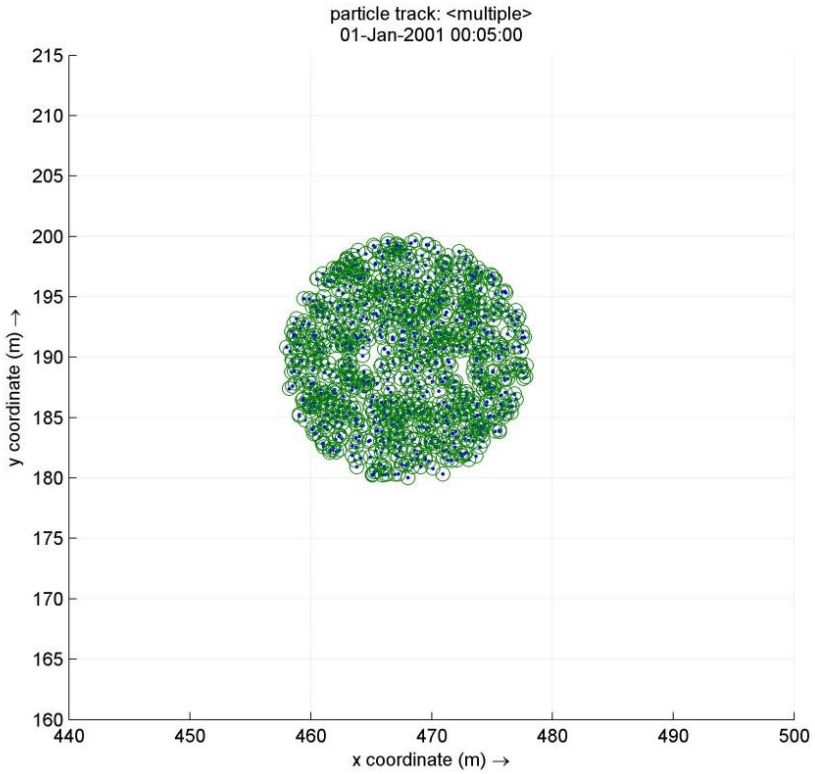

Figure 3.5 Verification of wind friction (3% with current of 0.375 m/s and wind speed of 12.125 m/s) – blue is the starting position and green circles the end position (no dispersion), seen from the top

Since the effect of the current on the transport is exactly balanced by the effect of the wind, it can be seen that, as expected, the particles remain in the same position. The size of the patch of particles also remains as it is since the dispersion coefficients are set to 0. It can therefore be concluded that the wind friction and the effect of the wind on the advection of the floating particles have been implemented correctly.

3.3.4 Conclusion of wind friction and transport of floating particles.

From the verifications in this section, it can be concluded that the effect of wind friction on the advection of floating particles has been implemented correctly in D-PART.

3.4 Verify horizontal dispersion process

3.4.1 Objectives

The objective of this verification is to show that the horizontal dispersion process has been implemented correctly in D-PART.

3.4.2 Implementation in D-PART and model setup

The dispersive step is calculated independently from the advection. Dispersion in both the horizontal and the vertical direction is based on a random walk setting one “dispersive step” per timestep. The direction is selected randomly. For each timestep the dispersive step distance for each individual particle in the model is selected randomly from a range between 0 and a maximum step (Deltares, 2018).

The *maximum* displacement of each particle for each time-step is :

$$\Delta S = \sqrt{6 \cdot D \cdot \Delta t} \tag{2.1}$$

With D the dispersion coefficient (m^2/s) and Δt the timestep in seconds.

For the verifications a uniform flow of 0.375 m/s, a dispersion coefficient of common value of 1 m^2/s and a timestep of 300 seconds were used.

3.4.3 Results

With the given dispersion coefficient and timestep the maximum displacement of a particle for each timestep is 42.4 m. Figure 3.6 below shows the expected horizontal displacement (in both x and y direction) after 1 and 2 timesteps after release. It is noted here that the shape of the distribution after step 1 is a square, buts shows as a rectangle since Figure 3.6 has a different horizontal and vertical scale. In fact the horizontal dispersion in along and across direction are equal. The center point per time step is changing in horizontal direction with 112.5 m as a result of the time step and the uniform flow velocity.

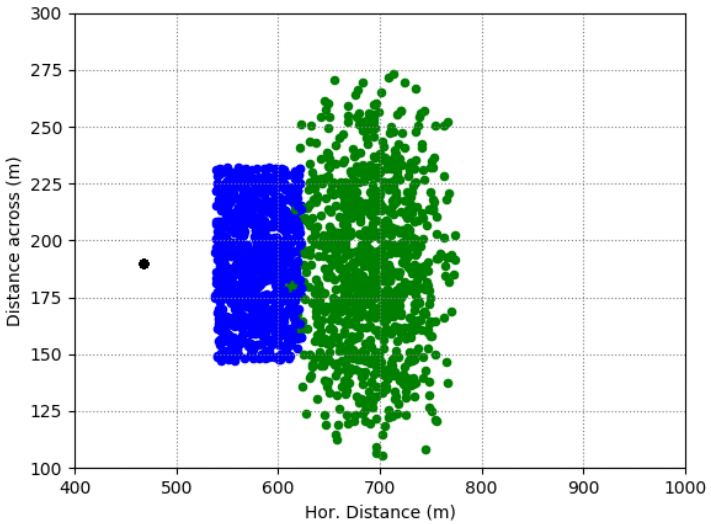

Figure 3.6 Horizontal position of particles after 0 (black), 1 (blue) and 2 (green) timesteps

Due to dispersion and a point source, a circular shape would be expected, a rectangular distribution is observed shortly after particle release. The reason for the rectangular distribution is that in D-PART the displacement in the x and y direction are set independently. Within a few timesteps the effect of this becomes insignificant. This is shown in Figure 3.7 with two distributions, one directly after release and the second 30 minutes after release. The distribution is nearly circular, considering the stochastic nature of the horizontal dispersion process and the limited number of particles (1000).

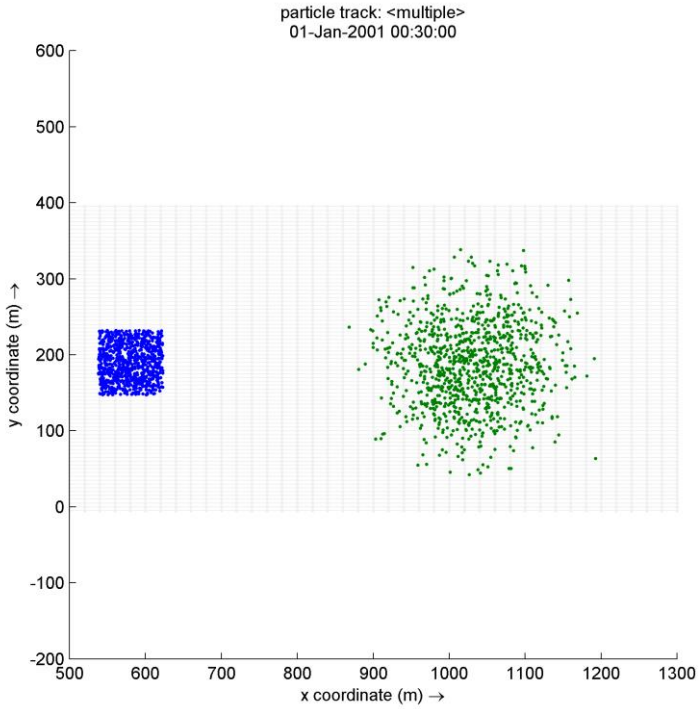

Figure 3.7 Horizontal position of particles shortly after release (blue) and after 30 minutes after release (green)

3.4.4 Conclusion

From the verifications can be concluded that the dispersion process has been implemented correctly, considering the stochastic nature of the process in D-PART.

Please note that in the modelling process the value of the dispersion parameter will be selected in relation to the grid resolution of the hydrodynamic model (dispersion parameter describes essentially the effect of sub-grid turbulence and eddies) and whether a 2D or 3D model is used. For 3D models, the dispersion coefficient is in the order of 0.1-1 m^2/s but for a 2D model it can be 1-2 orders of magnitude larger.

3.5 Verify vertical dispersion process

3.5.1 Objective

The objective of this verification is to show that the vertical dispersion process has been implemented correctly in D-PART.

3.5.2 Implementation in D-PART and model setup

In the vertical the same principles hold as for the horizontal dispersion and the implementation in the vertical is also described by Equation 1.2.
The vertical dispersion coefficient is significantly lower than the horizontal dispersion coefficient (Deltares, 2018b) and normally in the order of 10^{-3} to 10^{-6} m^2/s.

The same flow conditions (uniform velocity of 0.375 m/s) was used for this verification. For a dispersion coefficient of 10^{-3} the maximum displacement in the vertical per timestep is about 1.3 m. Examining the results shown in Figure 3.8 the maximum extent of the particles increases by 1.3 m per timestep, as expected.

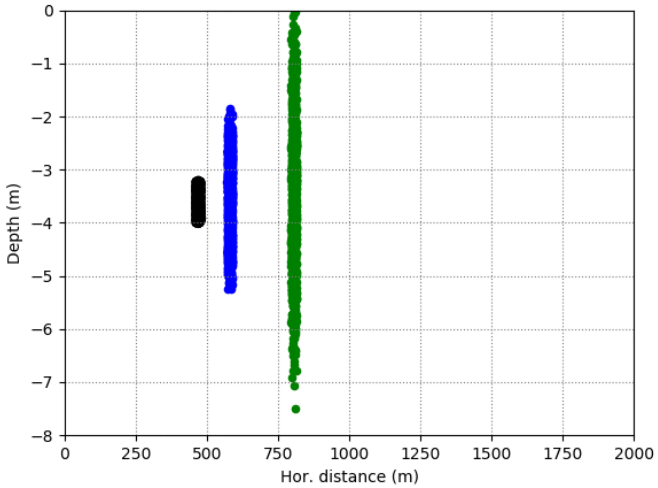

Figure 3.8 Vertical dispersion of particles. Black is the initial discharge distribution, blue is the distribution after 1 timestep and green the distribution after 3 timesteps

For this verification the horizontal dispersion was switched off to allow a good analysis of the vertical particle distribution. With no horizontal dispersion the distribution of the particles is strictly vertical, hence the particles in the figure appear stacked in the vertical only.

3.5.3 Conclusion

It is concluded that the vertical dispersion process is implemented correctly.

3.6 Verify dispersion process for a bank discharge

3.6.1 Objective

The objective of this verification is to show that the dispersion from a continuous discharge from a bank agrees with analytical solutions.

3.6.2 Implementation in D-PART and model setup

To verify a bank discharge with an analytical solution, it is required that the hydrodynamics does not include a horizontal or vertical velocity gradient, because with such a velocity gradient, an analytical solution is not available. Hence the same model setup as for the verification of the horizontal and vertical dispersion process is used, i.e. a flow velocity of 0.375 m/s. The same horizontal dispersion coefficient of 1 m^2/s is used, with the vertical dispersion set to 0.

The discharge is located on one bank and discharges in the top layer. The particles have a neutral buoyancy which means that without a vertical diffusion process they will remain in the top layer. The simulation of the particles is therefore equivalent to 2D horizontal transport (depth averaged) without a horizontal or vertical velocity gradient. The situation is outlined in the figure below.

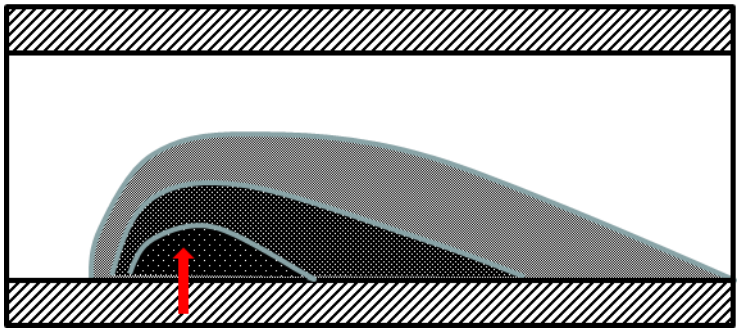

Figure 3.9 Verification outline of horizontal dispersion for an example bank discharge

The discharge is defined as 100 kg/s. D-PART does not add a discharge volume.

For the situation shown here, an analytical solution exists and follows from:

$$C(x,y) = A \cdot \exp\left\{\frac{u}{2D}x\right\} \cdot K0\left\{\frac{u}{2D}\sqrt{x^2+y^2}\right\} \tag{3.3}$$

where A is the discharge flux over the depth (kg/m/s) and is calculated by:

$$A = \frac{L}{\pi DH} \tag{3.4}$$

With L is the discharge load and H the depth(2D). The flow velocity is denoted by *u*, *x* and *y* represent the longitudinal and lateral co-ordinates respectively (m), *D* is the horizontal dispersion coefficient and *K0* the modified Bessel function with order 0. These equations were implemented in an Excel spreadsheet so that the results can be compared with the modelled results.

3.6.3 Results

The analytical and simulated results of the verification are shown in Figure 3.10 by dots and continuous patches, respectively. It can be seen that the theoretical distribution of the plume agrees with the modelled distribution.

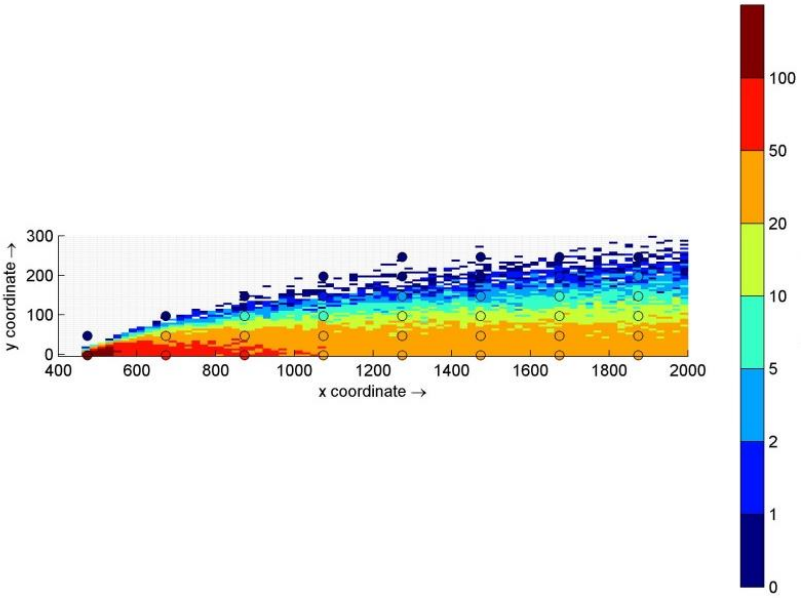

Figure 3.10 Horizontal concentration distribution after a continuous bank discharge, compared with a theoretical solution (markers), colour scale for both are the same. Concentrations less than 0.01 kg/m^3 are not shown.

3.6.4 Conclusion

It can be concluded that the horizontal dispersion/advection process in D-PART has been implemented correctly.

3.7 Verify transport in a river bend

3.7.1 Objectives

The objective of the verification is to demonstrate that transport in a riverine bend with secondary flow gives a good description of reality. An analytical result cannot be derived, so the result will only be compared with expected behaviour.

3.7.2 Implementation in D-PART and model setup

Hydrodynamic model

For this verification a hydrodynamic model was set up. The general dimension (length/width and depth) of the model was similar as the model that was used for earlier verifications (see section 3.2.2.1). The overall length of the channel is around 20km and 400m wide with the same grid resolution as before. The depth was again set at 8 m. The bend of the river was modelled to the actual bend in the *Nieuwe Maas*, around the location where Allseas carried out their monitoring. The hydrodynamic model is therefore a schematic model of this area.

The model was forced with a constant water level of 0 m at the western boundary and a constant inflowing discharge of 1200 m^3/s on the eastern boundary, distributed uniform over the cross section. The model outline is shown in Figure 3.11.

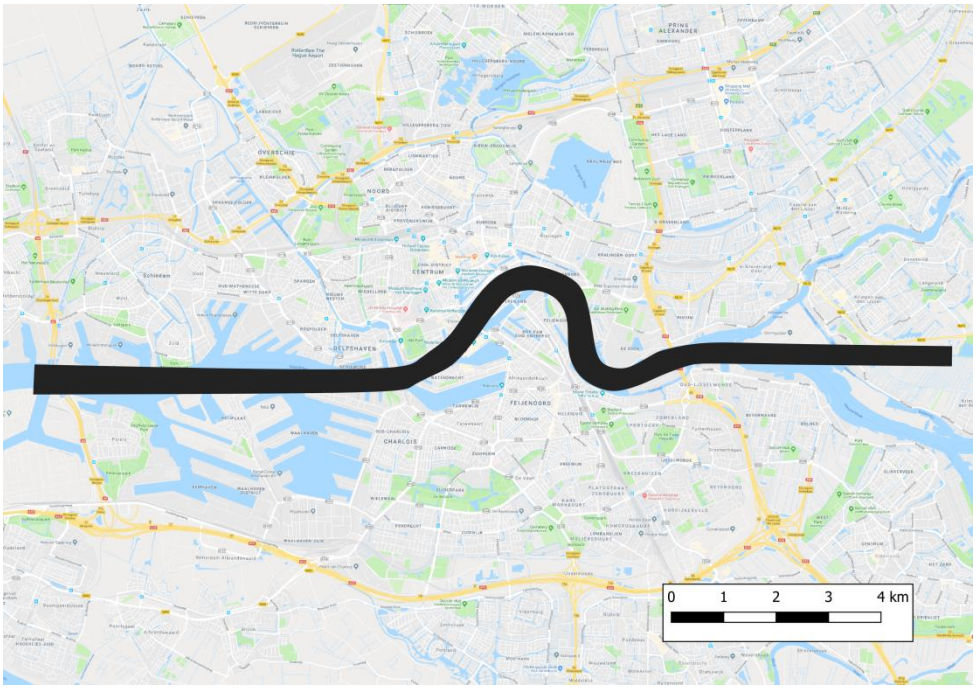

Figure 3.11 Model extent of the river bend mapped on the Nieuwe Maas in Rotterdam

The radius of the bend is approximately 1000 m, which defines the main characteristic of the bend.

The resolution of the grid is 10 m (about 5 m in width and 20 m along the river) although it does vary slightly throughout the grid. The model was run for a period of 2 days (48 hours).

The particle model setup
Three cases were set up with a variation in the falling:

- Buoyant particles with a rising velocity of -0.0001 m/s (equals about -8 m/d)
- Falling particles with a fall velocity of 0.0001 m/s
- Neutral buoyant particles (fall velocity of 0)

A continuous discharge was defined upstream of the river bend and the model uses 14000 particles. The discharge was distributed across the river. It is assumed here that the buoyant particles have already reached near surface region and the falling particles the near bed region when they enter the model. Hence, the buoyant particles were released in the surface layer and the sinking particles in the lowest layer near the bed. The neutral particles were also released in the surface layer to allow an investigation of cross-directional current (such as secondary flows in bends). All discharges start at t=0. For these three cases the horizontal dispersion was set to 1 m^2/s and the vertical dispersion was switched off to ensure that the particles are only transported in the vertical due to vertical flows and not by dispersion. The choice of zero vertical dispersion was made to highlight a weak vertical transport due to the secondary flow, if present.

In the river bend a weak secondary flow is expected to develop, due to the relatively wide river bend. Particles may follow that flow path. For higher rising speeds the generally low secondary flow may be insufficient to drag the particle down, whereas neutral particles may be transported downwards with this secondary flow. Furthermore, it is expected that velocities near the bed are lower than near the surface and that this can be seen in the simulated particle tracks.

3.7.3 Results

Vertical velocity gradient

Figure 3.12 below shows the position of the particles around the point where the main plume passes the bend, 4 hours into the release. The black dots represent the particles that are buoyant, whilst the red dots represent the sinking particles.

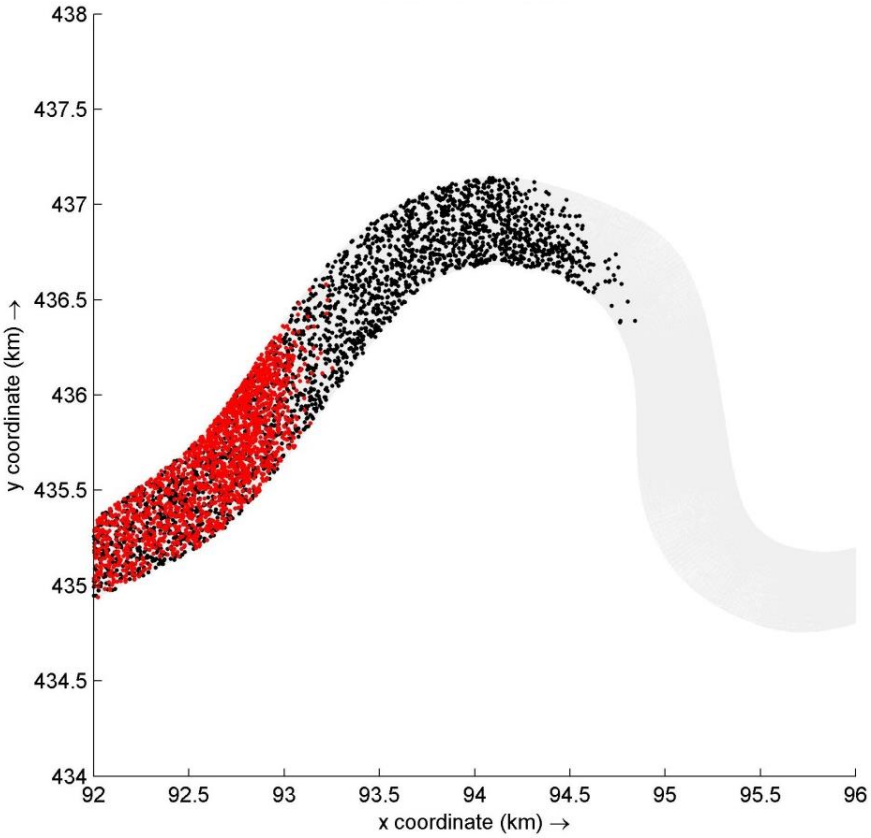

Figure 3.12 Position of particles 4 hour after start of the release, with black buoyant and red sinking particles

The figure clearly indicates that the buoyant particles that are near the surface travel faster than the sinking particles that are near the bed. This verification shows therefore that the velocity gradient is well represented in the model and that the particle tracking model takes account of this vertical velocity gradient. It can also be seen that in the cross section current velocities are higher on the inside of the main bend which causes the particles to travel faster.

Figure 3.13 and Figure 3.15 show a 3-dimensional presentation of a number of randomly selected particle tracks travelling around the river bend.

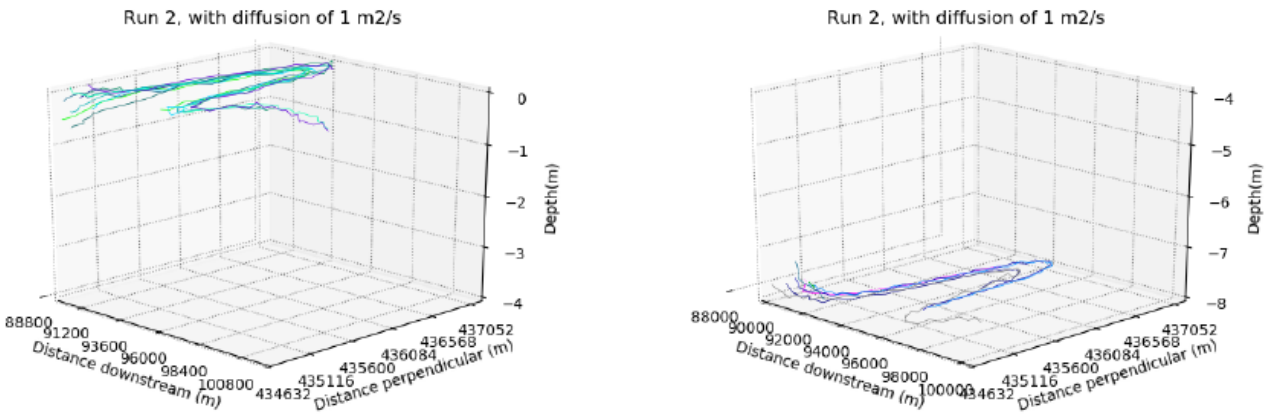

Figure 3.13 Verification of particle transport in a river bend for particles with the tendency to rise (left) and the tendency to sink (right)

The hydrodynamic model does show a secondary current pattern, such as shown in Figure 3.14. At the water surface a flow is present from the inner to the outer bank, which causes a vertical flow downwards near the outer bank (0-50 m along cross section in Figure 3.14). Near the bed the secondary flow is directed towards the inner bank.

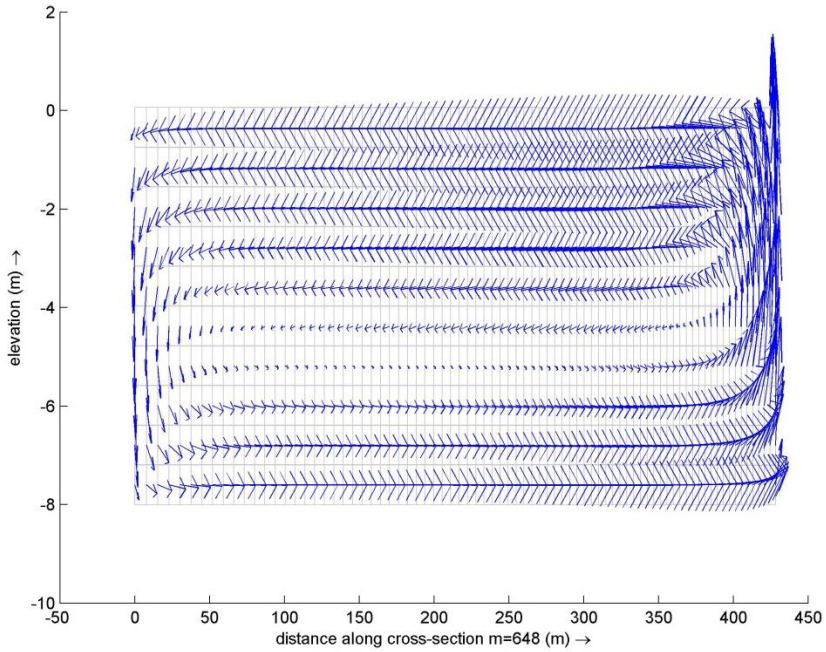

Figure 3.14 Cross sectional current velocities in the river bend (0 is on the north side, 425 on the south side)

For floating and sinking particles (Figure 3.13) the effect of secondary flow in a bend cannot be seen. For the model verification with neutral buoyant particles, the effect can be seen (Figure 3.15).

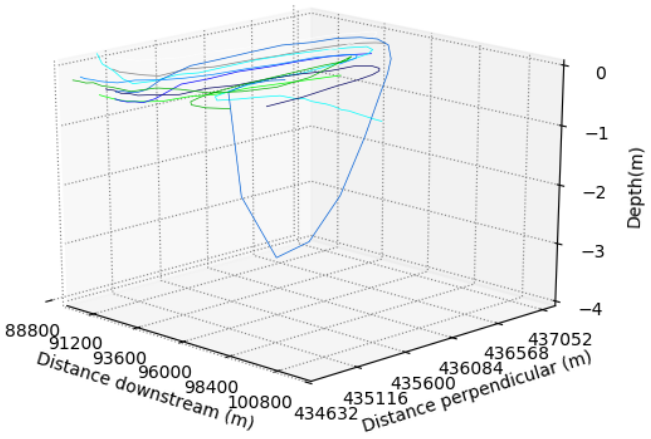

Figure 3.15 Verification of particle transport with neutral buoyancy in a river bend

The effect is of the secondary flow is very small and is only visible when the particle is at the outer edge of the bend. After an investigation of the flow model results, it was observed that the vertical flow velocity that is generated is relatively small, compared to the horizontal flow velocity of approximately 0.375 m/s. The effect is small due to the actual conditions in the river bend (combination of flow velocity, curvature of the bend and bathymetry). When particles have a negative or positive buoyancy forcing them towards the water surface of river bed, they cannot be transported downwards or upwards, because the advection due to the vertical flow velocity is smaller than the falling or rising velocity. The transport of the neutral buoyant particles show that the flow model does reproduce the secondary flow and that the particle model will follow these flow lines.

3.7.4 Conclusion

With the shown examples, it is concluded that the effect of the secondary flow can be modelled with the combination of FLOW and D-PART. In the verification case the effect is small and could only be visualized for neutrally buoyant particles.
In addition, the model simulates the velocity gradient that exists due to the bottom shear well. This results in particles travelling faster near the surface compared to near the bed.

3.8 Verify floodplain deposition, resuspension and transport

3.8.1 Objective

The objective of the verification is to verify the processes when a floodplain is present. This floodplain can flood from time to time and the model should represent the relevant processes as expected. In particular the focus is on the processes:

- Falling of suspended particles;
- Stranding of floating particles;
- Deposition and resuspension and advection on the floodplain.

3.8.2 Implementation in D-PART and model setup

Hydrodynamic model

The hydrodynamic model is an extension of the straight channel model (400m wide) as presented in Section 3.2.2.1. The extension was a floodplain with a width of 500 m. A detail of the bed level is shown in Figure 3.16. The main channel bed level was set at -8 m and the floodplain at -1 m.

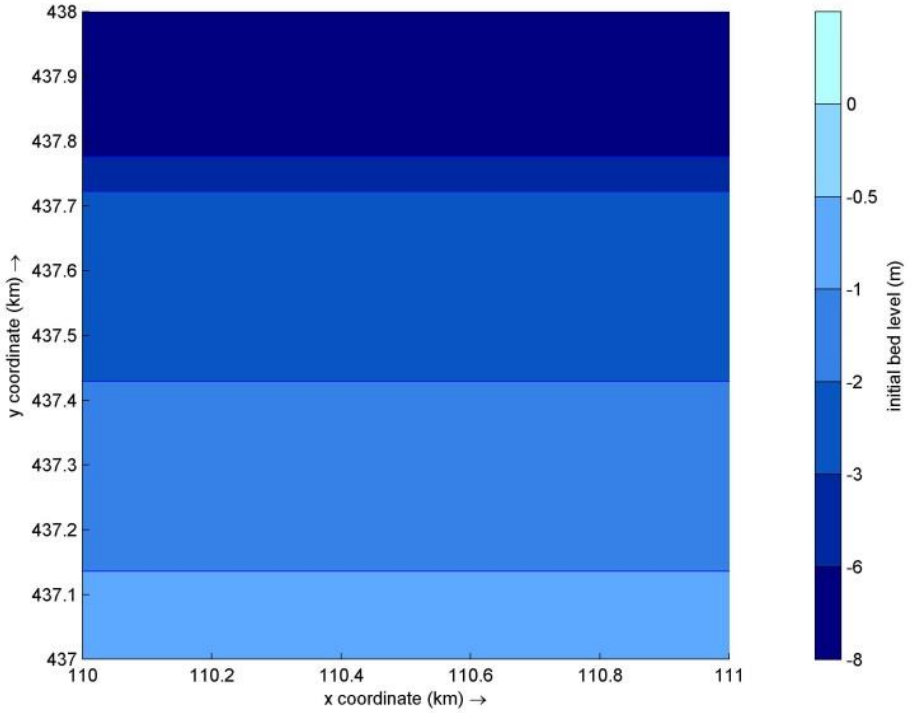

Figure 3.16 Model bathymetry (detail)

For this verification the model was set up to calculate the flow velocities, meaning that a vertical velocity gradient resulted. The model also includes a groyne (fig 3.17) of about 50 m into the main channel to allow a verification on the processes around such a feature. Behind the groyne, a flow circulation may develop that may capture litter that flows down from the river. As with the previous models, the grid cell size of the model is 5 m across and 20 m along the river.

The hydrodynamics have been set up in such a way that the model starts with just a summer discharge (defined by 1200 m^3/s) with water levels below that of the floodplain (Figure 3.17). This is followed by a period of an increase in discharge, up to 8000 m^3/s with water levels higher than the bed of the floodplain followed by a reduced discharge with water levels again reducing again to levels below the bed level of the floodplain to verify stranding of particles in the floodplain. Finally, another flood period follows to verify processes that deal with resuspension of particles.

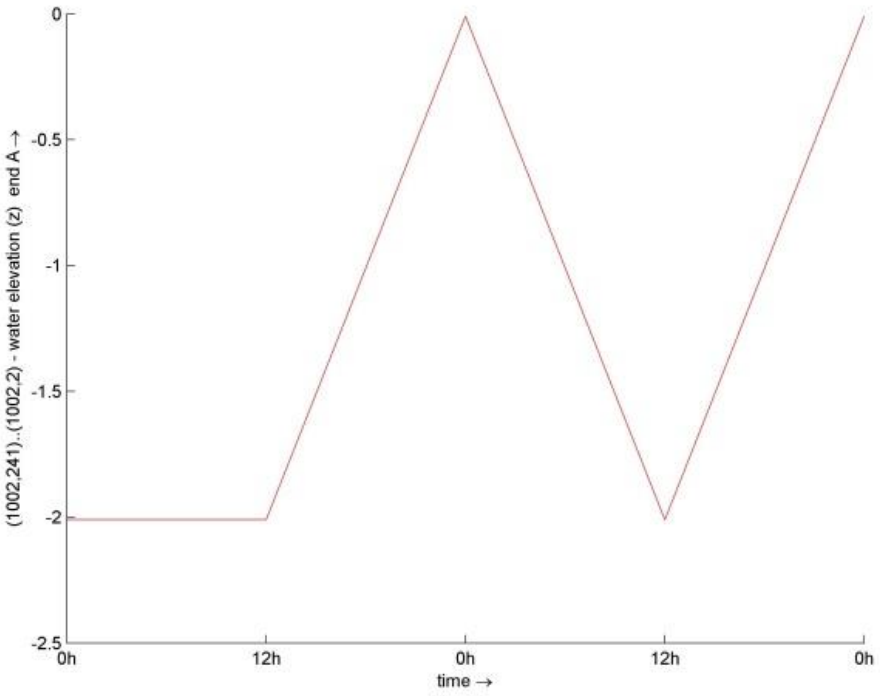

Figure 3.17 Water level variation as a function of time for the flooding/drying verification

The particle model setup

The release of the particles is the same as for the other verifications, which means a continuous discharge focussing on particles with a very low fall velocity and floating particles. Sinking particles were not considered here since they settle relatively quickly in the main channel and do not have a real mechanism to be transported onto the floodplain. Furthermore, this model application does not include wind. For the floating particles deposition was not switched on, whereas this process was switched on for the particles with low fall velocity.

In D-PART particles can deposit on a floodplain, due to the following three mechanisms:

- Due to drying cells: When cells on the floodplain run dry and the deposition process has been switched off, the particles remain in suspension but cannot be transported back to the river and are therefore stranded. The reason is that even when the model considers a cell to be dry, a certain amount of water will remain in the cell (with a water depth of a few centimetres). As a result, the particles cannot be transported out of that cell even if actual deposition has been switched off. Hence, the deposition is definitive.

- Due to deposition: With deposition process switched on, particles can only settle on the bed with a fall velocity pointed towards the bed. The particles remain there provided the critical shear stress for erosion is not exceeded. If the shear stress exceeds that of the critical shear stress for erosion, all particles in that grid cell will erode. There is no limitation of the erosion flux. For rising particles and neutrally buoyant particles, deposition cannot occur even with the deposition process switched on. When a cell becomes dry with these latter particles contained in them, they will not be advected (the cell is considered dry so there is no water movement) but they will remain in suspension.
- Due to stranding of floating particles: floating particles cannot deposit to the bed, except when a specific wetting/drying process has been switched on. With that switch set to on, floating particles will stick to the bed when the flow model considers a cell to be dry. Once the particle has stuck to the bed due to this process, it cannot refloat if the cell refloods.

3.8.3 Results

Hydrodynamic model

The hydrodynamic model behaves as expected. The floodplain floods during high water and becomes dry during the low discharge period. The groyne that is included in the model leads to the development of eddies (see Figure 3.18).

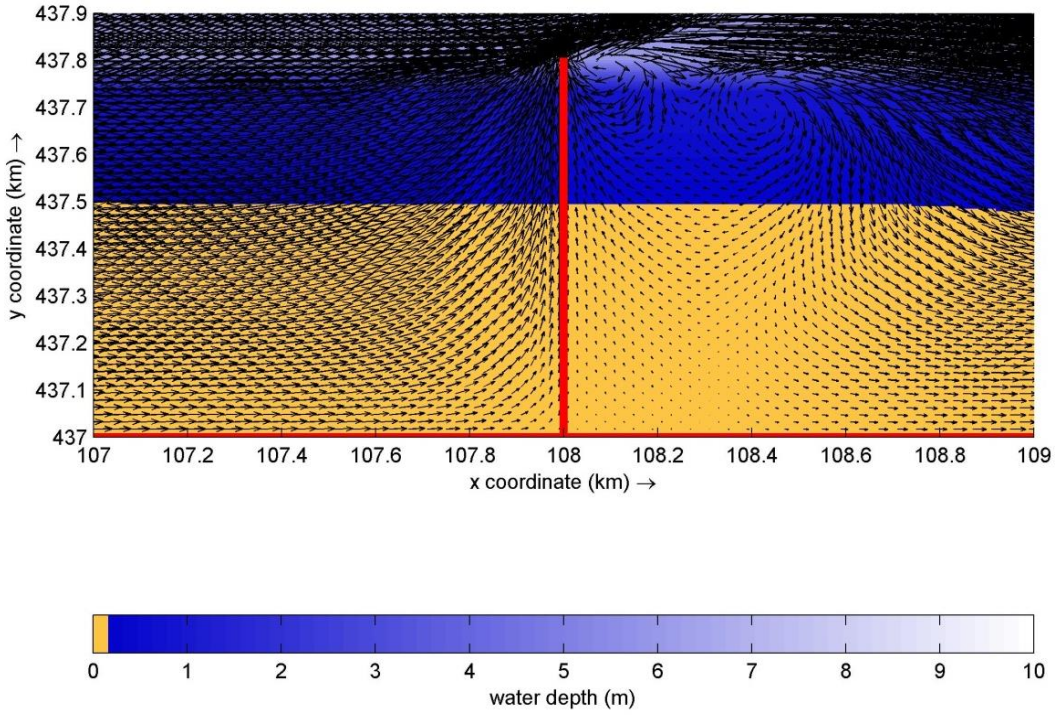

Figure 3.18 Flow velocities around a groyne during high discharge of 8000m³/s

An investigation into the nature of the eddy it is noted that the location and size of the eddy depend on the water level and flow velocities. Occasionally two eddies develop temporarily (Figure 3.18).

D-PART model

The floating plastic particles follow the flow lines of the eddy as expected (Figure 3.19).

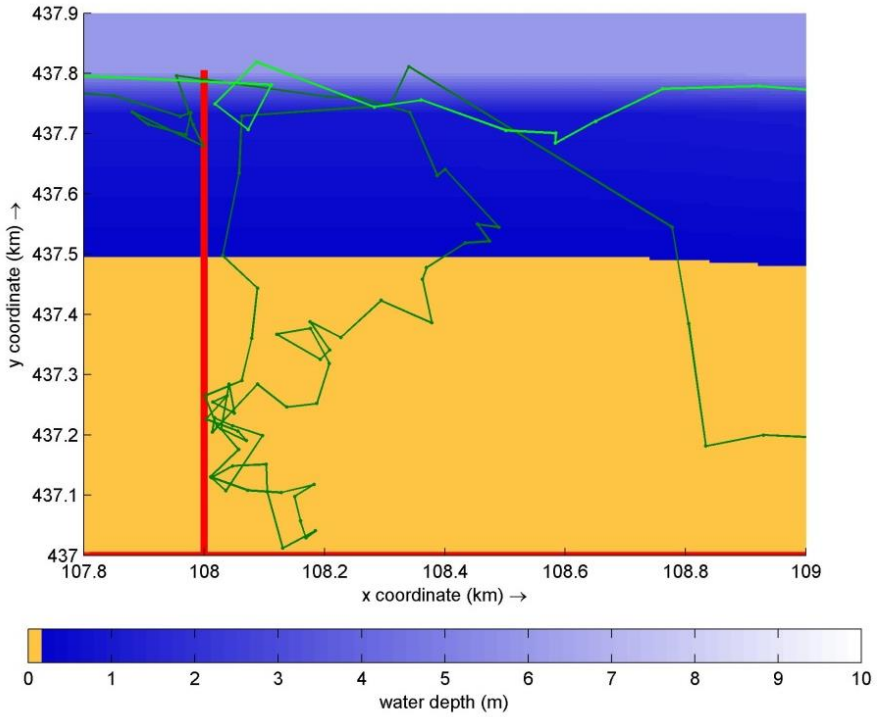

Figure 3.19 Example particle tracks with a groyne and floodplain; Flow is from left to right.

Figure 3.19 shows essentially two cases. The first particle is travelling along a relatively small eddy and is then caught by the main current and moves further downstream. The second particle is also caught in an eddy during the flood period and travels onto the floodplain where it remains for a little while after which it moves downstream. During this period there is a flow velocity towards the floodplain and the particle travels with this flow velocity onto the floodplain. The accuracy of the particle tracks will be affected by the timestep.

Stranding of floating particles

One verification involved floating particles travelling downstream and stranding on the drying floodplain. In this verification floating particles were introduced in the model with the option of sticking to drying flats switched on, which is a separate process from deposition of suspended particles (not used for floating particles). From the results it can be seen that the (macro) plastic particles stick to drying flats (represented by the black dots, Figure 3.20).

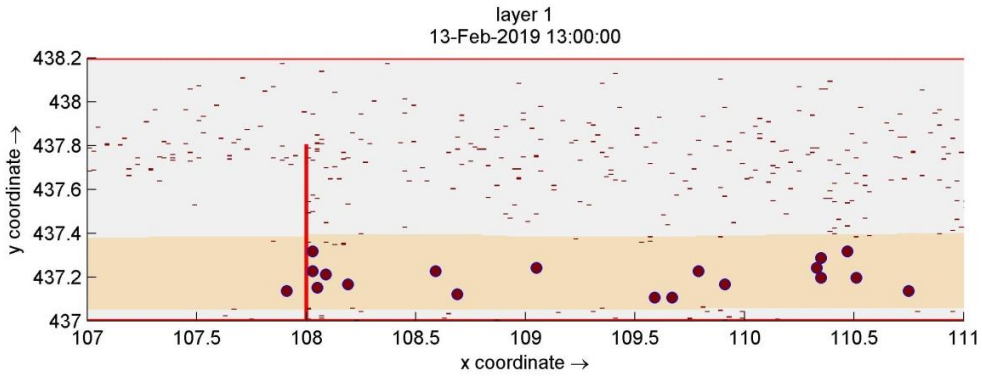

Figure 3.20 Example particles sticking to a drying floodplain,

The floating particles appear to deposit mainly behind the groyne rather than before. The majority of the particles that enter the floodplain during the flood are transported back to the main channel and a relatively few are left behind and settle on the floodplain. This is because the floodplain has a small bed gradient towards the main channel and flow velocities are directed towards the main channel when water levels drop transporting the main fraction of the floating particles back to the main stream before the floodplain becomes dry and the particles stick to the dry cell.

It is noted that the drying flats process that is implemented in D-PART does not allow refloating particles, i.e. once they stick to the bed, they remain there. Hence if this process is to be included in the actual simulations, then the use of this model will provide areas where the plastics may stick to the bed, but not provide information on where the plastics will go when the floodplain is reflooded. Only when the 'tracer' module is used this process can be switched on by using suitable critical shear stresses for setting and resuspension. But this module does not allow wind forcing to act on the particles themselves, but only via the hydrodynamics. This means that the wind will need to be included in the hydrodynamic model so that the particles that are near the surface are affected by the changes in the surface flow velocity due to wind.

From this verification it can be concluded that the wetting and drying process in which floating particle can settle on the floodplain is behaves as implemented.

Deposition and resuspension of particles on a floodplain

A final test was conducted using plastics that are suspended in the water column and that have a fall velocity of 0.0001 m/s to test the deposition and resuspension process. A fall velocity is needed to activate the process. Shear stresses will drive the deposition and erosion process. The maximum shear stress (when flow velocities are at its highest around mid-tide) in the hydrodynamic model is shown in Figure 3.21.

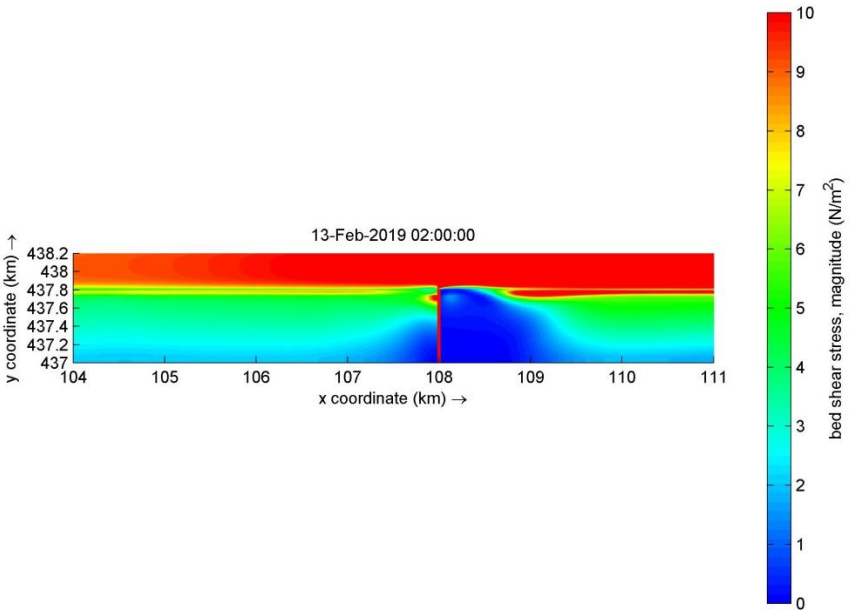

Figure 3.21 Maximum bed shear stress in the hydrodynamic model.

The highest shear stresses are in the main channel and occur towards the end of the flood. On the floodplain the shear stresses are considerably lower and in the wake of the groyne, the shear stresses are at its lowest and hence this area is most susceptible to deposition and accumulation of material.
Two runs were carried out, one with deposition only without resuspension (setting the critical shear stress for erosion to a very high value of 10 Pa with a deposition critical shear stress of 0.01 Pa) and one with critical shear stresses for both of 0.01 Pa, which gives an active deposition and erosion process. An example of the output is shown in Figure 3.22 and Figure 3.23. Shear stresses in D-PART are calculated (Deltares, 2018) using a Chézy coefficient and local velocity.

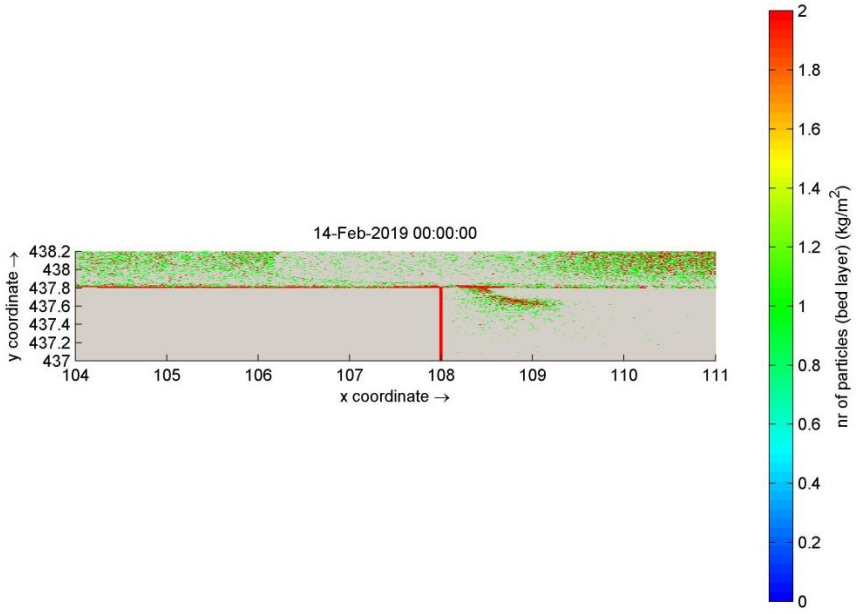

Figure 3.22 Example of particles depositing on the river bed and floodplain, with deposition only

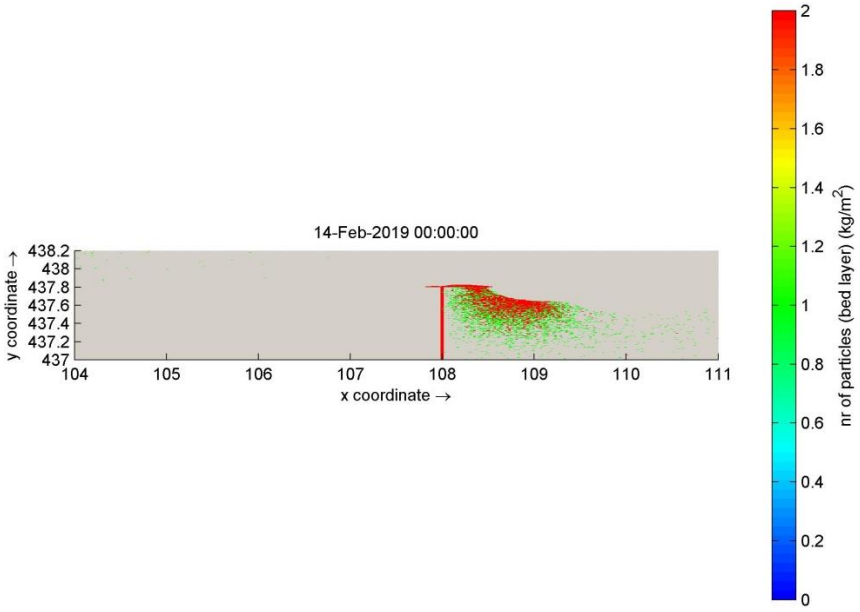

Figure 3.23 Example of particles depositing on the river bed and floodplain, with deposition and erosion

With only deposition it can be seen that deposition takes place foremost in the main channel. This occurs when shear stress is lower that the critical value. Since this happens before and after the high water, many particles will settle in the main channel and cannot be eroded. Particles do reach the floodplain and some will settle there. As expected, no erosion takes place. The distribution of the particles on the bed has a similarity of the spatial distribution of the shear stress in the hydrodynamic model, because particles remain settled when shear stress remains below the critical shear stress for erosion. In the main channel in the vicinity of the groyne shear stresses tend to be somewhat higher which is why the number of particles in that area are lower than elsewhere in the channel. Here the choice of the critical shear stress can be very sensitive.

When erosion is also active then the distribution of the particles on the bed is shown in Figure 3.23. Here the shear stress exceeds that for erosion in the main channel, hence no particles are visible there. These particles can then be transported onto the floodplain during the high water periods, which is why the amount on the floodplain is higher that without erosion. Only on the floodplain, just behind the groyne particles settle and remain there and can therefore accumulate. An overall development of the amount of settled material is shown in the figures below (Figure 3.24 and Figure 3.25), confirming the findings.

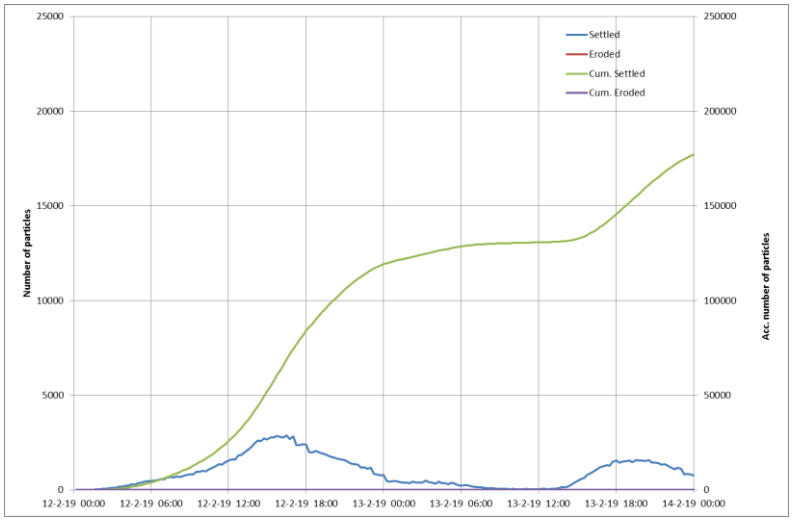

Figure 3.24 Amount (per timestep) and cumulative amount of settled material on the bed for deposition only

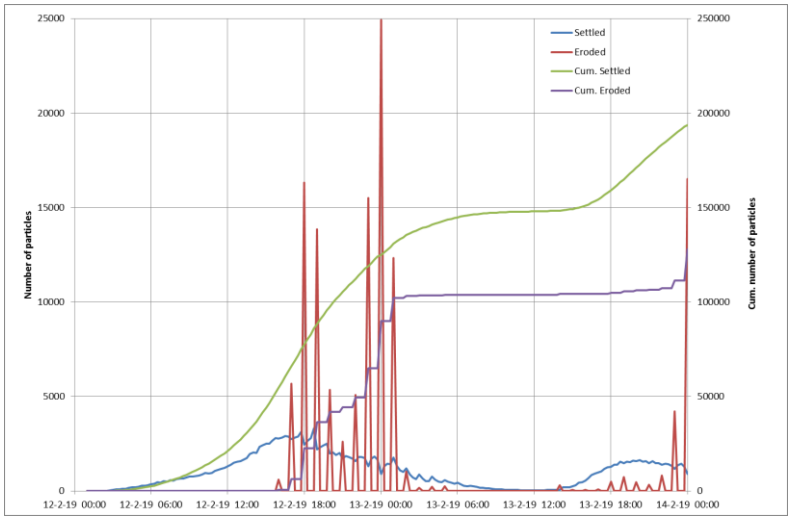

Figure 3.25 Amount (per timestep) and cumulative amount of settled and eroded material on the bed

The water levels during the shown periods are shown in Figure 3.17. In these figures high water occurs at 13-2-19 00:00 and at the end of the run. It can be seen that the material start to erode just before 18:00, when the shear stress build up and exceed the critical shear stress for erosion. This is also the reason why the deposition of material reduces at that point, because the same critical shear stress value is used for both processes. The reason for the sharp peaks in Figure 3.25 is that all particles in a grid cell are eroded when the critical shear stress in that cell exceeds the critical value. There is no flux limitation in D-PART for the erosion flux. Hence the model results agree with expectations.

3.8.4 Conclusion

Three processes that relate to the interaction with the riverbed have been investigated:

- Falling of suspended particles;
- Stranding of floating particles;
- Resuspension and advection on the floodplain.

The processes of deposition and resuspension act in the model as expected. Deposition and erosion in the D-PART model are in line with the derived maximum shear stress distribution as calculated by the FLOW model. It is noted that when erosion takes place all particles come back into suspension without a limitation of the flux, i.e. the amount released from the bed per timestep is not limited by physical processes. Since this is unrealistic, resuspension is often not included in particle tracking modelling. The functionality to model the wetting and drying and the effect this has on the transport of the plastic material, in particular in relation to the stranding on the floodplain and the possibility to refloat once water enters the floodplain again, is limited.

3.9 Overall conclusion for the verifications of D-PART for macroplastic items

The processes that are implemented in D-PART appear to have been implemented correctly and agree with the descriptions as included in the D-PART manual. The stranding of floating particles on drying cells as well as the deposition/erosion process can be used but is very sensitive to the values of the critical shear stress model parameters.

A limitation is that resuspension can be modelled only by allowing erosion of all deposited material in a cell when the shear stress is higher for a moment than the critical shear stress of the particles. This probably leads to overestimation of resuspension at those moments and underestimation after a period with the same flow condition.

A clear disadvantage of PART is that for longer simulation periods the required number of particles to be tracked can be very large (in the order of millions) and that has consequences for the run-time but especially for the memory usage.

4 Verification software module WAQ

4.1 Introduction

D-Water Quality, WAQ for short, is the general water quality module in the Delft3D suite of models (Deltares, 2018b). It has been used extensively for a wide variety of water quality problems. For the purposes of this project the process module within D-Water Quality was extended with processes specific to microplastics, as far as these are actually known.[2] The basis for this is described in an article by Unice et al. (2019). The process formulations described in the article are for tyre and road wear particles (containing both rubber and abrasive road material), but it is expected that microplastics behave in a very similar way, as the formulations describe general mechanisms, such as the falling and the aggregation of particles.

As with the particle tracking model a number of well-defined cases have been modelled to verify that the results of the model are in agreement with the a priori expectations. These cases are for a large part identical to the cases described for D-PART. For details we refer therefore to the previous chapter.

Due to the mathematical representation of the transport and processes of substances used in WAQ, namely a grid of computational cells in which the concentration is known via a single representative value only, certain physical processes of interest are difficult to represent correctly, such as the influence of wind on floating particles. Also, it is impossible to suppress dispersion or dispersion completely as a consequence of the finite size of the grid cells. The advantage however of the modelling approach is that interaction between substances, such as in this case aggregation of plastic particles and suspended sediment, can be modelled.

4.2 Verify advection and falling/rising velocity

4.2.1 Objectives

The objective of this verification is to show that combination of advection (transport of the particles by flow) and falling/rising of particles is calculated correctly.

By setting the vertical dispersion to a small value, the effect of falling or rising of the particles can be elucidated. The falling and rising velocities were set to 30 m/day and the vertical dispersion coefficient was set to $1.0 \cdot 10^{-7}$ m^2/s.

4.2.2 Model set-up

4.2.2.1 Hydrodynamic model setup

The hydrodynamic model was the same as for D-PART – see section 3.2.2.1

4.2.2.2 Implementation

For the purpose of simulating falling particles the standard process called “sedimentation of IM1” (inorganic matter, first fraction) was used with a constant falling velocity of 30 m/day or 0.34 mm/s. As the flow velocity is 0.375 m/s in the hydrodynamic model and the channel is 8 m deep, it is expected that the particles will sink to the bottom in approximately 0.27 days and travel over 8.6 km.

[2] *For this purpose D-Water Quality offers the so-called Open-PLCT approach. This extension was only used for the realistic river modelling, as the standard processes library covers the verification cases.*

The particles are supposed to fall only, no deposition onto the bottom is to occur.

To ensure that a clear pattern is shown, the boundary condition was such that only in the first three layers at the top any material would come into the system with a concentration of 1 mg/l.

4.2.2.3 *Results*

The calculation covered a long enough period to reach an equilibrium, that is, two days – the residence time for water in the model system is 0.6 days. As can be seen in the picture (Figure 4.1), the substance as released near the surface on the left side reaches the bottom around 6 to 8 km and then moves along the bottom in a fairly thin layer. The plume spreads out due to horizontal dispersion (dispersion coefficient set at 1 m^2/s) and numerical effects of the finite grid size.

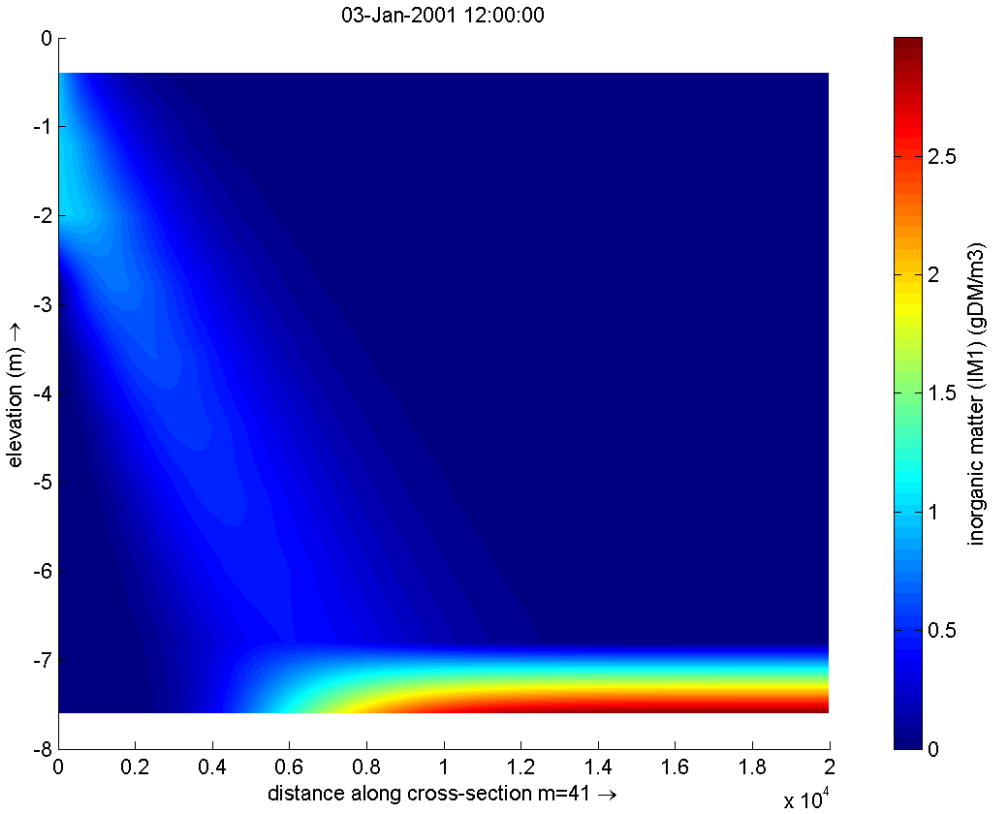

Figure 4.1 Concentration of falling particles in WAQ, cross-sectional view. The particles are released in the top-left corner and are transported along the channel, while sinking towards the bottom.

The “touchdown” occurs earlier than the 8.6 km that was predicted because the material is in fact released over a layer of 2 m, so the (mean) depth over which the particles should fall is shorter than the nominal 8 m. With this in mind a corrected estimate is (7/8)·8.6 = 7.7 km. (Note: due to artefacts in the plotting program the water column is represented as starting at 0.5 m and ending at 7.5 m, instead of the full 8 m it actually is.)

4.2.3 Rising particles with a constant velocity

By setting the fall velocity to a negative value we can simulate rising particles (particles lighter than water). This has been done based on the same hydrodynamic model. The result is shown in Figure 4.2. It is in fact the mirror image of Figure 4.1: the boundary condition was set to 1 mg/l in the lowest three layers and the particles can be seen to rise to the surface where they are subsequently transported in a thin layer to the right side of the model area.

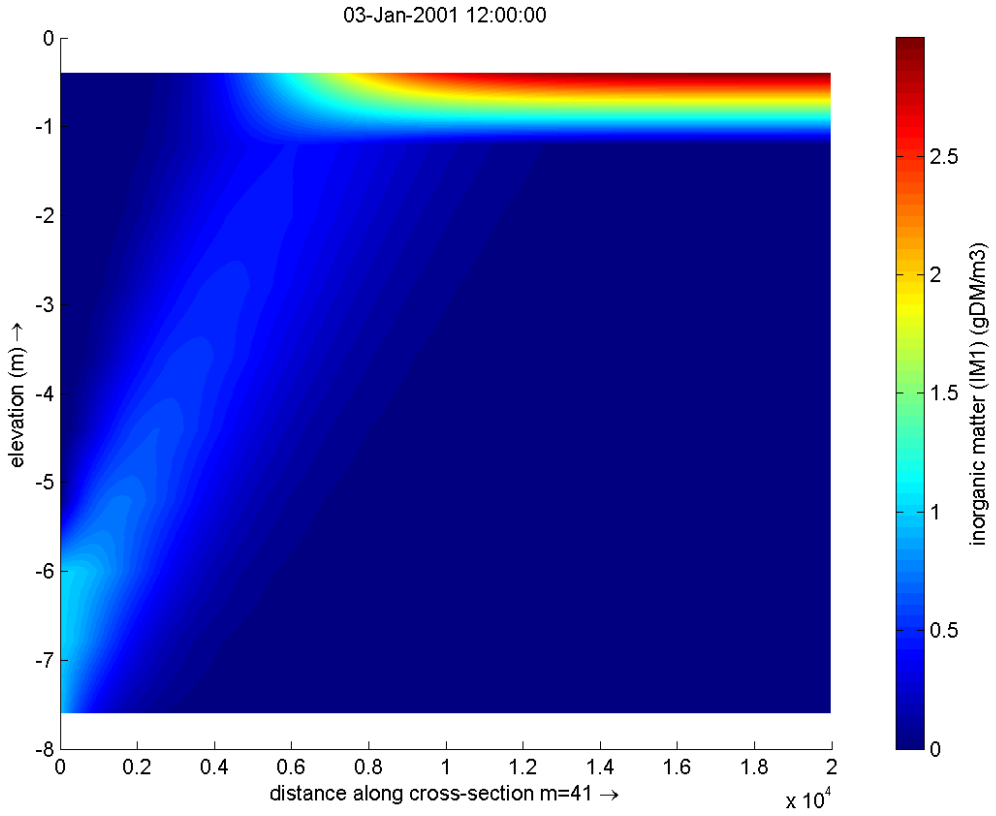

Figure 4.2 Concentration of rising particles in WAQ, cross-sectional view. The particles are released in the bottom-left corner and are transported along the channel, while rising towards the surface.

All the remarks that were made with respect to the first verification case also hold for this.

4.2.4 Conclusions regarding falling and rising

The results of the two verification cases agree with the expectations. WAQ can be used to simulate both falling and rising particles in a river system.

4.3 Verify the effect of wind friction at surface on transport

The verification case where *floating* particles are traced through the system makes no sense for WAQ, because the substance that represents the particles will always be distributed over at least one grid layer. A particle is only transported with the wind induced flow averaged over the layer. The effect of the wind directly on the particle at the very surface is not included,

This verification case has therefore not been considered for WAQ.

4.4 Verify horizontal dispersion process

Testing horizontal dispersion has been done extensively in the WAQ validation document (Deltares, 2018). In this document the numerical aspects can be found. The main conclusion is that horizontal dispersion works as expected.

4.5 Verify vertical dispersion process

Testing vertical dispersion has been done extensively in the WAQ validation document (Deltares, 2018). For this transport phenomenon the conclusion holds as for horizontal dispersion.

4.6 Verify dispersion process for a bank discharge

4.6.1 Objective

The objective of this verification is to show that the dispersion from a continuous discharge from a bank agrees with analytical solutions.

4.6.2 Implementation

The implementation is identical to that of D-PART – see section 3.6.

In this case, however, we have used a conservative substance, that is, a substance which is not involved in any processes. It is released via a continuous source at one bank of the river stretch with a rate of 100 kg/s. The source is located in the top layer.

4.6.3 Results

The concentration pattern for this verification case is shown below as a contour plot where each colour represents a concentration range.

The concentration pattern largely resembles the pattern sketched in Figure 3.9: the concentration along the x-axis decreases slowly while the substance disperses sideways.

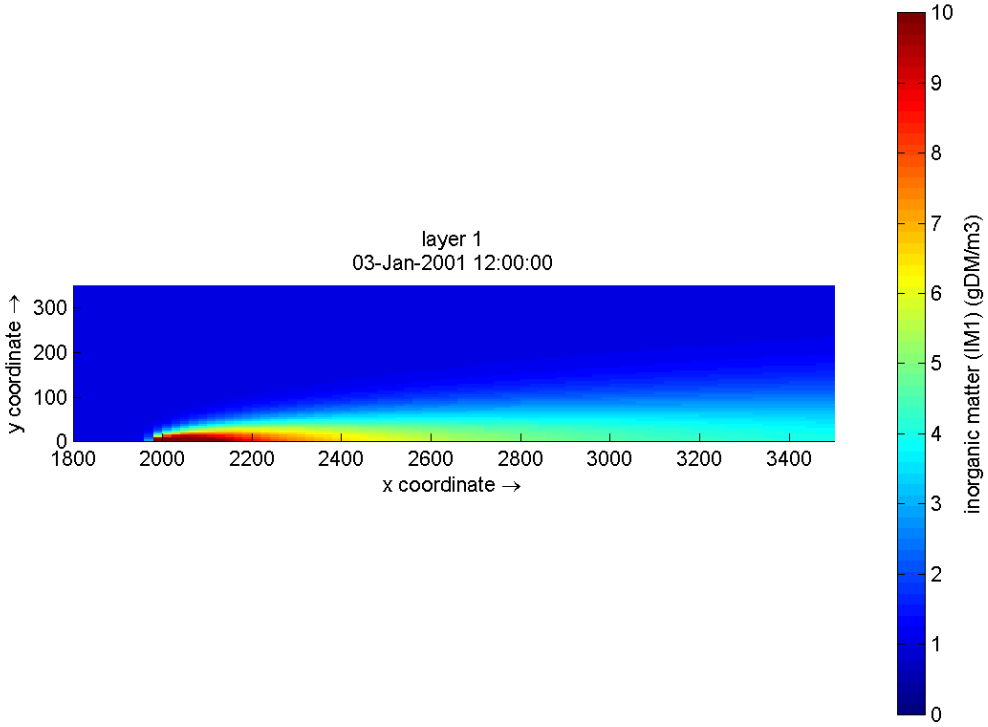

Figure 4.3 Concentration pattern resulting from a continuous source at one bank in a river. The transverse direction has been enlarged with respect to the direction along the flow to highlight the pattern (the model area is 20 km long and 500 m wide, which would result in a very narrow rectangle otherwise; the flow is from left to right).

4.6.4 Conclusion

The spreading of the substance along the flow and perpendicular to the flow is in agreement with the theoretical pattern, except that the opposite bank quickly influences the pattern, because the substance cannot spread beyond the bank. This makes a comparison with the analytical solution difficult. Similar cases with an “unconfined” spreading have been considered in the validation document (see Deltares 2018). These cases showed proper compliance to the analytical solution.

4.7 Verify transport in a river bend

The objective of this verification case is to show that secondary (spiralling) flow is taken into account in the transport calculations. For D-PART this has been done by tracing individual particles but for WAQ this is not possible, as there is nothing that can be traced in this way. An alternative might have been to use a local waste load and a very low dispersion coefficient to keep the material together within the model. This would have required a very careful selection of the waste load location and a very careful consideration of what is to be displayed.

As it is far from trivial to specify the expected results, this case has not been considered further in the context of D-Water Quality.

4.8 Verify floodplain deposition and transport

4.8.1 Objective

The objective of this verification is to verify the processes when a floodplain with a groyne is present. Such a configuration is typical for rivers in the Netherlands:

- Deposition can occur in zones in the vicinity of the groyne where a slowing-down of the flow occurs.

4.8.2 Implementation in WAQ

4.8.2.1 Hydrodynamic model

Again, the hydrodynamic model is the same as that used in the corresponding verification case for D-PART.

4.8.2.2 Water quality model

For WAQ the substances chosen to represent the situation are IM1 (inorganic matter) and IM1S1 (inorganic matter in the sediment layer on the bottom). The fall velocity was set to 0.1 m/day and the critical shear stress for deposition to 0.05 Pa. With the initial condition set to zero, the substance is transported into the system via the boundary concentration (set to 10 mg/L) only.

The hydrodynamics is dynamic in character, that is, it varies over time:

- During the first phase the water level rises to flood the plain besides the main channel
- In the second phase it falls, so that the plain becomes dry again, and then a second flood wave occurs, flooding the plain again.

Because of this, it is difficult to represent the result in a static document. Only the end result is shown.

4.8.3 Results

In the figure below, the concentration of IM1 near the surface is shown (mg/L) together with the amount of material that has deposited on the bottom (expressed as g/m^2).

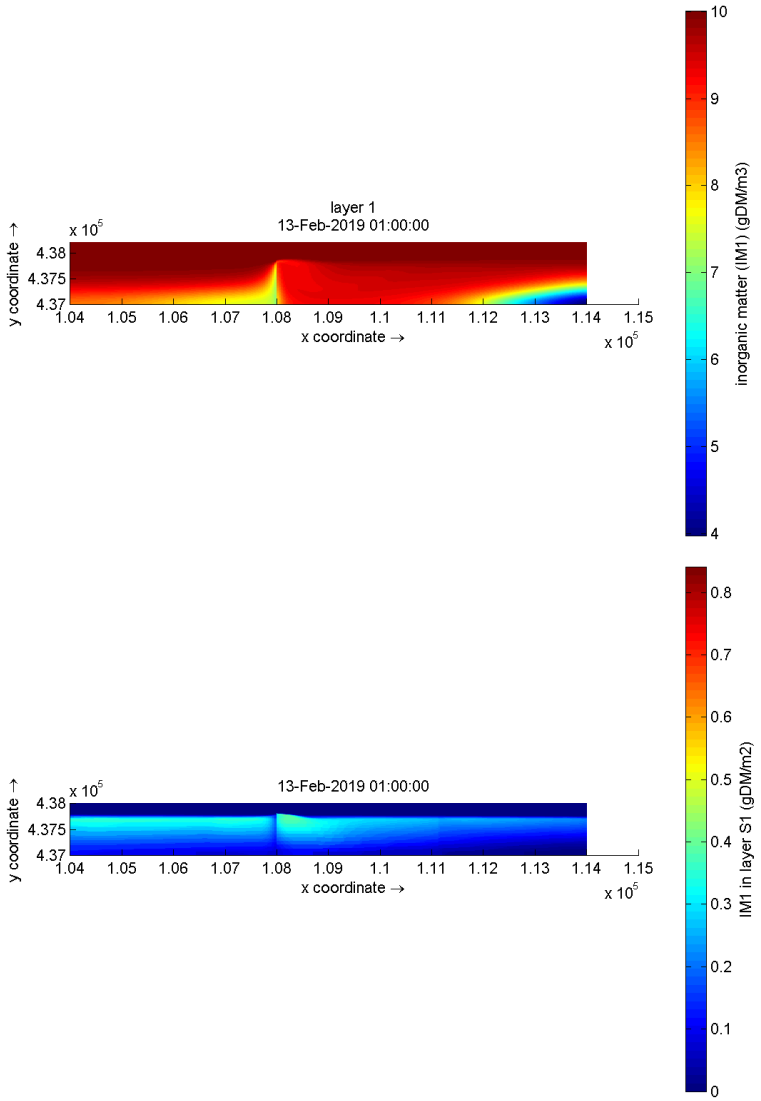

Figure 4.4 Concentration in the water of IM1 (mg/l) and on the bottom (IM1S1; g/m^2, accumulated from the start of the calculation period). The direction perpendicular to the flow direction has been enlarged to better show the concentration distribution. The groyne is visible as a discontinuity in the pattern at about two thirds of the way. The flow is from left to right. The snapshot was taken after 23 hours into the calculation.

In the lower figure, the main channel is clearly visible at the top as a dark rectangle – there the flow velocity is much too high for deposition to occur. This does occur, however, in the shallow lower part of the model area: the flow velocities are much lower there and as a consequence matter settles onto the bottom and remains there. The effect of the groyne is also quite clearly visible as a “fault line” in the concentration of suspended material (left) and less so in the accumulation of bottom material.

4.8.4 Conclusion

While it is not possible to compare the model results with an analytical solution (no analytical solution is known and it is very unlikely one can be constructed), the concentration patterns are what you would expect: deposition only occurs on the floodplain and the groyne causes a disruption in the pattern where it generates spatial variation resulting in zones with additional deposition.

The results for this particular verification differ using WAQ or using PART for a number of reasons:

- PART cannot import the shear stress data from the hydrodynamic model directly, so it has to recalculate the shear stress.
- The parameters controlling the deposition differ in the two models. The critical shear stress for deposition in the WAQ calculation was 0.05 Pa, which was lower than the shear stresses as seen in the hydrodynamic results for the main channel. For the PART calculation, however, an even lower critical value was chosen. This should have resulted in even less deposition in the main channel. This is a point of attention.

4.9 Overall conclusion for the verification of WAQ for microplastics

Using the standard processes library, it is possible to simulate the verification cases in a satisfactory way.

Advantages of using WAQ for the simulation of microplastics are:

- Easy incorporation of additional or specific processes, such as deposition and aggregation.
- Arbitrarily long simulation periods, the required memory resources are independent of the length of the simulation period.

Disadvantages of using WAQ are:

- It is not possible to consider *floating* particles.
- The underlying mathematical representation has as a consequence that concentration patterns cannot be finer than several grid cells. PART, however, can naturally reveal sub-grid details.

5 Pilot realistic river modelling for macroplastic items using D-PART

5.1 Hydrodynamic modelling

5.1.1 Introduction

For the pilot realistic modelling the focus was on the location where Allseas carried out their field monitoring, which was about 1km to the west of the van Brienenoordbrug in Rotterdam. It was considered that the 3D OSR-NSC-model, nested in the 2D OSR-Haven model was the most suitable model that covers the study area, because it is a 3D model with the highest resolution available and furthermore is well verified (Kranenburg, 2015).The Port Authority Rotterdam approved the use of this model for this project. Details of the model can be found in Kranenburg et al. (2015).

In summary, the OSR model consists of two models. The *OSR-Havenmodel* covers a large area including the lower Rhine and Meuse branches and a part of the North Sea and is simulated depth averaged using WAQUA. The *OSR-NSC* model is a detailed model nested in the *Havenmodel* and includes the *Nieuwe Maas*. It is solved in 3-dimensions using TRIWAQ. WAQUA and TRIWAQ are modules of SIMONA, which is a modelling suite developed for Rijkswaterstaat and has significant similarities to the Delft3D-FLOW module. The extent of the models and a detail of the 3D model grid around the monitoring site shown in Figure 5.1.

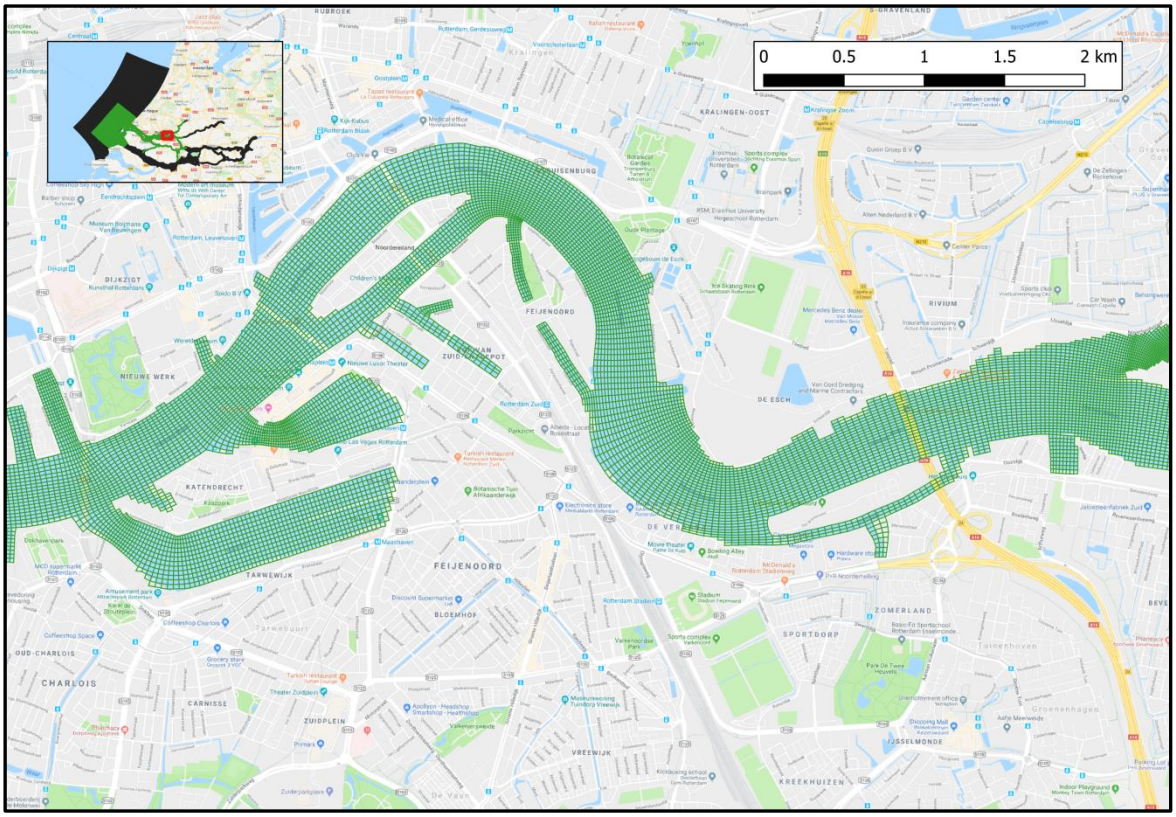

Figure 5.1 Overview of the extent of the OSR model (insert) and detail around the monitoring locations

5.1.2 Horizontal and vertical resolution

The resolution of the OSR-NSC model is three times that of the *OSR-Havenmodel* and near the study are this means that the grid resolution of the *OSR-NSC* is approximately 20x30m. The model has 10 sigma layers, specified as a percentage of the local depth (Table 5.1).

Table 5.1Vertical layer distribution of the OSR-NSC model

(counting from the surface)	Thickness (% of local depth)
1	12
2	12
3	11
4	11
5	11
6	11
7	11
8	9
9	6
10	6

From the vertical layering it is noted that the highest vertical resolution of the model is near the bed (layer 9 and 10).

5.1.3 Forcing

The model was set up for the period 1 February – 3 March 2018. We have assumed a condition that is derived from an annual average discharge at Lobith of 2225 m^3/s. This means that for the boundary condition of the 2D model, the real discharges at *Tiel* (*Waal*) and *Lith* (*Maas*) during that period have been replaced by values of 1510 m^3/s and 200 m^3/s (annual average discharge of the Maas) respectively. On the western boundary of the OSR-haven model water levels are specified. A nesting procedure leads to water level boundary specification for the western boundary of the OSR-NSC model and discharges at the river boundaries. The wind forcing that is used is taken from observed wind at Hoek of Holland for the modelled period (Figure 5.2).

The OSR model does not include waves, but includes the effect of wind on currents (due to wind shear stress. Salt intrusion from the sea is included.

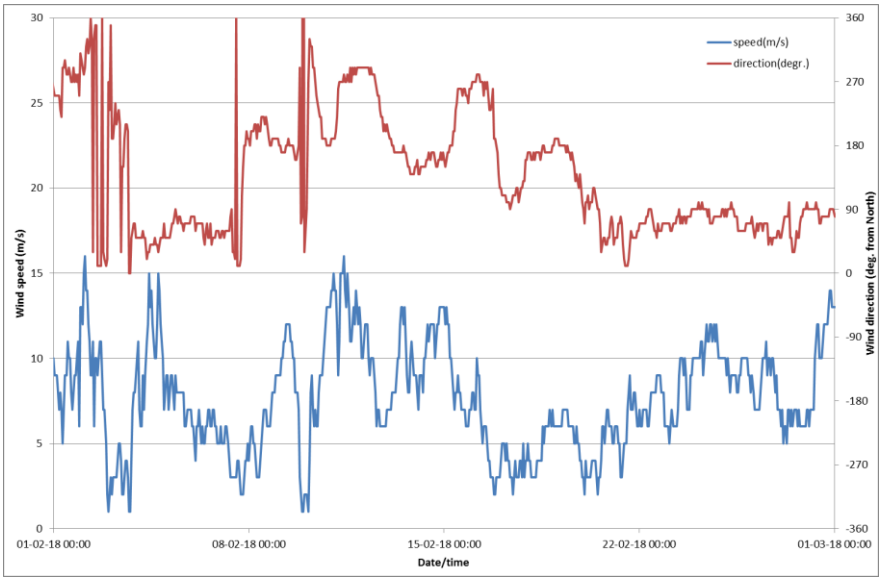

Figure 5.2 Wind speed and direction at Hoek van Holland (2018)

5.2 Particle tracking modelling with D-PART

5.2.1 Objective

The particle tracking was set up using the OSR-NSC model to cover the entire FLOW period (1 February to 3 March). The objective of the modelling is to investigate how plastics with different characteristics may be distributed in the river and which factors affect this distribution.

5.2.2 Particle model setup

The particle model was set up to model macroplastic items with different characteristics. Litter may float, tend to sink and tend to rise towards the surface. These settling and rising processes are included in the particle tracking model. For floating particles, the effect of wind drag on the transport of floating objects is also included in the model setup. Hence three main types of litter were used in the modelling. With a varying falling and rising velocity a total of seven scenarios were set up:

Floating particles

- Wind drag coefficient of 1% (based on findings/data of The Ocean Cleanup)

- Rising particles
  - Velocity = 0.0001 m/s (0.1 mm/s which is equivalent to about 8.5 m/d)
  - Velocity = 0.01 m/s (about 85 m/d)
  - Velocity = 0.2 m/s (1700 m/d)
- Falling particles
  - Velocity = 0.0001 m/s (0.1 mm/s which is equivalent to about 8.5 m/d)
  - Velocity = 0.01 m/s (about 85 m/d)
  - Velocity = 0.2 m/s (1700 m/d)

The lowest vertical velocity, which may be more representative of micro plastics, have been used to address objects that may have very low speeds due to their density (very close to that of the surface water) in combination with their shape (such as plastic bags).

The horizontal dispersion coefficient was set at 1 m^2/s and the vertical dispersion coefficient at 1.10^{-5} m^2/s. These values are typical for these types of models, although they are in the lower range. Data to verify these model parameters are not available and the final particle distribution in the vertical is a combination of the vertical dispersion and the falling/rising velocity. Higher or lower values of the dispersion coefficient will result in faster or slower distribution of particles in the horizontal and vertical, but will in general not alter the main results, although some changes would be expected. This was not investigated further in this study.

Bouncing of the particles at the bed and water surface has been switched off, such that it was not needed to reduce the time step. A fall velocity of 0.0001 m/s was included as one of the model to represent a falling velocity that is in the same order of magnitude as the dispersion displacement.

The two main upstream boundaries are the *Beneden Merwede* and the *Lek* branches. The boundary conditions were set up in such a way that the plastic concentration is represented by a unit concentration of 100 units/m^3. Since the river is still under influence of the tide, particles are only discharged during the periods when the discharge is directed seaward. This way an approximate constant concentration of 100 units/m^3 near the boundary is achieved. The rising particles are released near the surface and the sinking particles near the river bed and all are distributed across the river. For each simulation 5,000,000 particles were used.

For the output, monitoring points were introduced in addition to the ones already in the flow model, as shown in Figure 5.3.

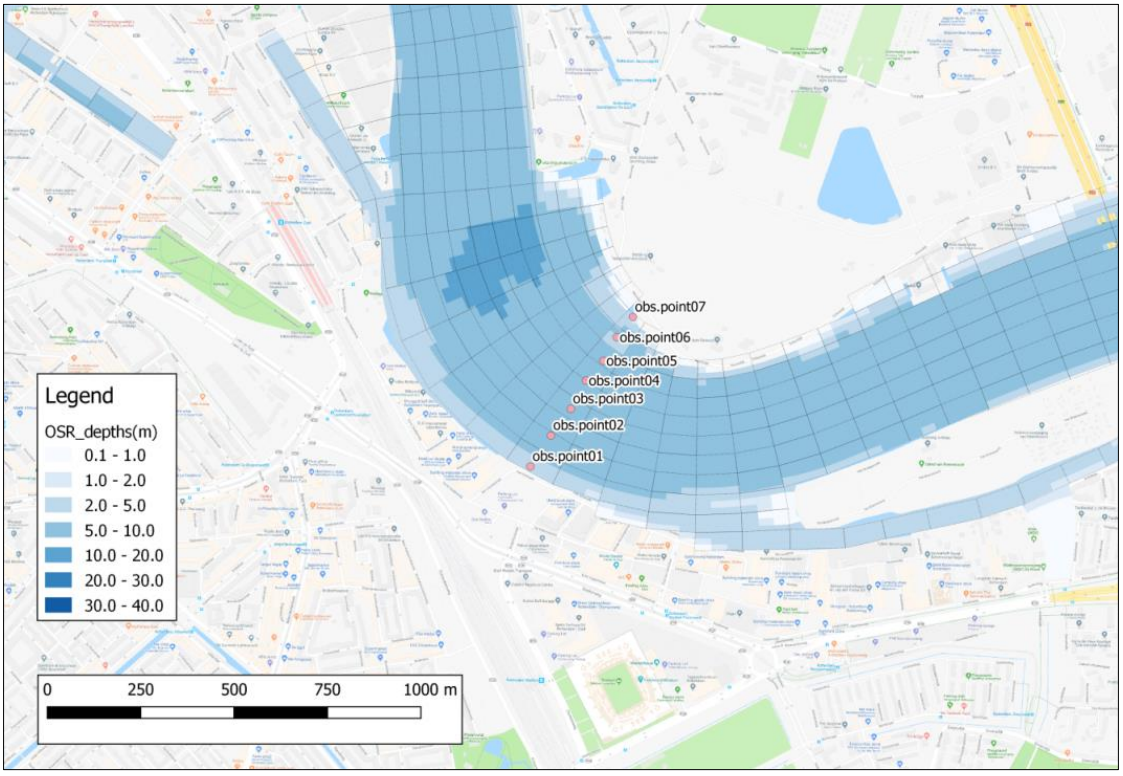

Figure 5.3 Model grid and depth of the OSR model and positioning of monitoring points in D-PART near the Allseas site

5.3 Results

5.3.1 Hydrodynamics

The hydrodynamic model was run from 1 February 2018 for a period of 4 weeks. The first two weeks are used as a warm-up period (to distribute the initial salt concentrations) and to stabilise currents. The last 15 days (spring-neap period) are used to run the particle tracking model. The area is characterised by a tidal movement. The water level varies with the semi-diurnal tide. Also meteorological conditions affect the water level (Figure 5.4). In particular, an increase in water level due to a storm surge can be observed around 11 February.

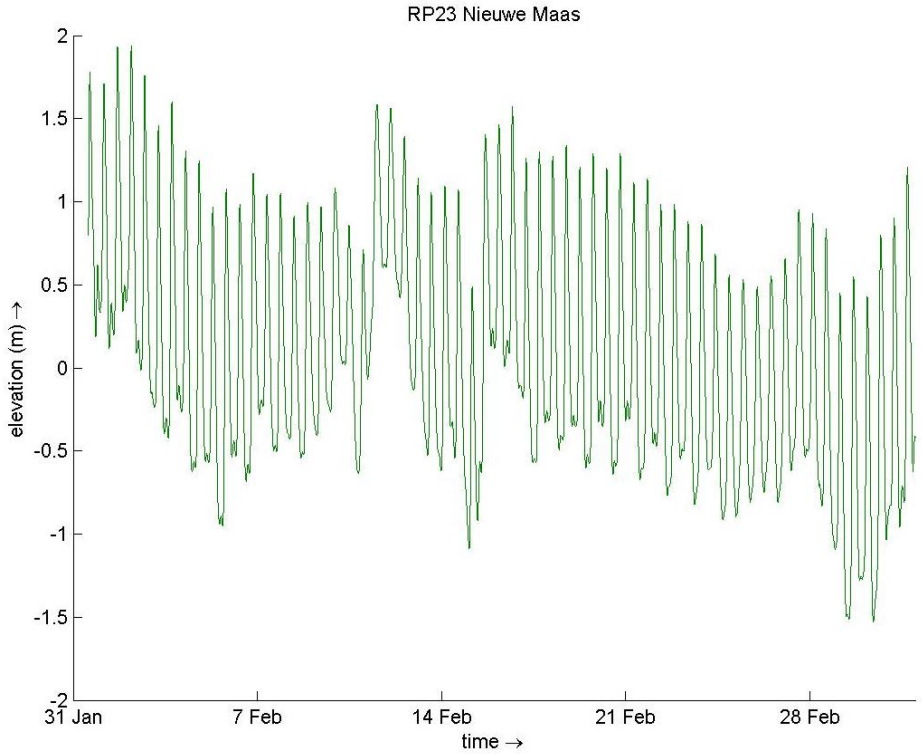

Figure 5.4 Water levels near the monitoring locations in the Nieuwe Maas

The tidal flow velocities can be more than 1 m/s in the main channel for both the flood as well as the ebb tide (Figure 5.5).

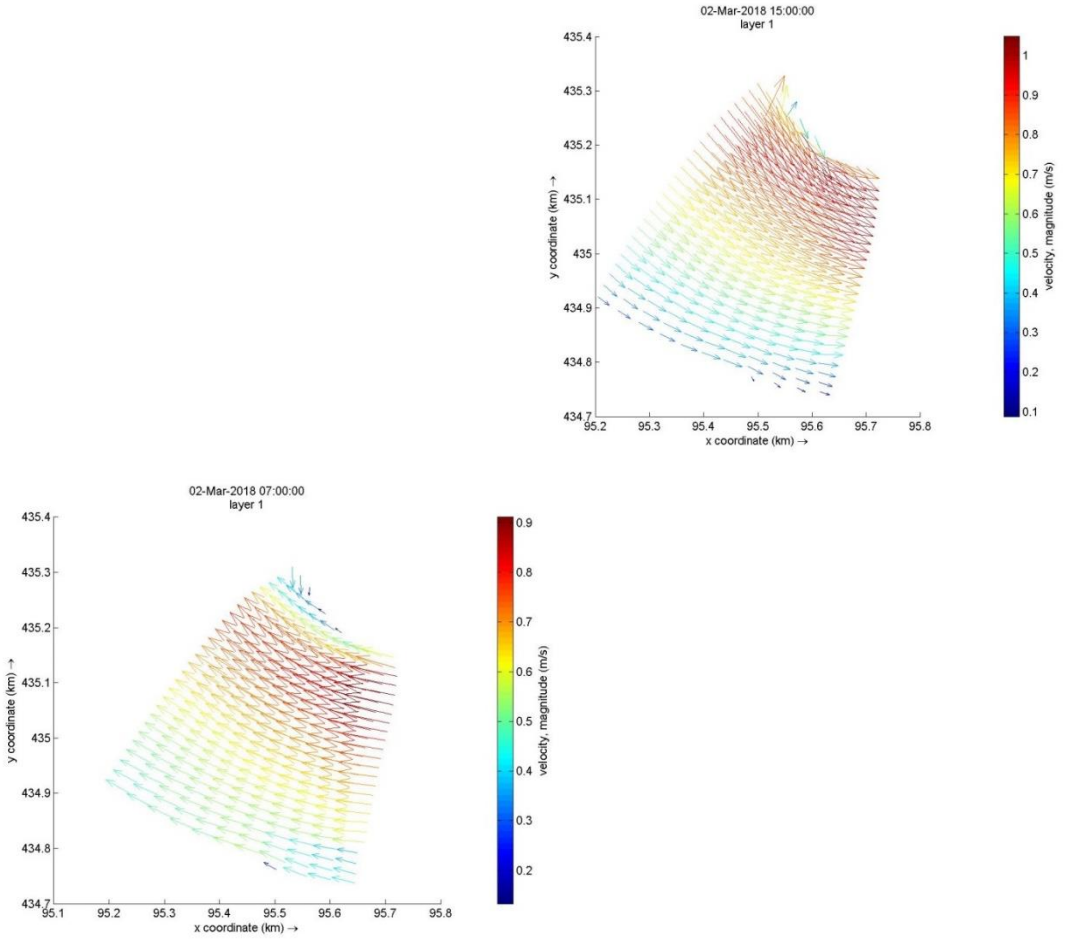

Figure 5.5 Flow velocities during ebb (left) and flood(right)

When examining the vertical flow velocities in the cross section near the monitoring location, it can be seen that a circular pattern occurs from time to time, see Figure 5.6. This figure shows a cross-sectional view of a circular pattern during the ebb tide located to the south of the centreline of the main channel with flow velocities in the order of a few centimetres per second. However, vertical flow velocities are small in comparison to the horizontal (tidal) flow velocity and the secondary cell is only present in part of the cross-section, due to the bed shape.

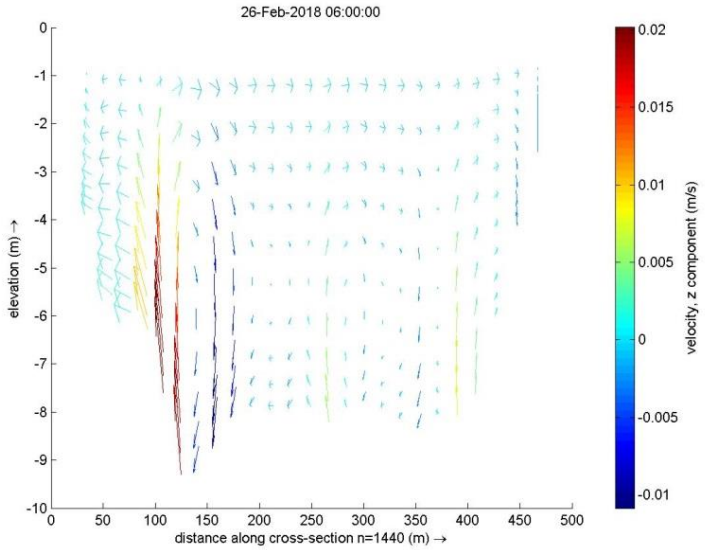

Figure 5.6 Vertical flow velocities at the cross section near the monitoring stations

5.3.2 Floating particles

The surface floating plastics vary in their location in the river. There are times when they are close to the northern side and at other times at the southern side (Figure 5.7).

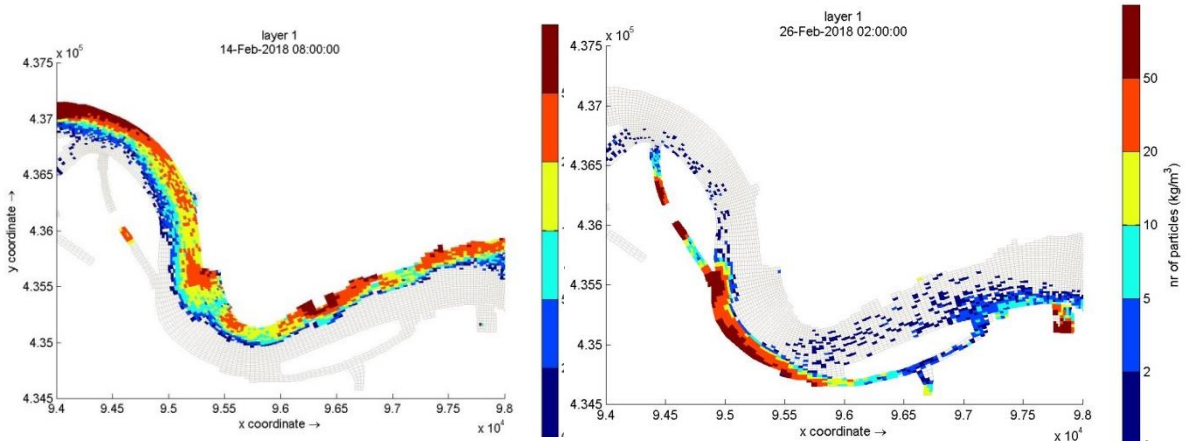

Figure 5.7 Distribution of floating plastics for two wind conditions (southerly-left, northerly-right)

This is the effect of the wind acting on the horizontal transport. On the 14th February the winds were mainly from southerly directions (Figure 5.2) whilst on 26th February they are mainly from the east/north-east. From the figures it can be concluded that the wind plays an important role for the floating plastics. The areas of highest concentration vary with wind strength and direction. For this reason, there is no fixed location where concentration or flux of macroplastic items is highest.

5.3.3 Rising particles

In this study three rising velocities were applied for plastic items (Section 5.2.2). It is generally noted that the results for plastics with 10 mm/s and 200 mm/s rising velocity are very similar. Figure 5.8 shows that the results with the low rising velocity of 0.1 mm/s are quite different from the other two. For the higher rising velocities, the effect of the wind is clearly visible in the distribution of the particles (right in Figure 5.8).

In the model these are particles that remain very close to the water surface, although they remain suspended in the water and do not become floating.

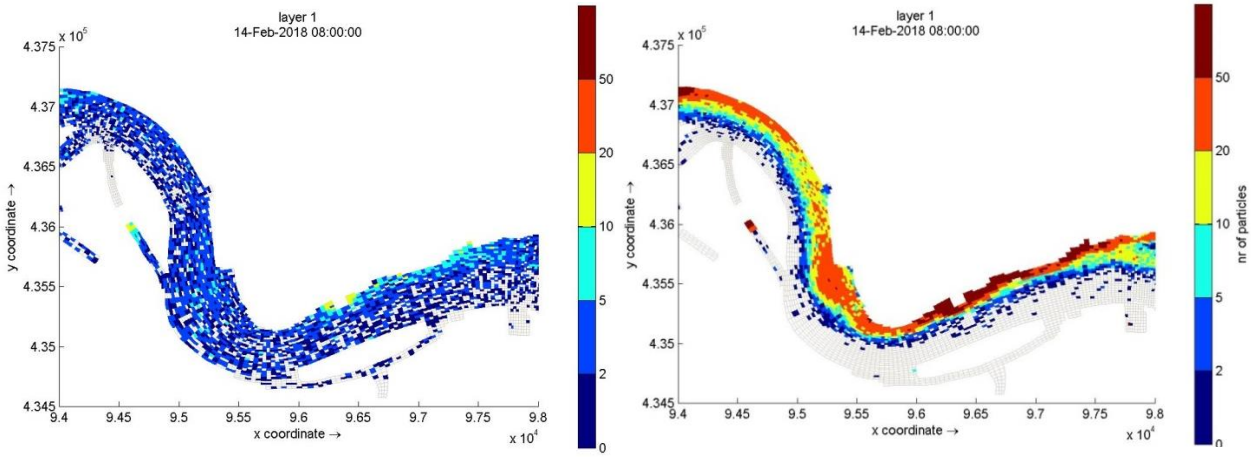

Figure 5.8 Distribution buoyant plastics in the surface layer for two rising velocities (0.0001 m/s-left, 0.01 m/s-right)

The similarity of the right image of Figure 5.8 with Figure 5.7 (left image) shows that the wind is an important factor for the plastic transport. For the plastics with a low rising velocity, the vertical dispersion results in vertical spreading of the particles over the water column. In other words, vertical mixing occurs continuously. Since the effect of the wind is highest in the top layer, the wind has less effect for the case with low rising velocity (Figure 5.8, left image). As a result, the effect of the wind is counteracted by continuous redistribution of particles due to the vertical dispersion.

For the case with a low rising velocity, the vertical dispersion results in a vertical distribution of particles, with the highest numbers near the surface and lowest near the bed. This vertical distribution results in lower numbers near the surface compared to particles with higher rising velocities. The simulations with the higher rising velocities only show particles in the surface layer and none in the layers below the surface layer. Figure 5.9 shows an example of the time development of the concentration near the surface and the bed (small rising velocity) in the centre of the *Nieuwe Maas* indicating that particles are found in the lower model layers, but that there is a vertical concentration gradient with the highest concentration near the surface, which is consistent with the expected distribution. The results are shown to be sensitive to the selection of the vertical dispersion, in combination with the falling/rising velocity.

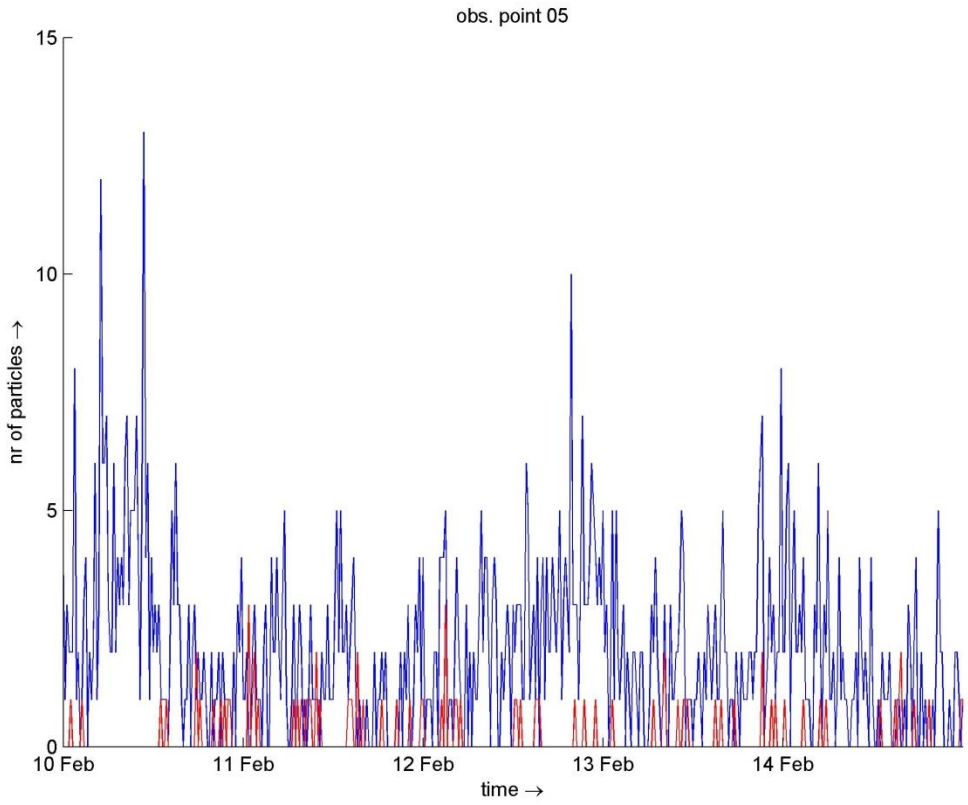

Figure 5.9 Particle concentration for the surface (blue) and bed (red) layer, for particles with rising velocity of 0.1 mm/s at observation no 5, on the inside of the river bend

Since the wind does not affect these rising particles directly, the advection of the plastics is driven by the flow velocities. The wind acts on the flow velocities in the hydrodynamic model leading to the particles drifting towards the northern side of the river for the two higher rising velocity values. The effect of any secondary flow on the particle transport could not been seen.

Figure 5.10 illustrates the wind effect on distribution of the particle concentration across the *Nieuwe Maas*. It can be seen that the concentrations are highest on the northern side in the period between 7 and 17 Feb (approximately) and that during the period after 21 February the concentrations on the south side are higher (blue line). Between 21 and 28 February the wind was mainly blowing from easterly/north easterly directions, whilst around 15 February the wind direction was more from the south. The simulated particle concentrations across the *Nieuwe Maas* can generally be explained by the effect of the wind.

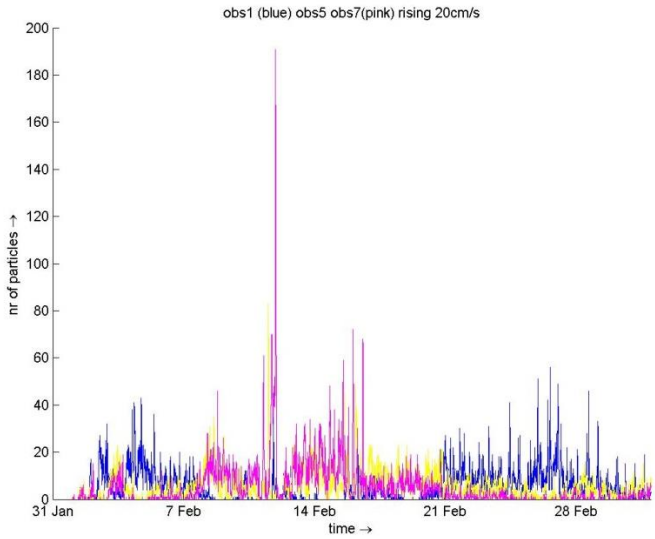

Figure 5.10 Particle concentrations for three observation locations in the top layer, on the north (obs7-pink), middle (obs5-yellow) and the south (obs1-blue) side of the river

Particle fluxes from the model provide an indication of the amount of plastics that may be captured in certain periods. The derived fluxes for two periods for the rising particles are shown in Figure 5.11. During the first period (8 Feb. to 11 Feb) winds are mainly from the south (Figure 5.2) whilst the second period (26 Feb to 29 Feb) they are mainly from the east to north-east.

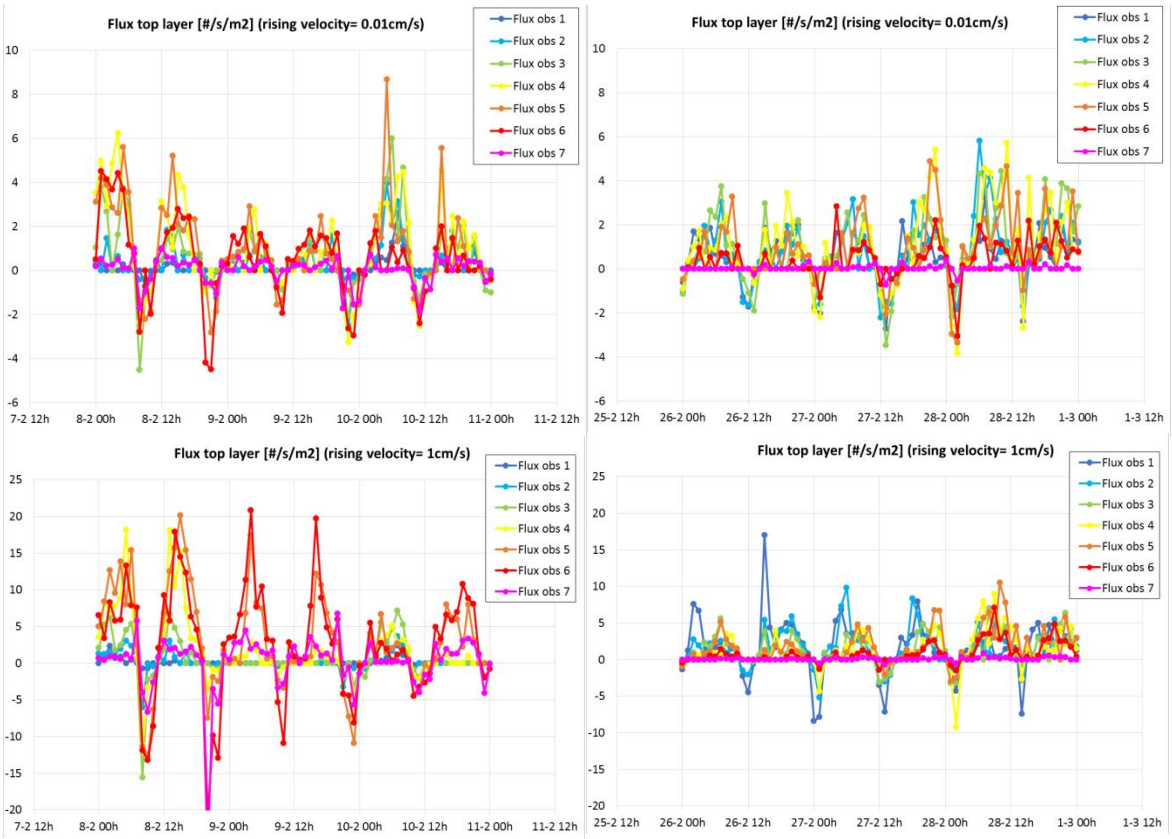

*Figure 5.11 Near surface particle fluxes (current velocity * concentration) at the 7 observation locations across the Nieuwe Maas for two different rising velocities and for two periods; positive flux occurs during ebb tide.*

From the figures above (Figure 5.11) can be seen that during the period with mainly southerly winds (figures on the left), the fluxes at stations 5 and 6 dominate during the flood (positive flux). For location 7 the fluxes are lower, due to the lower current velocities close to the northern river bank (for details see Figure 5.12). For the low rising velocity, the effect of the wind direction is small compared to the higher rising velocity. For winds from the east to northeast, the opposite effect can be seen, in particular for the higher rising velocity.

As an example, Figure 5.12 shows for one period and for the rising velocity of 10 mm/s the flow velocity and particle concentration separately to show how the flux is composed. The peak flow velocities during ebb are highest for obs3, obs4 and obs5, as expected. The reason for the low flux in the top layer during ebb at obs7 is that the flow velocity is an order of magnitude lower than in the middle of the channel. During flood, the peak flow velocity magnitude is similar for the 7 observation points. The variation across the channel is smaller than during ebb for this specific cross section. For that reason, the landward directed fluxes are substantial for each of the observation points.

The wind direction in the period of this example was in between north and east (Figure 5.13). The wind is likely to have generated a surface flow towards the southern bank. The plastic particles in the top layer were transported to the outer bend, resulting in a relatively high concentration in the outer bend. This is likely to be the dominant cause for the high flux at obs1 near the southern bank and similarly for the low flux at obs7 near the northern bank.

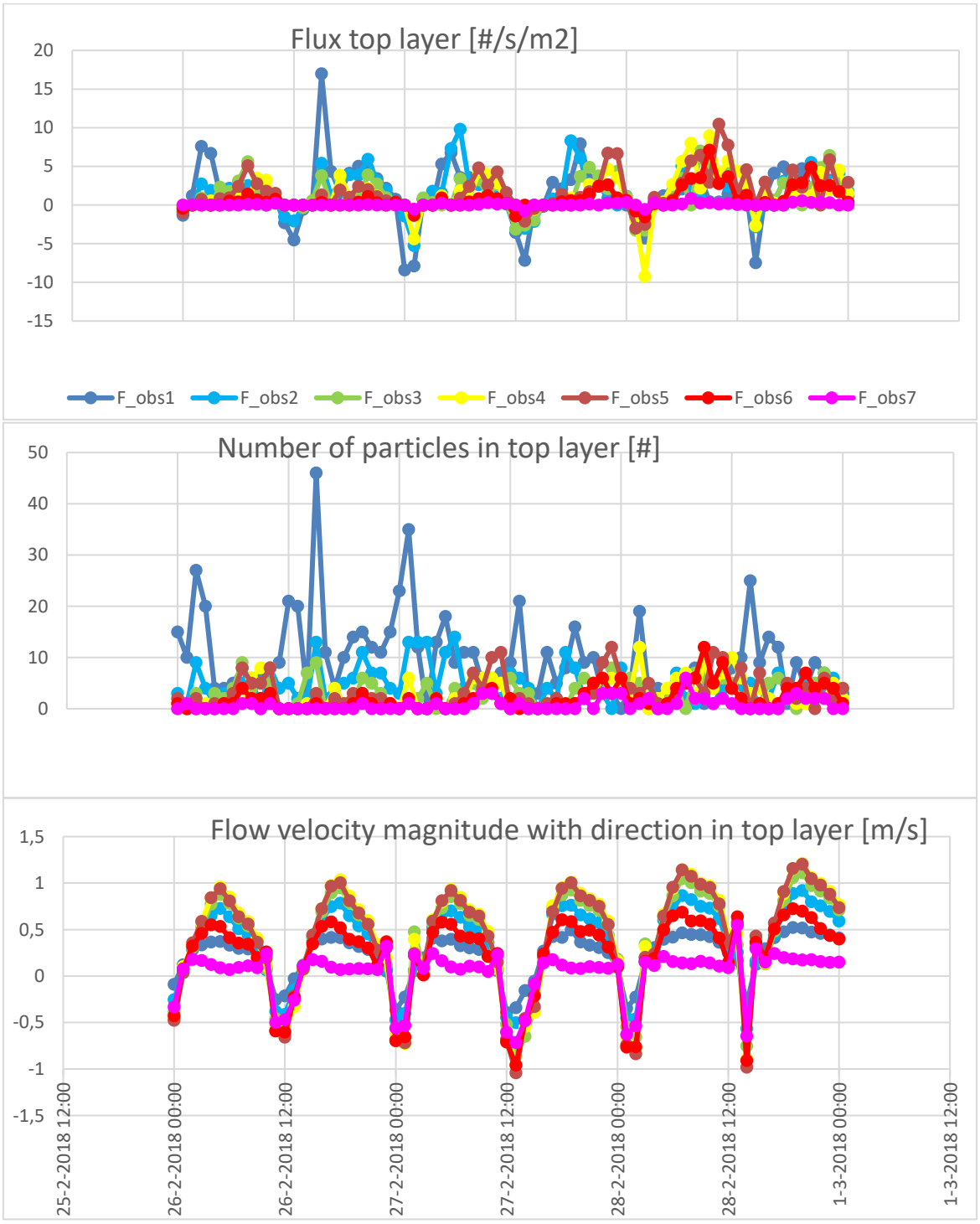

Figure 5.12 Near surface particle flux, concentration of plastic particles and flow velocity at the 7 observation locations across the Nieuwe Maas for a period of three days for particles with a rising velocity of 10 mm/s.

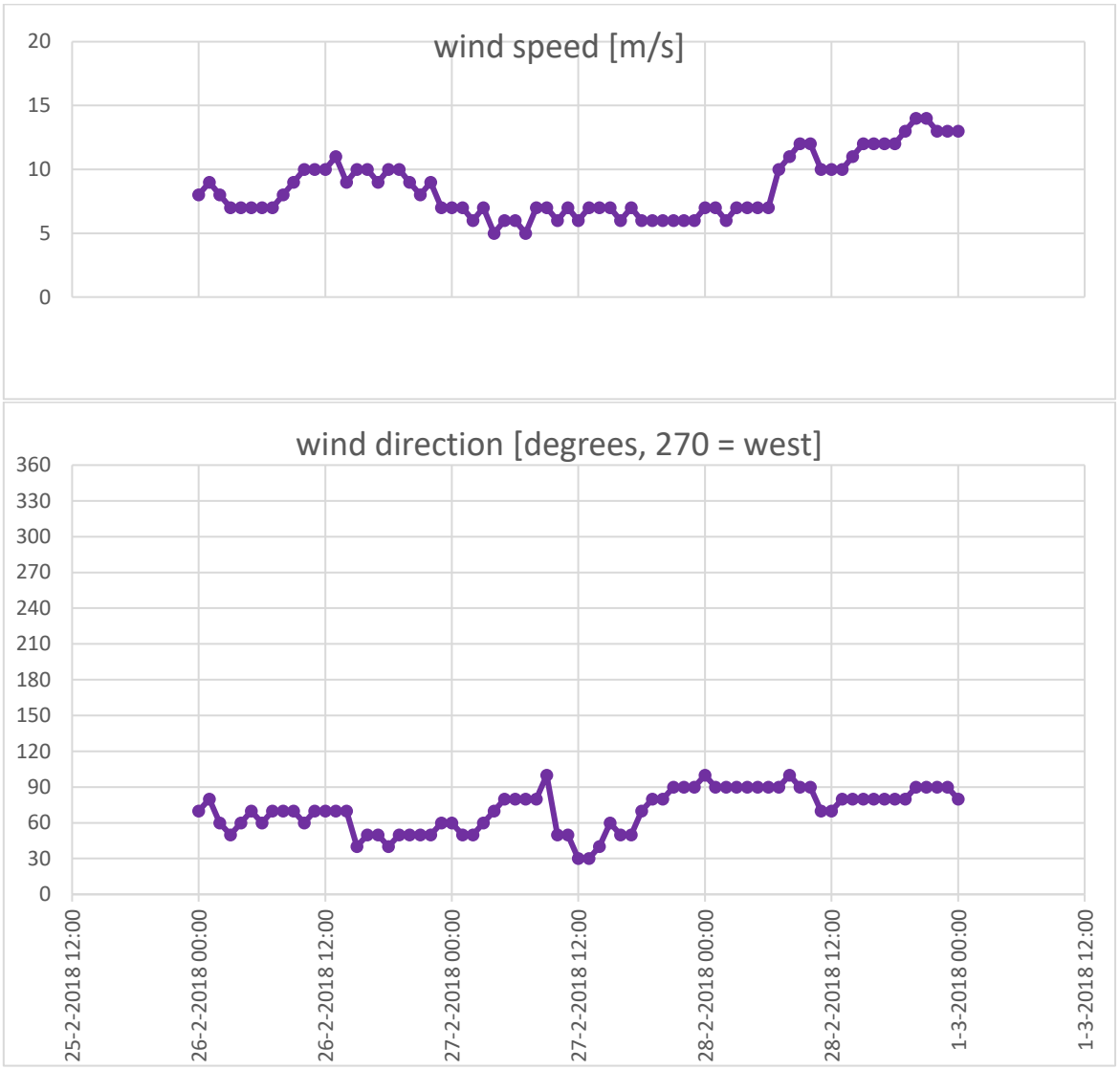

Figure 5.13 Wind speed and direction for the same period of three days as in Figure 5.12.

Another observation from the results is that particles can accumulate in the harbours from time to time (see e.g. circled areas in Figure 5.14 and Figure 5.15). Where they accumulate will depend on the wind conditions. There may also be times when the plastics are transported back out of the harbour so the accumulation may be temporary, again depending on wind conditions.

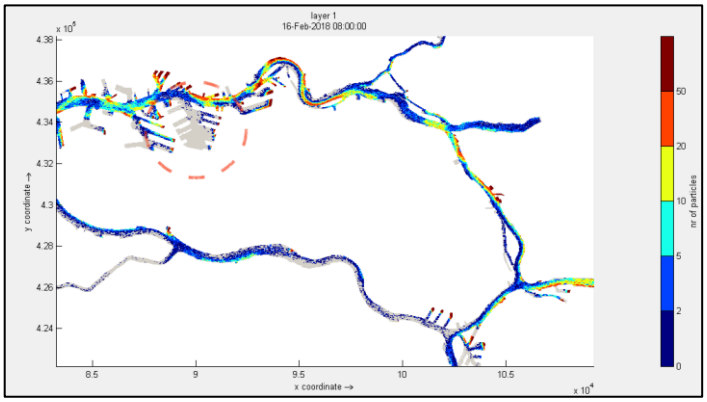

Figure 5.14 Rising particle concentrations on 16 Feb, during mainly westerly winds

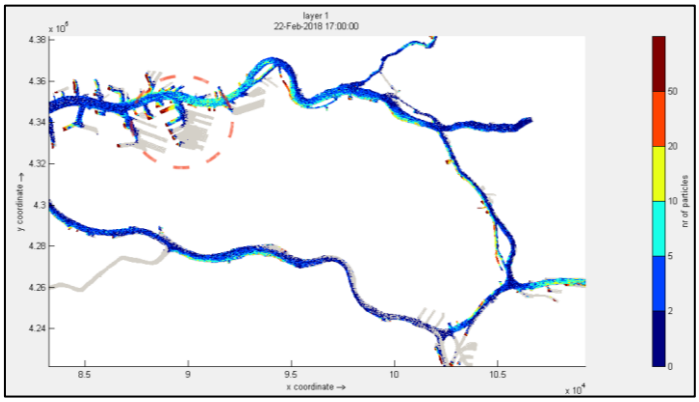

Figure 5.15 Rising particle concentrations on 22 Feb, during mainly easterly winds

Overall concentrations of the particles with a tendency to rise are transient and dependent on wind conditions.

5.3.4 Falling plastics

For the falling particles the same vertical velocities were applied as in Section 5.3.3, but now directed downwards. The general characteristics of the particle transport in the vertical is similar. However, for the falling particles the highest concentration is found near the bed, although particles are also found near the surface. This can be seen in Figure 5.16 for a point in the centre of the *Nieuwe Maas*.

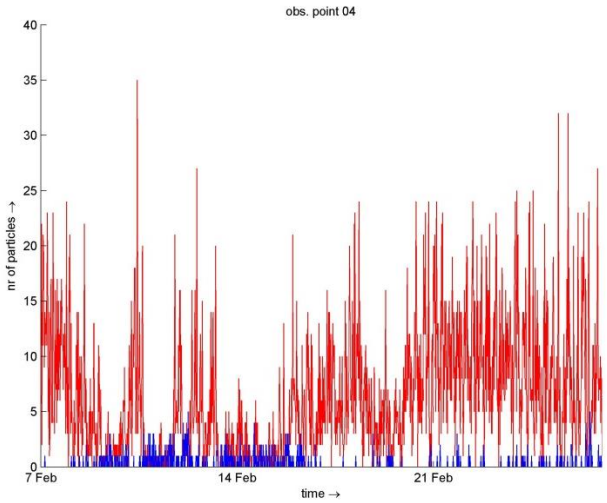

Figure 5.16 Particle concentration for the surface (blue) and bed (red) layer, for particles with falling velocity of 0.1 mm/s

Figure 5.16 indicates that for obs4, the concentrations are significantly higher for the case with the lowest falling velocity than those observed in the model for the rising particles at obs5 in the previous section (Figure 5.9). Obs5 is somewhat closer to the inner bend, but the reason for the difference is that the rising particles are predominantly in the top layer, with higher flow velocities than near the bed. Near the surface they travel faster through the system and as a result a larger share of the rising particles is transported out of the model than for the falling particles that are concentrated near the bed.

It is noted that the concentrations for the particles with a fall velocity of 10 and 200 mm/s are only found in the lowest layer (not shown). Due to the large fall velocity, the particles remain near the bed.

Particle fluxes for two falling velocities and two periods are shown in Figure 5.17.

*Figure 5.17 Near bed particle fluxes (current velocity * concentration) at cross-sectional observation locations for falling particles for different falling velocities and periods*

The reasons behind the correlation of the fluxes with the wind direction are less clear than for the near surface (rising) particles, although a link can be made. The first period (8 Feb top 11 Feb) with winds mainly from southerly directions (see Figure 5.2) appear to be dominated by locations 2 and 3, i.e. towards the south part of the bend. The outer stations do not show any particles, confirming that the falling particles tend to remain more in the main channel. The falling particles near the bed are also located towards the other side of the river compared to the rising particles near the surface. This is due to the cross-sectional current that develops due to the wind. When the wind is from the south the near surface current is directed towards the north with a near-bed current directed to the opposite direction (to the south). For winds from the east to north-east, the opposite occurs.

It is also interesting to note that the fluxes for the different stations for the low (0.1 mm/s) and higher (10 mm/s) falling velocities appear similar. This is not the case for the rising particles. This indicates that the bed form has an important influence on the distribution of the falling particles near the bed. The falling particles are transported primarily in the deepest part of the river.

Generally, concentrations of particles with high falling or rising velocities in the layer where they accumulate, are higher than for particles with low falling/rising velocities. This is due to the distribution of particles over the vertical when the falling/rising velocities are small (see Figure 5.9 and Figure 5.16) and in the same order of magnitude as the spreading velocity due to vertical dispersion. With higher falling/rising velocities, the particles are only present in the bed or surface layer and this results in higher concentrations in these layers.

The falling particles remain near the bed with a preference of the deepest part of the cross section. There is a variation of the location of the highest concentration in the cross-section. This may be related to the tide induced current direction (e.g. Figure 5.18) but can also be affected by cross-sectional current that may occur and that may be wind induced.

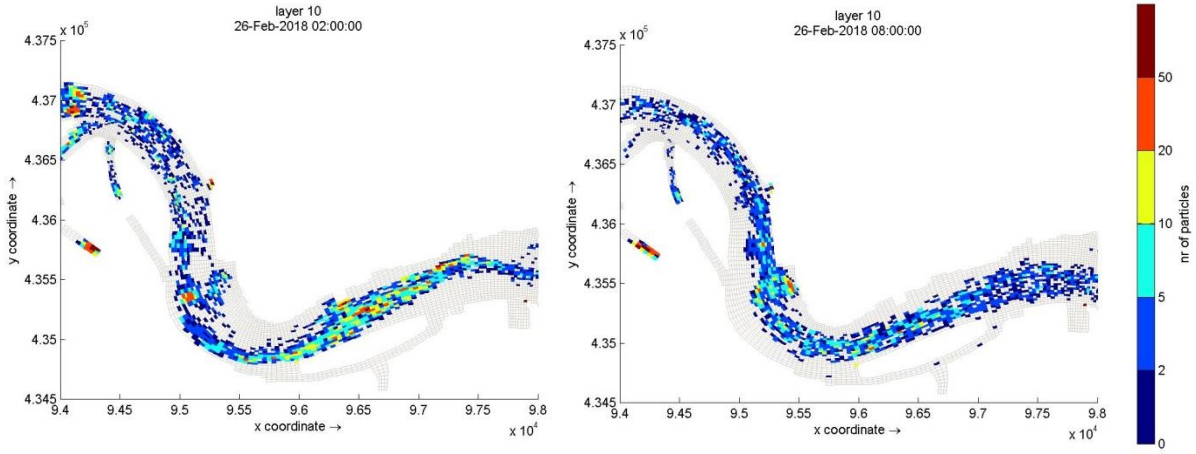

Figure 5.18 Particle concentration near the bed layer at two times (flood-left, ebb-right), for particles with sinking velocity of 10 mm/s

The results of the modelling show accumulation in the centre of the harbours near the bed (Figure 5.19), but the amount will depend on the actual conditions. These particles are transported into the harbour during the flood. The velocities in the harbour are very low and as a result these particles tend to remain in the harbour for longer periods.

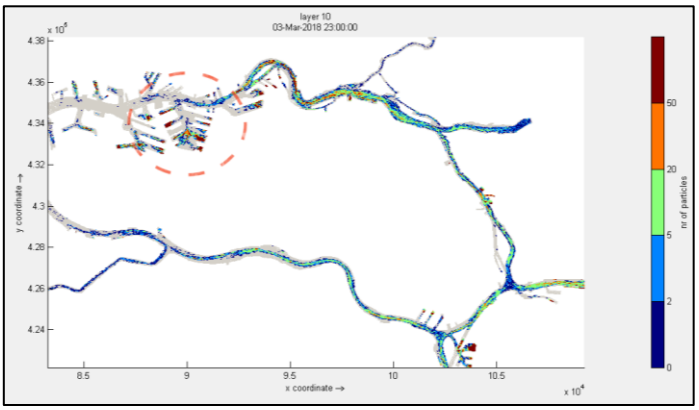

Figure 5.19 Distribution of falling plastics at the end of the simulation

The distribution of the particles in the main river and in harbours with a tendency to sink is different from the distribution of particles with a tendency to rise or floating particles. The dependency of the wind conditions is far less pronounced for the falling particles, as may be expected. A consistent picture of accumulation areas or areas with elevated flux do not emerge other than that the highest concentration tend to be more towards the main channel of the river and near the bed. In harbours some accumulation resulted.

5.4 Conclusions of the particle tracking modelling

A number of key conclusions can be drawn from the pilot realistic river modelling for macroplastic items:

- Floating plastics are significantly affected by the wind friction and therefore the wind strength and direction. Where the highest concentrations are found is directly linked with these wind conditions. The plastics may also collect in harbours in the area and accumulate there, but wind can also transport it to other parts in the harbour or back out of the harbour.
- Particles with a tendency to sink were found to accumulate in harbours. In contrast to floating plastics, the effect of wind on accumulation of sinking particles is limited and any accumulation is more towards the centre of the harbour.
- Plastics with a low falling or rising speed (here 0.1 mm/s) do accumulate more near the surface (rising) or bed (sinking) but are also found over the entire water column, due to the combined effect of vertical dispersion and cross-sectional flow velocities. A vertical concentration gradient exists with the highest concentrations near the surface for rising plastics and near the bed for the falling plastics. The extent of this is uncertain due to the dependency of the vertical dispersion and falling/rising velocities.
- Plastics with a higher vertical velocity (10 and 200 mm/s) are only found in the surface layer or in the layer just above the bed and not in other layers.
- Plastics that are near the bed travel downstream at significantly lower velocities than near the surface.
- Plastics near the surface, but still suspended, are subject to wind effects, due to the cross-current developing in the surface layer due to wind. The area where these plastics accumulate will therefore depend on the wind direction. The wind strength will affect the extent to which this occurs.
- Plastics near the bed are not directly affected by the wind conditions, although the location of highest cross-sectional concentration varies, likely to depend on flow conditions (flood/ebb) and existence of cross-sectional flow velocities. There is a tendency that during southerly winds particles are transported to the south bank, which is in agreement with the secondary circulation that occurs. Hence, the particles near the bed are transported in opposite direction compared to near-surface rising particles.

6 Pilot realistic river modelling WAQ

6.1 Objective

As with the D-PART model, for the realistic river modelling the OSR-NSC model was chosen for the entire period of 1 February to 3 March. In this case we focused on microplastics instead of macroplastic items. The objective of the modelling is to investigate how microplastics with different characteristics may be distributed in the river and which factors affect this distribution. To this end a set of 24 unique types of microplastic particles was selected (Table 2.4) and the spreading of these plastics through the river system was calculated.

These falling/rising velocities are much higher than those commonly encountered for organic or inorganic suspended particles (in the order of several m/day). These are generally much lighter (organic) or much smaller (diameter in the order of 60 µm) than the microplastics included in this study. This has a consequence that plastic particles may fall more readily in quiescent waters than “natural” particles.

6.1.1 Model set-up

The model set-up consists of two components: the transport by the flow and the distinguished processes specific to plastics. The transport is taken care of by the generic part of WAQ, as it has been in the software verifications. The hydrodynamic model for the Rhine-Meuse estuary is responsible for providing the geometry as well as the flow-field over the selected period (see chapter 5 for more details).

The following processes were considered:

- Falling or (if they are lighter than the ambient water) rising of microplastics. In case of falling, the particles will sink towards the bottom and if the flow is weak enough, settle onto the bottom. Resuspension, however, was not included. There is hardly any information to be found in literature about resuspension of (micro)plastics. By not including this process a worst-case estimate of the amount of plastic in the river bed is obtained.
-
- Aggregation with suspended sediment. While most of the plastic particles either sink rapidly or rise rapidly (see below), the particles that have almost the same density as that of water may start to sink if sediment particles stick to them.
- For the calculation of the falling/rising velocities we used equation 2.4 provided by Waldschläger and Schüttrumpf (2019).
- For the calculation of the aggregation rate we used the same formulation as was described in Unice et al. (2019). The aggregation efficiency was set to 0.01, a best estimate (Besseling 2018).
- The horizontal and vertical dispersion coefficients were set to 1 and 10^{-7} m^2/s, respectively.

To model the transport and fate of the microplastics we combined a single type of suspended sediment (density 2650 kg/m^3 and a diameter of 0.2 mm) with a single type of microplastic. Given the uncertainties involved in the behaviour of microplastics in water and the expected low concentrations of microplastics in this river system, it would have been “overkill” to model any interaction between microplastics of the same or different type.

The initial and boundary conditions for the various substances were:

- Initial concentration of 0 mg/l for all substances
- Boundary concentration for the substances representing plastics: 25 µg/m^3 or 25 ng/L, roughly the concentration found in the measurements.
- The boundary concentration for suspended solids was set to 30 mg/L.
- The waste loads in the hydrodynamic model are all inlet/outlet pairs, so recycling of water. The corresponding concentrations have been set to zero. (All of these waste loads are located far from the area of interest).

6.2 Results

6.2.1 Group 1: heavy particles

For plastic types 1 and 2 (fall velocities respectively 170 and 341 m/day, see table 2.4; type 3 with a fall velocity of 852 m/day gave rise to the aforementioned instability) the patterns are very similar. Only the pattern for type 2 is shown below.

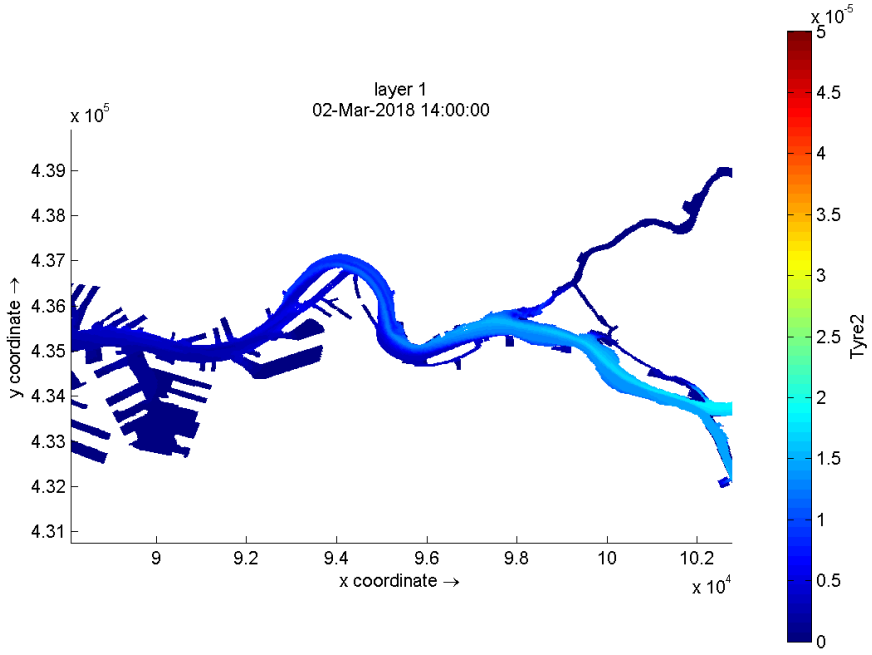

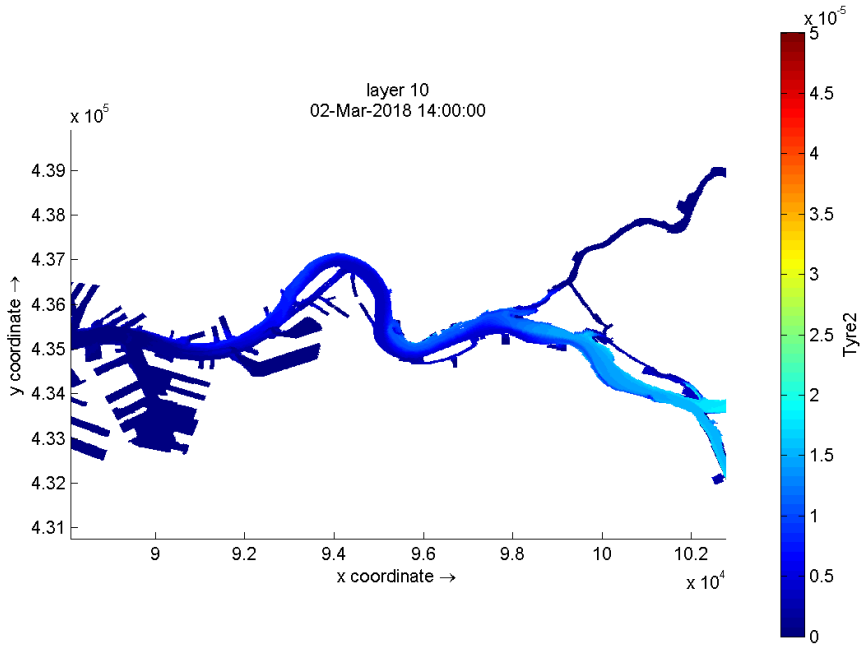

Figure 6.1 Concentration pattern for type 2, at the surface (layer 1) and the bottom (layer 10). Values in mg/l. The snapshot was taken after two months, one day and 14 hours into the calculation.

The concentration levels in the top and the bottom layers are quite comparable, but it can be seen that the particles at the bottom are spread out more to the western part. This is a consequence of the tidal dynamics – the water at the surface and the water at the bottom move differently over the tidal cycle.

The plastic that has settled on the bottom (and because resuspension was not taken into account, accumulates there) can be found in the harbour area, rather than in the reach with the Brienenoordbrug, see Figure 6.1. The sedimentation of the plastics in the main part of the Nieuwe Maas is probably due to prolonged periods of more or less stagnant water, when the tidal inflow is compensated by the river outflow. The fact that resuspension of microplastics was not taken into may exaggerate the effect. For the harbours themselves it is unlikely whether resuspension plays a role.

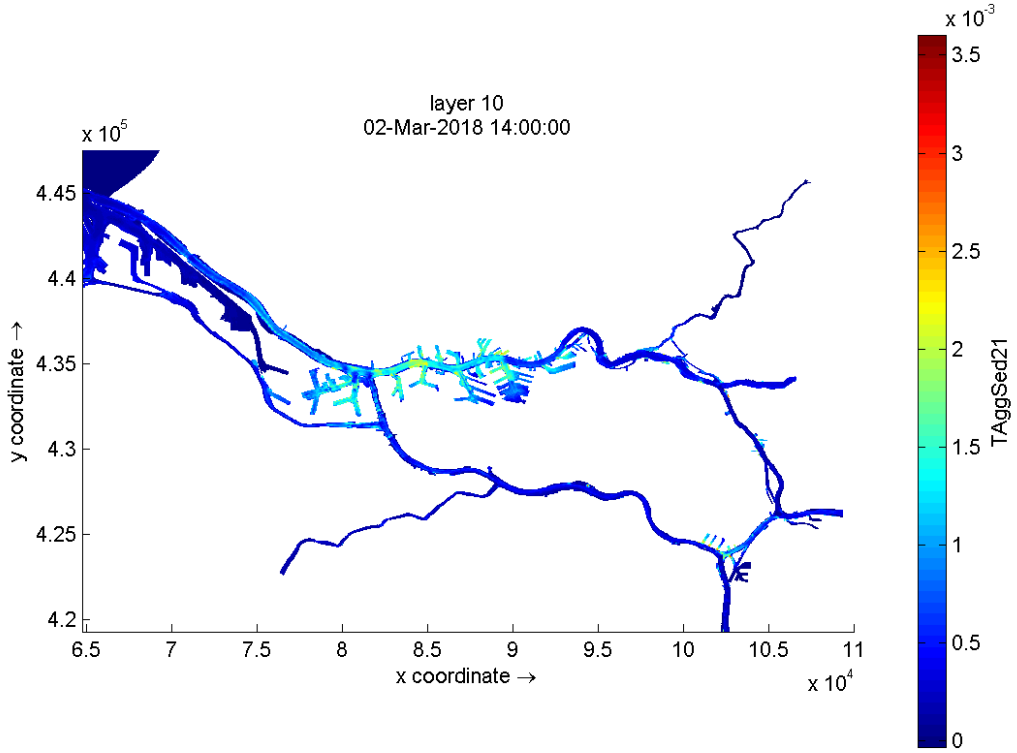

Figure 6.2 Deposition of plastics in the model area (g/m^2).

Besides the Rotterdam harbours there are a few other areas where depositions can be found, but these are minor.

The vertical distribution of the concentrations in a section near the Brienenoordbrug is shown below. It appears that in the centre of the river the concentration is fairly uniform over the vertical – and the highest in the deeper parts of the river (the lighter shades) – and near the river banks there is a slight decrease.

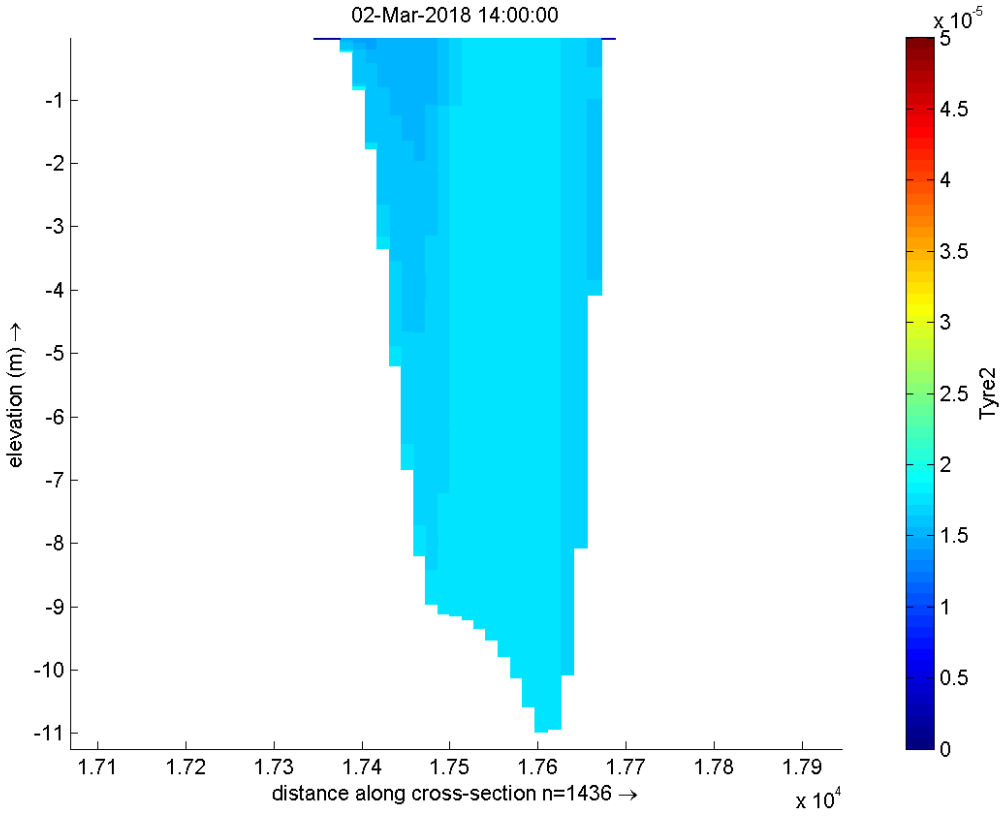

Figure 6.3 Distribution of plastic concentration within a cross-section near the Brienenoordbrug (mg/l).

6.2.2 Group 2: light plastic types

The light particles (type 4, 5 and 6, rising velocities respectively 1.4, 2.9 and 7.2 m/day) with a density of 970 kg/m^3 tend to rise to the surface. Unfortunately fraction 6 showed signs of instability, despite the fairly low rising velocity, so this fraction has been left out of the analysis. Fraction 5 is shown as a typical example; all other fractions show very similar results.

As can be seen in Figure 6.4 (surface layer) and Figure 6.5 (bottom layer), the particles are not spread out evenly over the river cross section. The concentration patterns differ slightly, but it is likely more due to the vertical distribution of the flow field than due to the upward motion of the plastic particles: the timeseries of the concentration at a location in the middle of the river, just downstream of the Brienenoordbrug shows that differences in the concentration over the vertical are minimal (Figure 6.6). The difference in the horizontal pattern is more likely due to the river water at the surface moving seaward and the river water at the bottom moving landward.

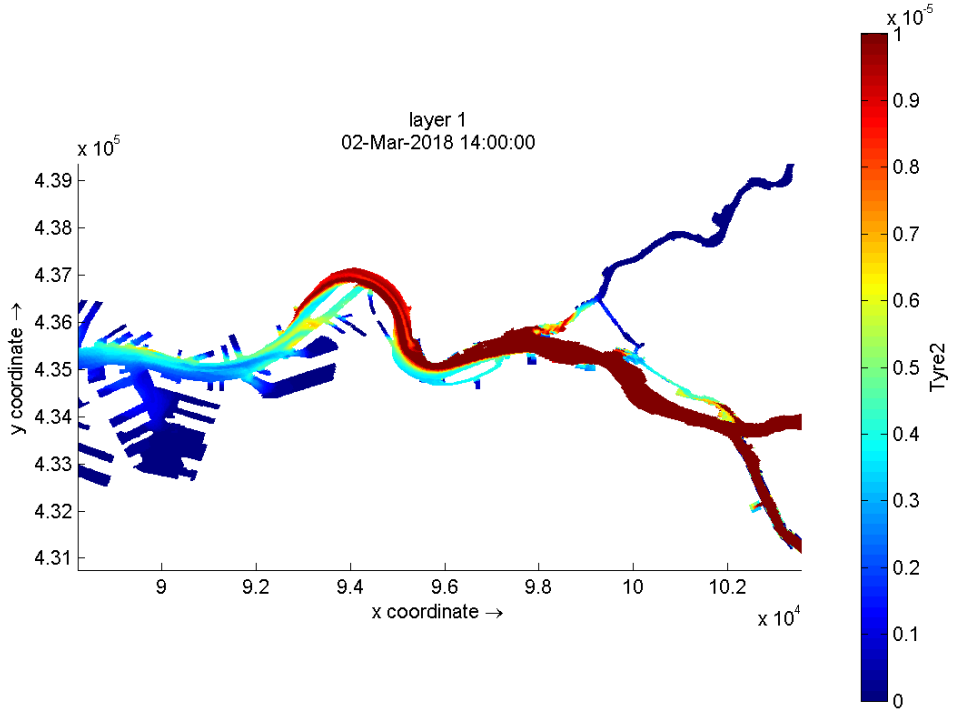

Figure 6.4 Concentration of fraction 5 in the surface layer.

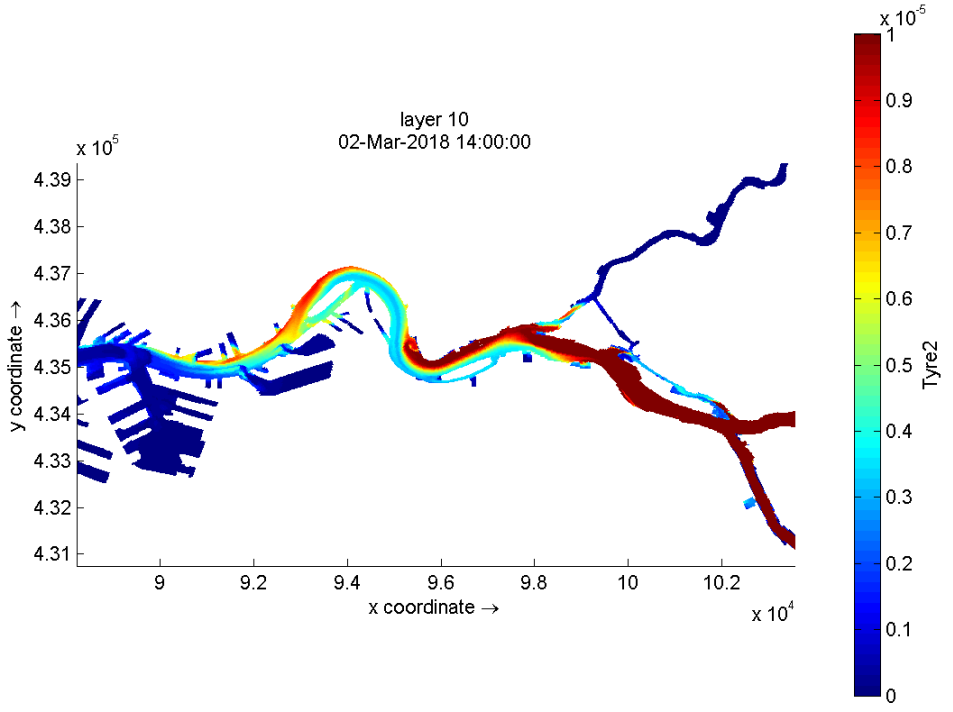

Figure 6.5 Concentration of fraction 5 in the bottom layer.

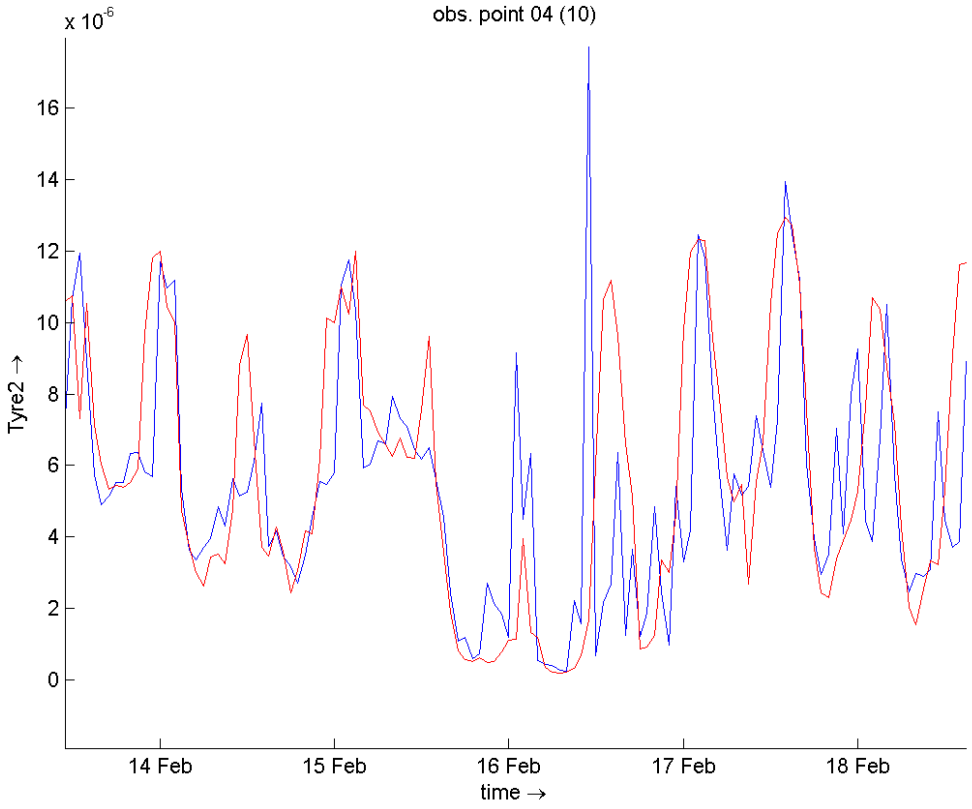

Figure 6.6 Timeseries of the concentration of fraction 5 at a location in the middle of the river. The blue line is for the surface layer, the red line for the bottom layer.

6.2.3 Aggregation and vertical concentration distribution

A noticeable characteristic of all plastic types in the calculation is that the “aggregated” fractions (that is, plastic particles with a sediment particle attached as modelled via the aggregation process) occur in much higher concentrations than the non-aggregated particles.

Table 6.1 summarises the characteristics of all fractions in terms of total mass in the system and concentration distributions at a monitoring point downstream of the Brienenoordbrug near one of the banks of the river at the end of the calculation period (March 3, 23:00, one hour before the end). At this moment the concentration at the surface is higher than at the bottom for all types, but this is not a general trend. In time it varies whether the top or bottom layer has the highest concentration (Figure 6.6).

Table 6.1 Overall characteristics of the non-aggregated microplastics at a moment at the end of calculation period. For those fractions for which the calculation became unstable a "—" is shown instead. An observation point fairly close to the right river bank (northern bank) was chosen, but all observation points showed similar concentrations.

No.	Total mass (kg)	Concentration at surface (g/l)	Concentration at bottom (g/l)	Mass ratio aggregated/ non-aggregated
1	1782	$3.034 \cdot 10^{-6}$	$1.798 \cdot 10^{-6}$	4.9
2	1777	$3.034 \cdot 10^{-6}$	$1.798 \cdot 10^{-6}$	4.9
3	--	--	--	--
4	1824	$3.427 \cdot 10^{-6}$	$1.778 \cdot 10^{-6}$	9.2
5	1818	$3.427 \cdot 10^{-6}$	$1.778 \cdot 10^{-6}$	9.2
6	--	--	--	--
7	1824	$3.234 \cdot 10^{-6}$	$1.970 \cdot 10^{-6}$	4.1
8	1815	$3.224 \cdot 10^{-6}$	$1.960 \cdot 10^{-6}$	4.1
9	1807	$3.197 \cdot 10^{-6}$	$1.935 \cdot 10^{-6}$	4.1
10	1819	$3.427 \cdot 10^{-6}$	$1.777 \cdot 10^{-6}$	9.2
11	--	--	--	--
12	--	--	--	--
13	1785	$3.047 \cdot 10^{-6}$	$1.804 \cdot 10^{-6}$	4.9
14	1779	$3.039 \cdot 10^{-6}$	$1.801 \cdot 10^{-6}$	4.9
15	1777	$3.036 \cdot 10^{-6}$	$1.800 \cdot 10^{-6}$	4.9
16	1786	$3.036 \cdot 10^{-6}$	$1.799 \cdot 10^{-6}$	4.9
17	1779	$3.035 \cdot 10^{-6}$	$1.798 \cdot 10^{-6}$	4.9
18	1777	$3.035 \cdot 10^{-6}$	$1.798 \cdot 10^{-6}$	4.9
19	1785	$3.043 \cdot 10^{-6}$	$1.802 \cdot 10^{-6}$	4.9
20	1778	$3.038 \cdot 10^{-6}$	$1.800 \cdot 10^{-6}$	4.9
21	1777	$3.036 \cdot 10^{-6}$	$1.799 \cdot 10^{-6}$	4.9
22	1786	$3.036 \cdot 10^{-6}$	$1.799 \cdot 10^{-6}$	4.9
23	1779	$3.035 \cdot 10^{-6}$	$1.798 \cdot 10^{-6}$	4.9
24	1777	$3.035 \cdot 10^{-6}$	$1.798 \cdot 10^{-6}$	4.9

Several observations can be made from table 6.1:

- The total mass in the system is surprisingly constant – the overall variation is several percent only. As the total mass is proportional to the mean concentration, we may conclude that the plastic concentration depends very little on the type of plastic in the Rhine/Meuse estuary.
- This is confirmed by the plastic concentration in the selected monitoring point, even though the variation between the plastic types is roughly 10%.
- As far as the aggregated versus non-aggregated plastics results are reliable, the "light" plastic fractions tend to be subjected to more aggregation than the "heavy" plastics. A possible explanation for this (in view of the model formulation) is that rising particles encounter more sediment particles, as they move in opposite directions.

6.3 Discussion

In comparison to PART, the results from WAQ show concentration distributions that are remarkably uniform over the vertical. This was unexpected, given that the settling/rising velocities for the plastic particles are quite large – tens to hundreds of meters per day.
To check that the vertical transport is correctly implemented in WAQ (an additional check with respect to the verification cases), we did a calculation with the OSR model for type 1, which has the tendency to fall. We replaced by a stylised hydrodynamic model, one without any vertical flow (the channel model used in section 4.6, the discharge from the river bank). The vertical profile that resulted at a point downstream (Figure 6.7) shows that the plastics are concentrated in the lower layer. Apparently, the flow in the OSR results in much more mixing of the water column, which is probably due to substantial vertical flow velocities.

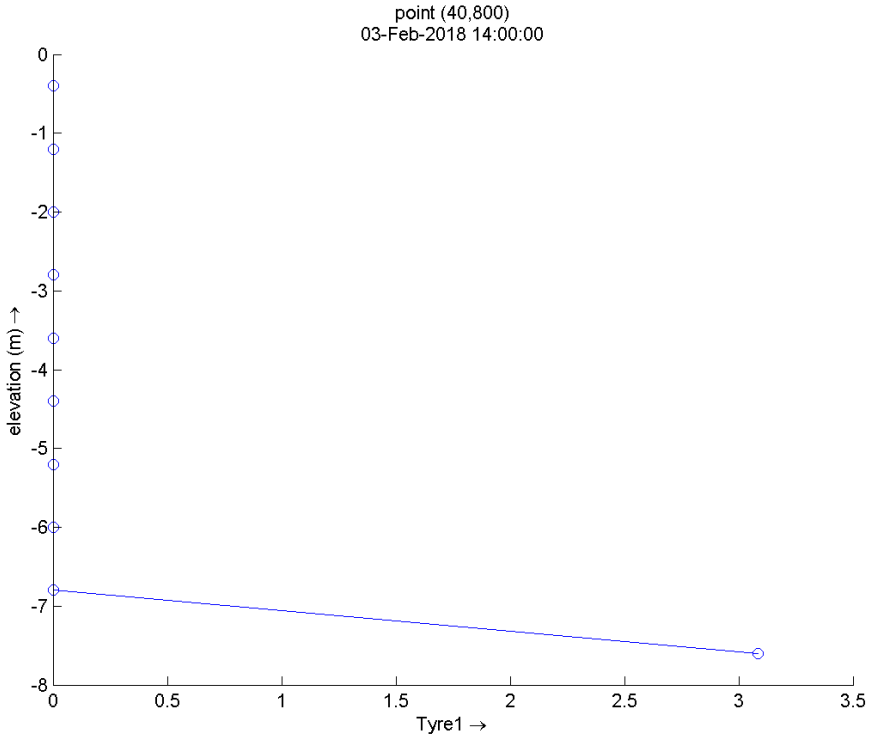

Figure 6.7 The vertical concentration profile at a point downstream. The ratio of the concentrations at the top and bottom is roughly 1:10000, all the plastic particles are concentrated in the bottom-most layer.

An explanation for the difference in vertical distribution with the flow calculated by the OSR model is that in D-PART (with the bouncing turned off) the particles that reach the bottom experience the *local* vertical and horizontal velocities from interpolation of the grid flow velocities, which are very small. The consequence is that they cannot easily be transported off the bottom again. The same holds for the surface (in case of light plastic particles). In WAQ, however, the flow velocities as calculated per grid cell are being used for the concentration in that entire cell. Therefore, the vertical mixing in D-PART is suppressed with respect to WAQ. For large particles the net effect in D-PART is likely to be close to reality – large pieces of plastic are heavy and are not easily moved by the weak flow. It does make D-PART less suitable, though, for microplastics or easily moved particles in general, if the bouncing has to be turned off for numerical reasons. For the particles with low fall velocities WAQ is more suitable to model their transport.

6.4 Conclusions from the realistic modelling using WAQ

For the realistic modelling using a realistic flow field and (limited) fall and rising velocities, the horizontal and vertical distribution of microplastic particles seems to be largely independent of the precise type of plastic.

Both plastics that are denser than water and plastics that are lighter than water show a fairly even distribution over the vertical and the horizontal distribution appears to be governed by the river flow only. Nonetheless, some conclusions may be drawn with respect to the distribution over the river:

- The highest concentrations in the water are found in the deeper parts of the river's cross-section. In the shallower parts the concentrations are somewhat lower, possibly due to deposition but more likely, as it also clearly occurs for the lighter plastic types, due to the limited mixing with the water in these shallow parts.
- Deposition occurs mainly in the harbour region, hardly any deposition occurs in the upstream parts of the river.

7 Synthesis

7.1 Plastics characterization

The positioning of a cost-effective system to remove plastics from a river largely depends on the plastics flux through the cross-sectional area covered by such a system. Since different plastic items/particles behave differently, the zones with the highest flux may vary, depending on the size and properties of the plastic. Because of its relatively large volume to surface ratio, a larger plastic item with a density higher than water will have a larger fall velocity than a smaller particle with the same density. The transport of microplastic particles (here defined as: 1 to 5 mm) and macroplastic items (5 mm and larger) is dealt with separately in this study. Furthermore, a distinction is made between plastic particles larger than 1 mm with a tendency to fall (density larger than the surrounding water) and particles with the tendency to rise (density smaller than the surrounding water). In addition to their size and density, the shape of particles determines their vertical behaviour within the water column. Plastic items found in rivers and their characteristics are listed in appendix A. From this list a selection was made based on the most typical microplastic particles (Table 2.4) and macroplastic items (Table 2.3) found in rivers. For the modelling of the plastic fluxes, we used the characteristics of these most typical items.

7.2 Relevant planform features, forcings and processes

Similar as for the plastic items, we listed the processes that determine the plastic flux, the relevant forcings and the relevant planform features, including planform geometry, constructions such as groynes and zones with different roughness. For a general river, we attempted to select the most important variables at the spatial scale of a river reach (Table 7.1). The selection was based on expert judgement. The most relevant forcings include the tides and the river discharge. The water level is the result of the different forcings. Per reach and even within a reach, the river planform features most relevant for the plastic flux may differ. In time, the effect of river planform features on the plastic flux may be different. An example of the dynamic character is related to the plastic concentration in floodplains. The concentration is likely to increase in a floodplain due to resuspension of stranded plastic particles from the bed, when the water level increases and the flow velocity in the floodplain becomes substantial. Another example of the dynamic interaction between the forcings and planform features is the effect of groynes on plastic accumulation, which is largely affected by the water level. The circulation pattern behind a groyne depends on the level of submergence. The temporal variation of the river discharge is important as well. Plastic fluxes are likely to be highest when the river discharge rises to a peak value (rising limb of the hydrograph) and not when the river discharge is at its peak.

Table 7.1 Selected river planform features, forcings and processes most relevant for the transport of plastics

River planform features	Forcings	Processes

• Bend (the more curved, the higher the spiral flow intensity)
• Floodplain presence and water level of inflow
• Constructions (e.g. weirs, groynes)
• Patches with different roughness (e.g. vegetated shore)
	• Tidal range
	  ○ One or two directional flow
	  ○ Absolute flow velocity
	• River discharge
	  ○ Flow velocity
	• Wind (for rising particles)
	• Suspended sediment concentration (for microplastic particles)
		• Advection
		• Falling and rising of plastic particles
		• Wind drag (for floating macroplastic items)
		• Mixing of water column by turbulence
		• Deposition
		• Resuspension
		• Entangling in vegetation
		• Hetero aggregation (for microplastic particles)

Assuming that Table 7.1 describes the most important factors for reaches in many rivers, an idea discussed during the course of the project (between Allseas and Deltares) is to simulate plastic flux for all the possible combinations to fill in existing knowledge gaps. This approach to obtain general knowledge from a set of simulations would need to include combinations of: several tidal ranges, several river discharges, several wind conditions and several suspended sediment concentrations for various planform features. This would lead to a large number of simulations, even without considering the selected processes and the different typical plastic characteristics. Still, due to the large sensitivity of the results to the planform features, the (general) results may not necessarily be representative for other river reaches. For example, for a reach with a combination of a bend, a floodplain and patches with vegetation the spatial distribution of these features is not likely to be simulated in the set of simulations. The effect of the interactions of only these planform features is still unknown. Such interactions may also occur with the forcings. Accordingly, we believe that it is hard to generate general knowledge and guidelines that can be applied to every river reach.

From the literature survey a general finding was obtained, though. Because tides can generate bidirectional flow and high flow velocity magnitudes, a plastic item may pass a location in an estuary or tidal river several times. A system to collect plastics is likely to be particularly effective at such a location. The chance that a particle is captured by the system is larger than in a river with only one-directional flow and lower flow velocities. Additionally, the flood tide transports plastics from the sea side to the system, where it can be collected. Moreover, aiming to collect plastics before they reach the ocean, the system should be positioned close to the ocean to limit the sources of plastics to the river seawards of the system. Based on these findings from literature, a draft guideline is formulated:

Optimal locations for plastic collection in rivers are within the reach where both ebb and flood flow occur.

7.3 Suitability of models

In this study, we used D-PART to model the transport of macroplastic items and WAQ for microplastics. Generally, model results were as expected. Important processes as advection of plastic items with the flow and wind drag can be modelled and the resulting vertical distribution of plastic items is reasonable. Qualitatively, trends in the model results show similarities as trends in the observations (Allseas, 2018), as will be addressed further in this synthesis. Generally, the models are suitable to model the transport of plastic items and their distribution in a river reach.

A quantitative comparison of the results of the pilot realistic modelling with the observations was not yet carried out for two reasons: firstly, the boundary conditions for plastic concentrations and composition are not available (e.g. it is unknown how these vary at the upstream boundary with river discharge) and secondly, the results of the surveys in the *Nieuwe Maas* have a number of limitations. Although 28 surveys have been carried out already in 2018, statistically the number of surveys at one location is limited. Furthermore, the density of the captured plastic items is unknown, such that is unknown what the characteristics of the plastic items in the model should be.

Another factor that makes a direct comparison with observations difficult is that the model does not include all processes that occur in reality. Although the main processes such as advection, falling and rising of particles and wind drag are included, some process descriptions may be limited or absent in the model. As an example, the process of trapping of plastics by vegetation is not included. The surveys, however, suggest that concentrations of plastic and organic matter (vegetation) are correlated (trend 2 from the surveys: both hard plastic and organic matter were higher at the surface and at 5 m depth than at 2.5 m depth).

From software verifications and pilots realistic modelling, macroplastic items are best modelled using D-PART and microplastic particles (1 to 5 mm) using WAQ, which is in line with the approach chosen in this study. However, microplastics with a large fall velocity (e.g. type 3 and 12 in this study) may better be modelled using D-PART, whereas macroplastic items with a density close to the density of water can generally best be modelled using WAQ. A reason for this suitability of the two modules is that WAQ makes use of the flow velocity calculated per cell, which can cause the particles to spread too much over the vertical. Especially near the surface (particles with high rising velocity) or near the bed (high fall velocity), the locally interpolated flow field used in D-PART results in a better distribution in the water column. The exact particle densities from where the best suitable module changes cannot be given based on this study. As an indication, a fall velocity of 1 mm/s can be considered low and 100 mm/s can be considered high.

Since D-PART has limitations modelling deposition and resuspension near the bed, but can include the effects of wind reasonably well, D-PART is well suitable for modelling rising and floating particles. For falling particles, the limitations of processes near the bed need to be accounted for.

Regarding the modelled processes, WAQ is more complete. Besides a reasonable representation of deposition, also hetero-aggregation gave reasonable results in the software verifications. Resuspension can also be included in the modelling, although this was not thoroughly tested in this study. Additionally, a new implementation for the fall velocity with characteristics of the particles using Waldschläger and Schüttrumpf (2019) makes WAQ better suited for modelling the transport of microplastic particles.

Using D-PART, the software verification with a floodplain and a groyne showed that plastic deposition can be captured reasonably well. In our modelling approach, the number of particles using D-PART increases with simulation time. In that, memory usage can become a limitation. To limit the computation time, bouncing of particles at the bed and the water surface needs to be switched off for higher falling velocities. For these reasons, D-PART is especially useful for medium scale models and not too long time scales. Because of the particle approach, we have experienced that D-PART is more suitable for low concentrations than WAQ. Acknowledging the given limitations, we conclude that WAQ is particularly suitable for plastic particles with a low falling velocity and that D-PART is particularly suitable for plastic particles with a high rising velocity.

7.4 Zones with relatively high plastic flux

The absence of resuspension limits the D-PART model result in the realistic model of the *Nieuwe Maas.* Still, the spatial distribution of macroplastic items with the tendency to fall is that they are concentrated near the bed, as expected. Since transport downwards in the cross section will occur easier than upwards, this vertical distribution implies that most of these falling items are transported in the main channel. A draft guideline is formulated, from which follows that the system should be designed to also collect items close to bed:

> The optimal location to collect falling macroplastic items (e,g. PET drink bottles, fragments of polystyrene) is somewhere in the deeper part of the cross section.

Similar to the falling items, the vertical distribution of the macroplastic items with a tendency to rise shows that the large majority of these items are within the surface layer for the moderate and high rising velocity (0.01 and 0.2 m/s). The most items found in the ocean have rising velocities within these two values (LeBreton et al., 2018). Without wind, the particles with a rising velocity tend to be equally distributed horizontally in the top layer. A draft guideline is formulated:

> The optimal location to collect rising macroplastic items (e.g. bottle caps and fragments of polypropylene) is where the flow velocity magnitude is highest.

At such a location with high flow velocities, the flux of these rising plastic particles is highest. This location is often in the middle of the river, although flow velocities can be 80-90 % of the peak highest values closer the banks, where collection is more feasible.

As expected with the low density of foam (around 300 kg/m^3), foam particles were found near the surface both in the model results and in the surveys (trend 3 from the surveys). Trend 1 in the surveys (soft plastic litter items were found both at the water surface and at depths 2.5 and 5 m below the surface) was not in agreement with the simulated vertical distribution of macroplastic items with one rising velocity. Possibly the observed group of soft plastics include both rising and falling items, causing these items to be more distributed over the water column than in the surveys in the *Nieuwe Maas*.

7.5 Role of forcings on the zones with relatively high plastics flux

Acknowledging the limitations of the pilot realistic modelling, the results give insight in the most relevant forcings and processes in the *Nieuwe Maas*. The draft guideline that tides have a large effect is supported by the model results. On the other hand, the secondary flow in the bend of the *Nieuwe Maas* was found to be small. Minor effects on the distribution of macroplastic items were observed. However, this effect was smaller than expected, which may be related to our focus on one cross section. Perhaps the spiral flow was not yet fully developed at this cross section. Deposition of microplastic particles mainly occurs in the harbours, where flow velocities are low.

The model shows that the wind has a large effect on the floating macroplastic items. The plastic particles larger than 1 mm that have the tendency to rise, but remain within the water column, were clearly forced in downwind direction with the flow generated by the wind near the water surface. This agrees with the observed trend 4 (Wind enhances the concentration of floating plastic litter at the downwind side of the river). We also observed that falling particles near the bed were transported in the upwind direction. This may be explained by the downwind generated flow near the surface, which forces a return flow near the bed. Considering the dependency on the wind for the rising and floating macroplastic items, the best location to locate a system to collect plastics is different from day to day depending on the wind direction. Ideally, the system should be positioned depending on the wind forecast. When repositioning of the system on a daily or weekly basis is not feasible, the system is best positioned in a way that is downwind of the favourable wind direction (in the Netherlands a location close to the east bank in a north-south oriented channel would generally be a good location). A draft guideline is formulated:

> The flux of macroplastic items with the tendency to rise (or float) is likely to be much higher near the downwind river bank.

The software verification cases with a floodplain and a groyne showed that behind the groyne an area with accumulation of plastic particles is present. This was observed for both WAQ and D-PART. Although this does not necessarily mean that the plastics flux is relatively high, the accumulation resulted as expected qualitatively. Despite the limitations of the software modules, the verifications show that in a zone with low flow velocities particles may sink and deposit to the bed. Furthermore, trapping of rising items was simulated in a circulation behind the groyne. These results are in agreement with usual flow patterns at groyne fields. The exact location of the accumulation and circulation cells may need further justification though.

8 Conclusions and recommendations

8.1 Conclusions

Typical plastic particles were listed based on publications. From this list, we made a selection of the most typical macroplastic items (Table 2.3) and the most typical microplastic particles (Table 2.4). The rising (or falling) velocity of plastics was determined from the observed behaviour for the macroplastic items. For microplastics particles it was determined from a recently published paper (equation 2.4; Waldschläger and Schüttrumpf, 2019). These characteristics per type were used for modelling the plastic transport in the *Nieuwe Maas*. Typical processes controlling plastic transport for river reaches, as well as typical forcings and planform features relevant for this transport are listed in Table 7.1. Due to the large variety of the planform features in river reaches, the forcing differences, and their interactions, the processes dominant for plastic transport may differ per river reach.

From software verifications and pilots realistic modelling, we conclude that generally the models are suitable to model the transport of plastic items and their distribution in a river reach. Important processes such as advection, wind drag and settling of a plastic item are included in the models and results were generally as expected. Trends in model results are qualitatively similar as trends in the observations.

Regarding the two software modules that were used, we conclude that plastic items with a large fall velocity or rising velocity can better be modelled using the particle tracking module D-PART, whereas plastic items with a density close to the density of water can generally best be modelled using the module WAQ, in which more processes can be included.

We were able to define rough guidelines for optimal locations for collection of plastics from rivers. These guidelines can be summarised as follows:

4. Optimal locations for plastic collection in rivers are within the tidal zone in a river, where both ebb and flood flow occur.
5. The optimal location to collect falling macroplastic items (e.g., PET drink bottles) is somewhere in the deeper part of the cross section. As such, the system can best be designed to also collect items close to the bed.
6. During calm wind conditions, the optimal location to collect rising plastic particles (e.g. bottle caps) is where the flow velocity is highest.
7. During moderate and high wind conditions, wind plays a significant role. Accordingly, the flux of macroplastic items with the tendency to rise (or float) may be much higher near the downwind river bank.

8.2 Recommendations

Based on the analysis made during this first phase of the project, we are able to make a number of recommendations. These are clustered as follows:

Recommendations for the surveys in the *Nieuwe Maas*, which are being carried out in 2019:

1) It is good to monitor at the same three depths as previously monitored (in 2018) and at the same locations. More survey results at these locations covering more conditions will be more valuable than carrying out tests at more locations.
2) Due to the variation in the velocity profile, it is good to measure flow velocity at the three levels of the nets for determining the flow volume through the nets during a test.

3) Conditions for which observations are particularly relevant are with strong wind and with salt intrusion up to the cross section, including salt concentration observations. Salt intrusion may affect the distribution of plastic items by changing the flow and by making plastic items more buoyant.

Recommendations directly following from the modelling carried out in phase 1 are:

4) The modelled vertical distribution of particles using D-PART is different from WAQ. It is not obvious which distribution corresponds better with the observations. Additional analysis to identify the reasons of the difference and to validate both is needed.
5) We believe that it is relevant to include a schematic representation of the plastic collections system in the model. This can be made using a trapping efficiency, which may depend on the flow direction. In this way, we can identify the effectiveness of the system as a function of its location.

8.3 Outlook to phase 2

Allseas decided to contribute to reduce the amount of plastics in the ocean worldwide by collecting plastic litter from rivers. Allseas developed a system to collect plastic items from the river, aiming to remove plastic items in an efficient manner. In this report on phase 1 the overall objective was to determine guidelines where to position the system cost-effectively. In paragraph 0 we discussed the variety in conditions that can be found in river reaches. Therefore, we stated that the approach to obtain general knowledge from a set of simulations is unfeasible. We redefined the overall objective for phase 2 with Allseas, which can be formulated as to:

> *"Identify the locations along and across a river, in which Allseas plans to position the system, with high probability of finding a relatively high flux of plastic items"*

For each river where Allseas plans to position the system, Allseas will carry out a pilot sampling campaign to monitor what the concentration and composition of the plastic items in that river is. For each river case, the effective locations to collect plastic items need to be indicated. Based on the overall objective, the direct objectives of phase 2 can be set as follows:

1. Gain confidence in the performance of, and identify uncertainty in, the results of the detailed model of the *Nieuwe Maas*. Although we conclude that generally the detailed models are suitable to model the transport of plastic items and their distribution in a river reach, trends in the field observations in the *Nieuwe Maas* and trends in the model results were compared only qualitatively. Gaining more confidence in the model results, will also give more confidence in the formulated rough guidelines.
2. Prepare for supporting Allseas in future projects. Allseas aims to offer efficient and complete solutions for plastic collection from rivers. This direct objective is particularly related to rivers where knowledge about plastic transport is still limited and where Allseas plans to position the system to collect plastic items.

For each of the two formulated direct objectives several options are worked out. The options to meet direct objective 1 are formulated as to:

1. Carry out a sensitivity study and dedicated quantitative comparison of model results with field observations in order to verify trends in the model results with field observations. Although missing information on the plastic transport and composition and the simulation time hampers a direct comparison, trends in the observations and detailed model results can be compared indirectly. Using the detailed models and insights obtained in phase 1 (e.g. model particles with neutral buoyancy with WAQ and

particles with both high and low density with respect to water with D-PART), additional field observations that are carried out in 2019 and additional information on the characteristics of the sampled plastic particles, we can be most conclusive on the uncertainty of the model results. Additionally, from studying the sensitivity of model results to the most important parameters, the uncertainty can further be established. By studying the sensitivity of results to plastic characteristics (e.g. the density range of PE: 0.91 and 0.99 g/cm^3) the range of model results can be given. Since in the surveys the role of entangling of plastics vegetation seems to play a large role and this process is not included in the modelling, we propose to select the days when the amount of vegetation caught in the nets was limited.

2. The realistic modelling pilots are detailed modelling studies. This was possible, since a detailed model (*OSR-NSC*, thanks to Port of Rotterdam) was available. For a new river, usually such a detailed model is not available. Building an equally detailed three-dimensional model for a new river where the system is planned is probably not cost-effective. Therefore, we propose this option to compare field observations with model results of a coarser hydrodynamic model, as for the detailed model. We propose to use the relatively coarse Havenmodel (the coarse model of the OSR model). This depth averaged model of the Rhine-Meuse delta is available. A model that is similarly coarse is usually available for a river in a developed country. When the performance for the Rhine-Meuse delta is good, it is likely that the performance for similarly coarse models is good as well.

The options to meet direct objective 2 are formulated as to:

1. Use the rough guidelines (summarized in paragraph 8.1) in combination with expert opinion on hydrodynamics, river bed characteristics and plastic transport in rivers for each river case. We believe that further refinement of these guidelines would require significantly large effort for a limited added value. Accordingly, we recommend to use these rough guidelines as is with no further improvements. By combining them with our expert judgement for each river case, the location to collect plastic items can be grounded in a cost-effective way.
2. Dedicated detailed modelling on a project base. In this option a dedicated model will be setup, calibrated and validated for use for each river where the system is planned to be positioned. The dedicated model is as detailed as possible, given the data available for the hydrodynamics and plastic input. Deltares would do no further work in phase 2. Instead, a considerable investment is made in every project (framework agreement).
3. Rapid modelling case by case (Deltares does the modelling). In this option, we would carry out rapid modelling for the area of interest, with minimum effort for model setup and validation. No calibration would be involved. Besides modelling the transport of plastic items in the river reach from the model boundary, we can also include modelling the plastic emissions discharged into the river. Emissions of plastics are estimated based on largescale modelling studies (Jambeck et al. 2015), population density and the presence of roads. This option requires the preparation of rapid modelling guidelines and testing the rapid modelling approach in a known case to verify it.
4. Rapid assessment tool. Deltares builds a simplified modelling tool, which can be used by Allseas for each river case.

9 Bibliography

- Addamo, A, Laroche, P, Hanke, G. ***Top Marine Beach Litter Items in Europe***. Publications Office of the European Union, Luxembourg, 2017, ISBN 978-92-79-87711-7, doi: 10.2760/496717
- Allseas (2018) Plastic sampling in the Nieuwe Maas: Test Report Campaign no1 - River bend Van Brienenoord brug, number GE-185-03-R-15, version 11 December 2018.
- Barboza, L. G. A., Vethaak, A. D., Lavorante, B. R., Lundebye, A. K., & Guilhermino, L. (2018). Marine microplastic debris: An emerging issue for food security, food safety and human health. Marine pollution bulletin, 133, 336-348.
- Besseling, E., Redondo-Hasselerharm, P.E., Foekema, E.M. and Koelmans, A.A., 2018, Quantifying Ecological Risks of Aquatic Micro- and Nanoplastics, *Critical Reviews in Environmental Science and Technology*.
- Bruge A, Barreau C, Carlot J, Collin H, Moreno C, Maison P, 2017. ***Monitoring Litter Inputs from the Adour River (Southwest France) to the Marine Environment*****.** Journal of Marine Science and Engineering.
- Buschman, F.A., 2011, Flow and sediment transport in an Indonesian tidal network, Utrecht University, PhD thesis, ISBN 978-90-6266-288-3.
- Buschman, F.A., M. van der Meulen, A. Markus, M. Weeber and F. Kleissen, 2018, Roadmap voor de modellering van verspreiding microplastics in Rijkswateren, i.o.v. Rijkswaterstaat, Deltares kenmerk 11202218-003-ZKS-0002.
- Critchwell, K. and J. Lambrechts, 2016, Modelling accumulation of marine plastics in the coastal zone; what are the dominant physical processes, *Estuarine, Coastal and Shelf Science*.
- Crosti R, Arcangeli A, Campana I, Paraboschi M, Gonzalez-Fernandez D. 2018. ***'Down to the river': amount, composition, and economic sector of litter entering the marine compartment, through the Tiber river in the Western Mediterranean Sea***. Scienze Fisiche e Naturali.
- Deltares, 2018a, D-WAQ PART, Simulation of mid-field quality and oil spills, using particle tracking, User Manual, version 2.15
- Deltares, 2018b, D-Water Quality, Versatile water quality modelling in 1D, 2D or 3D systems including physical, (bio)chemical and biological processes, Version 5.06
- Deltares, 2018c, D-Water Quality, Validation document, draft.
- Deltares, 2018d, D-Water Quality Processes Library Description, technical reference manual.
- Derraik, J.G. The pollution of the marine environment by plastic debris: a review. Mar. Pollut. Bull. 2002, 44, 842–852.
- GESAMP, 2016. Sources, fate and effects of microplastics in the marine environment: part two of a global assessment. In: Kershaw, P.J., Rochmann, C.M. (Eds.), Rep. Stud. GESAMP No. 93, 220 p.
- González-Fernández, D, Hanke, G, and the RiLON network. ***Floating Macro Litter in European Rivers - Top Items***, Publications Office of the European Union, Luxembourg, 2018 doi: 10.2760/316058
- Jambeck, J.R., R. Geyer, C. Wilcox, T.R. Siegler, M. Perryman, A. Andrady, R. Narayan and K.L. Law, 2015, Plastic waste inputs from land into the ocean, Science, doi 10.1126/science.1260352.
- Kawecki, D., Scheeder, P.R.W. and Nowack, B., 2015, Probabilistic Material Flow Analysis of Seven Commodity Plastics in Europe, *Environmental Science and Technology*.

- Klein S, Worch E, Knepper T., 2015. ***Occurrence and Spatial Distribution of Microplastics in River Shore Sediments of the Rhine-Main Area in Germany***. Environmental Science and Technology. doi: 10.1021/acs.est.5b00492
- Kooi, M., E. Besseling, C. Kroeze, A.P. van Wezel and A.A. Koelmans, 2018, Modeling the Fate and Transport of Plastic Debris in Freshwaters: Review and Guidance, in book: M. Wagner and L. Scott (editors), Freshwater Microplastics: Emerging Environmental Contaminants?, pp. 125-152
- Lamb, H. (1994). Hydrodynamics (6th edition.). Cambridge University Press. ISBN 978-0-521-45868-9.
- Lebreton, Laurent C.M., Zwet, Joost van der, Damsteeg, Jan-Willem, Slat, Boyan, Andrady, Andreas and Reisser, Julia, 2017. River plastic emissions to the world's oceans. *Nature communications*. DOI: 10.1038/ncomms15611.
- Lebreton, L., B. Slat, F. Ferrari, B. Sainte-Rose, J. Aitken, R. Marthouse, S. Hajbane, S. Cunsolo, A. Schwarz, A. Levivier, K. Noble, P. Debeljak, H. Maral, R. Schoeneich-Argent, R. Brambini & J. Reisser (2018), Evidence that the Great Pacific Garbage Patch is rapidly accumulating plastic, *Scientific Reports*, DOI: 10.1038/s41598-018-22939-w
- Leslie H, Brandsma s, van Velzen M, Vethaak A, 2017. ***Microplastics en route: Field measurements in the Dutch river delta and Amsterdam canals, wastewater treatment plants, North Sea sediments and biota***. Environmental International.
- Mani T, Hauk A, Walter U, Burkhardt-Holm P., 2015. ***Microplastics profile along the Rhine River***. Nature Scientific Reports.
- Maes, T, van der Meulen, M, Devriese, L, Leslie, H, Huvet, A, Frere, L, Robbens, J, Vethaak, A., 2017. ***Microplastics Baseline Surveys at the Water Surface and in Sediments of the North-East Atlantic*.** Frontiers in Marine Science. https://doi.org/10.3389/fmars.2017.00135
- Maximenko, N., Hafner, J. and Miller, P., 2011, Pathways of marine debris derived from trajectories of Lagrangian drifters, Marine Pollution Bulletin.
- Morrit D, Stefanoudis P, Pearce D, Crimmen O, Clark P, 2014. ***Plastic in the Thames: A river runs through it*.** Marine Pollution Bulletin.
- Nizzetto, L, Bussi, B. Futter, M.N. Butterfield, D. and Whitehead, P.G., 2016, A theoretical assessment of microplastic transport in river catchments and their retention by soils and river sediments, *Environmental Science Process Impacts*.
- Ryan, P.G., 2015. Does size and buoyancy affect the long distance transport of floating debris? Envir. Res. Lett. 10, doi:10.1088/1748-9326/10/8/084019
- Sadri S, Thompson R. 2015 ***On the quantity and composition of floating plastic debris entering and leaving the Tamar Estuary, Southwest England***. Marine Pollution Bulletin.
- SAPEA, 2019, A scientific perspective on microplastics in nature and society, Evidence Review Report no. 4.
- Schone Rivieren, 2018. Report from monitoring of 2017 and preliminary results from 2018.
- Schumm, S.A. (1981) Evolution and Response of the Fluvial System, Sedimentologic Implications, in book: Recent and Ancient Nonmarine Depositional Environments: Models for Exploration, https://doi.org/10.2110/pec.81.31.0019.
- Schmidt, Christian, Krauth, Thomas and Wagner, Stephan, 2017, Export of Plastic Debris by Rivers into the Sea, *Environmental Science and Technology.*
- Seybold, H., J. S. Andrade, and H. J. Herrmann (2007), Modeling river delta formation, Proc. Natl. Acad. Sci. U. S. A., 104, 16804–16809, doi:10.1073/pnas.0705265104
- Siegfried, Max, Koelmans, Albert A., Besseling, Ellen and Kroeze, Carolien, 2017, Export of microplastics from land to sea. A modelling approach, *Water Research*

- Unice, K.M., Weeber, M.P., Abramson, M.M., Reid, R.C.D., van Gils, J.A.G., Markus, A.A., Vethaak, A.D., Panko, J.M., 2019a. Characterizing export of land-based microplastics to the estuary – Part I: Application of integrated geospatial microplastic transport models to assess tire and road wear particles in the Seine watershed. Science of the Total Environment. doi.org/10.1016/j.scitotenv.2018.07.368
- Urgert, 2015. ***Microplastics in the rivers Meuse and Rhine-Developing guidance for a possible future monitoring program*** (MSc Thesis)
- Van der Wal M, van der Meulen M, Tweehuijsen G, Peterlin M, Palatinus A, Virsek K, Coscia L, Krzan A., 2015. ***Identification and Assessment of Riverine Input of (Marine) Litter****.* Final Report for the European Commission DG Environment under Framework Contract No ENV.D.2/FRA/2012/0025.
- Vermeulen, B., 2014. Rivers running deep. PhD thesis Wageningen University; ISBN: 978-94-6257-206-5.
- Yossef, M. F. M. (2005). “Morphodynamics of rivers with groynes.” Ph.D.thesis, Delft Univ. of Technology, Delft, Netherlands
- Wohl, E., 2015, Chapter 9 - Rivers in the Critical Zone, *Developments in Earth Surface Processes* 19, https://doi.org/10.1016/B978-0-444-63369-9.00009-4

A List of plastic items

A.1 Macroplastic items

A.1.1 Foam

	min	max	class limits
Size (mm)	5	500	5-25-40-100-200-500
Density (10^3 Kg.m-3)	0.1	0.3	**0,1 ; 0,3**
Factor of occurrence	low	high	(low, medium, high)
Shape	*tbd*	*tbd*	spherical, sheet-like, cuboid, fiber/elongated

	Polymer	Size	Density	Item	Shape	Occurrence	TOP 10	Position (*)	(*) NL rivers
1	**PU**	5	0.1	**Pieces of foam**	cuboid	low	no		
2		25	0.1	Pieces of foam	cuboid	low	no		
3		40	0.1	Pieces of foam	cuboid	low	no		
4		100	0.1	Pieces of foam	cuboid	low	no		
5		200	0.1	Pieces of foam	cuboid	low	no		
6	**EPS**	5	0.3	**Fragments of EPS**	cuboid	high	yes	2 - 3	
7		25	0.3	Fragments of EPS	cuboid	high	yes		
8		40	0.3	Fragments of EPS	cuboid	medium	yes		
9		100	0.3	Fragments of EPS	cuboid	medium	yes		
10		200	0.3	Fragments of EPS	cuboid	low	yes		
11		500	0.3	Fragments of EPS	cuboid	low	yes		
12		40	0.3	**Drink cups EPS**	cylindrical, open end	medium	yes	0 - 10	
13		100	0.3	Drink cups EPS	cylindrical, open end	medium	yes		
14		100	0.3	**Food containers EPS**	cuboid	medium	yes	6 - 10	
15		400	0.3	Food containers EPS	cuboid	medium	yes		

A.1.2 Polypropylene

	min	max	class limits	
Size (mm)	5	500	5-20-25-40-70-100-200-500	(included 25mm as it is one of the limit classes used in beach monitoring for pieces of plastic)
Density (10^3 Kg.m-3)	0.91	0.91	**0.91**	
Factor of occurrence	low	high	(low, medium, high)	
Shape	*tbd*	*tbd*	spherical, sheet-like, cuboid, fiber/elongated	

	Polymer	Size	Density	Item	Shape	Occurrence	TOP 10	Position (*)
1	**PP**	40	0.91	**Drink cups PP**	cylindrical, open end	medium	yes	10 - 0
2		100	0.91	Drink cups PP	cylindrical, open end	medium	yes	
3		100	0.91	**Food containers PP**	cuboid	medium	yes	6 - 10
4		400	0.91	Food containers PP	cuboid	medium	yes	
5		20	0.91	**Bottle caps**	cylindrical, open end	high	yes	**4 - 0**
6		40	0.91	Bottle caps	cylindrical, open end	high	yes	
7		70	0.91	**Sticks (cotton-bud & lollipops)**	elongated	medium	yes	**2 - 3- 7 - 8**
8		80	0.91	Sticks (cotton-bud & lollipops)	elongated	medium	yes	
9		5	0.91	**String & cord PP**	elongated	medium	yes	**7**
10		25	0.91	String & cord PP	elongated	medium	yes	
11		40	0.91	String & cord PP	elongated	medium	yes	
12		100	0.91	String & cord PP	elongated	medium	yes	
13		200	0.91	String & cord PP	elongated	low	yes	
14		500	0.91	String & cord PP	elongated	low	yes	
15		5	0.91	**Fragments of PP**	cuboid	high	yes	**1**
16		25	0.91	Fragments of PP	cuboid	high	yes	

17		40	0.91	Fragments of PP	cuboid	medium	yes	**1**
18		100	0.91	Fragments of PP	cuboid	medium	yes	
19		200	0.91	Fragments of PP	cuboid	low	yes	
20		500	0.91	Fragments of PP	cuboid	low	yes	
21		5	0.91	**Fragments of PP**	sheet	high	yes	**1**
22		25	0.91	Fragments of PP	sheet	high	yes	
23		40	0.91	Fragments of PP	sheet	medium	yes	**1**
24		100	0.91	Fragments of PP	sheet	medium	yes	
25		200	0.91	Fragments of PP	sheet	low	yes	
26		500	0.91	Fragments of PP	sheet	low	yes	

A.1.3 Polyethylene

	min		**max**	**class limits**	
Size (mm)		5	500	5-25-40-60-100-200-500	(included 25mm as it is one of the limit classes used in beach monitoring for pieces of plastic)
Density (10^3 Kg.m-3)		0.93	1	**0,93 - 0,94 - 0,97 - 1**	
Factor of occurrence	low		high	(low, medium, high)	
Shape	*tbd*		*tbd*	spherical, sheet-like, cuboid, fiber/elongated	

	Polymer	**Size**	**Density**	**Item**	**Shape**	**Occurrence**	**TOP 10**	**Position (*)**
1	**LDPE**	200	0.93	**Plastic bags** (LDPE)	**sheet**	medium	yes	**9**
2		500	0.93	Plastic bags (LDPE)	sheet	medium	yes	
3	Mixed layers of PE, LDPE, HDPE	60	0.93	**Packets of crisps/sweets**	sheet	high	yes	**2 - 3**
4		400	0.93	Packets of crisps/sweets	sheet	high	yes	
5		60	0.97	Packets of crisps/sweets	sheet	high		
6		400	0.97	Packets of crisps/sweets	sheet	high		

7		60	1.00	Packets of crisps/sweets	sheet	high	yes	
8		400	1.00	Packets of crisps/sweets	sheet	high	yes	
9		5	0.93	**Fragments of LDPE**	**cuboid**	high	yes	**1**
10		25	0.93	Fragments of LDPE	cuboid	high	yes	
11		40	0.93	Fragments of LDPE	cuboid	medium	yes	**1**
12		100	0.93	Fragments of LDPE	cuboid	medium	yes	
13		200	0.93	Fragments of LDPE	cuboid	low	yes	
14		500	0.93	Fragments of LDPE	cuboid	low	yes	
15		5	0.93	**Fragments LDPE**	**sheet**	high	yes	**1**
16		25	0.93	Fragments LDPE	sheet	high	yes	
17		40	0.93	Fragments LDPE	sheet	medium	yes	
18		100	0.93	**sheets LDPE/ agriculture/industry**	sheet	medium	yes	6
19		200	0.93	sheets LDPE/ agriculture/industry	sheet	medium	yes	
20		500	0.93	sheets LDPE/ agriculture/industry	sheet	medium	yes	
21	**HDPE**	5	0.94	**Fragments of HDPE**	**cuboid**	high	yes	**1**
22		25	0.94	Fragments of HDPE	cuboid	high	yes	
23		40	0.94	Fragments of HDPE	cuboid	medium	yes	**1**
24		100	0.94	Fragments of HDPE	cuboid	medium	yes	
25		200	0.94	Fragments of HDPE	cuboid	low	yes	
26		500	0.94	Fragments of HDPE	cuboid	low	yes	
27		5	0.97	Fragments of HDPE	cuboid	high	yes	
28		25	0.97	Fragments of HDPE	cuboid	high	yes	
29		40	0.97	Fragments of HDPE	cuboid	medium	yes	
30		100	0.97	Fragments of HDPE	cuboid	medium	yes	
31		200	0.97	Fragments of HDPE	cuboid	low	yes	
32		500	0.97	Fragments of HDPE	cuboid	low	yes	
33		5	1.0	Fragments of HDPE	cuboid	high	yes	
34		25	1.0	Fragments of HDPE	cuboid	high	yes	
35		40	1.0	Fragments of HDPE	cuboid	medium	yes	

36	100	1.0	Fragments of HDPE	cuboid	medium	yes	
37	200	1.0	Fragments of HDPE	cuboid	low	yes	
38	500	1.0	Fragments of HDPE	cuboid	low	yes	
39	5	0.94	**Fragments HDPE**	**sheet**	high	yes	**1**
40	25	0.94	Fragments HDPE	sheet	high	yes	
41	40	0.94	Fragments HDPE	sheet	medium	yes	
42	100	0.94	**sheets HDPE/ agriculture/industry**	sheet	medium	yes	6
43	200	0.94	sheets HDPE/ agriculture/industry	sheet	medium	yes	
44	500	0.94	sheets HDPE/ agriculture/industry	sheet	medium	yes	
45	5	0.97	**Fragments HDPE**	sheet	high	yes	
46	25	0.97	Fragments HDPE	sheet	high	yes	
47	40	0.97	Fragments HDPE	sheet	medium	yes	
48	100	0.97	**sheets HDPE/ agriculture/industry**	sheet	medium	yes	
49	200	0.97	sheets HDPE/ agriculture/industry	sheet	medium	yes	
50	500	0.97	sheets HDPE/ agriculture/industry	sheet	medium	yes	
51	5	1.0	Fragments HDPE	sheet	high	yes	
52	25	1.0	Fragments HDPE	sheet	high	yes	
53	40	1.0	Fragments HDPE	sheet	medium	yes	
54	100	1.0	**sheets HDPE/ agriculture/industry**	sheet	medium	yes	6
55	200	1.0	sheets HDPE/ agriculture/industry	sheet	medium	yes	
56	500	1.0	sheets HDPE/ agriculture/industry	sheet	medium	yes	

A.1.4 Polystyrene

	min	max	class limits
Size (mm)	5	500	5-25-40-100-200-500
Density (10^3 Kg.m-3)	1.09	1.09	**1.09**
Factor of occurrence	low	high	(low, medium, high)
Shape	*tbd*	*tbd*	spherical, sheet-like, cuboid, fiber/elongated

	Polymer	Size	Density	Item	Shape	Occurrence	TOP 10	Position (*)
1	**PS**	5	1.09	**Fragments of PS**	cuboid	high	yes	**1**
2		25	1.09	Fragments of PS	cuboid	high	yes	
3		40	1.09	Fragments of PS	cuboid	medium	yes	**1**
4		100	1.09	Fragments of PS	cuboid	medium	yes	
5		200	1.09	Fragments of PS	cuboid	low	yes	
6		500	1.09	Fragments of PS	cuboid	low	yes	
7		5	1.09	**Fragments of PS**	sheet	high	yes	**1**
8		25	1.09	Fragments of PS	sheet	high	yes	
9		40	1.09	Fragments of PS	sheet	medium	yes	**1**
10		100	1.09	Fragments of PS	sheet	medium	yes	
11		200	1.09	Fragments of PS	sheet	low	yes	
12		500	1.09	Fragments of PS	sheet	low	yes	
13		40	1.09	**Drink cups PS**	cylindrical, open end	medium	yes	**0 - 10**
14		100	1.09	Drink cups PS	cylindrical, open end	medium	yes	
15		100	1.09	**Food containers PS**	cuboid	medium	yes	**6 - 10**
16		400	1.09	Food containers PS	cuboid	medium	yes	

A.1.5 PET

	min	max	class limits
Size (mm)	5	500	5-25-40-100-200-500
Density (10^3 Kg.m-3)	1.35	**1.4**	**1,35 ; 1,4**
Factor of occurrence	low	high	(low, medium, high)
Shape	*tbd*	*tbd*	spherical, sheet-like, cuboid, fiber/elongated

	Polymer	Size	Density	Item	Shape	Occurrence	TOP 10	Position (*)
1	**PET/polyester**	5	1.4	**Fragments of PET**	**sheet**	high	yes	**1**
2		25	1.4	Fragments of PET	sheet	high	yes	
3		40	1.4	Fragments of PET	sheet	medium	yes	**1**
4		100	1.4	Fragments of PET	sheet	medium	yes	
5		200	1.4	Fragments of PET	sheet	low	yes	
6		500	1.4	Fragments of PET	sheet	low	yes	
7		5	1.35	**Polyester string**	**elongated**	medium	no	7
8		25	1.35	Polyester string	elongated	medium	yes	
9		40	1.35	Polyester string	elongated	medium	yes	
10		100	1.35	Polyester string	elongated	medium	yes	
11		200	1.35	Polyester string	elongated	medium	yes	
12		500	1.35	Polyester string	elongated	medium	yes	
13		5	1.4	**Fragments of PET**	**cuboid**	high	yes	**1**
14		25	1.4	Fragments of PET	cuboid	high	yes	
15		40	1.4	Fragments of PET	cuboid	medium	yes	**1**
16		100	1.4	Fragments of PET	cuboid	medium	yes	
17		200	1.4	Fragments of PET	cuboid	low	yes	
18		500	1.4	Fragments of PET	cuboid	low	yes	

19		40	1.4	**Drink cups PET**	cylindrical, one end open	medium	yes	**10**
20		100	1.4	Drink cups PET	cylindrical, one end open	medium	yes	
21		100	1.4	**Drink bottle** 0,33 cl	cylindrical, one end open	high	yes	**4**
22		500	1.4	Drink bottle 1,5 l	cylindrical, one end open	high	yes	
23		100	1.4	**Drink bottle** 0,33 cl	cylindrical, one end closed	high	yes	**4**
24		500	1.4	Drink bottle 1,5 l	cylindrical, one end closed	high	yes	

A.1.6 Other macrolitter

	min	**max**	**class limits**
Size (mm)	5	500	5-25-40-100-200-500
Density (10^3 Kg.m-3)	1.14	1.3	1,14…1,24…1,3
Factor of occurrence	low	high	(low, medium, high)
Shape	*tbd*	*tbd*	spherical, sheet-like, cuboid, fiber/elongated

	Polymer	**Size**	**Density**	**Item**	**Shape**	**Occurrence**	**TOP 10**
1	**Cellulose acetate**	10	1.24	**Cigarette butts**	cylindrical	high	yes
2		20	1.24	Cigarette butts	cylindrical	high	yes
3	**PVC**	5	1.3	**Sheet (eg tarpaulin)**	sheet	low	no
4		25	1.3	Sheet (eg tarpaulin)	sheet	low	no
5		40	1.3	Sheet (eg tarpaulin)	sheet	low	no
6		100	1.3	Sheet (eg tarpaulin)	sheet	low	no
7		200	1.3	Sheet (eg tarpaulin)	sheet	low	no
8		500	1.3	Sheet (eg tarpaulin)	sheet	low	no
9	**PA / Nylon**	5	1.14	**String, line**	elongated	medium	yes
10		25	1.14	String, line	elongated	medium	yes

11		40	1.14	String, line	elongated	medium	yes
12		100	1.14	String, line	elongated	medium	yes
13		200	1.14	String, line	elongated	medium	yes
14		500	1.14	String, line	elongated	medium	yes

A.2 Microplastics

	min		max		classes
Size (mm)		0.3		5	0,3 - 1 - 2 - 5
Density (10^3 Kg.m-3)		0.2		1.4	0,2-0,4…0,85-0,90-0,91-0,92-0,94-1...1,05-1,08…1,14…1,3...1,4
Factor of occurrence	low		high		(low, medium, high)
Shape	*tbd*		*tbd*		spherical, sheet-like, cuboid, fiber/elongated

		Size	Density	Shape	Item	Occurrence	
1	**Spherules/Pellets**	1	0.2	Spherical	**EPS foams**	low	*90-93% of foams*
2		2	0.2	Spherical	EPS foams	low	*90-93% of foams*
3		5	0.2	Spherical	EPS foams	low	*90-93% of foams*
4		1	0.4	Spherical	EPS foams	low	
5		2	0.4	Spherical	EPS foams	low	
6		5	0.4	Spherical	EPS foams	low	
7		1	0.91	**Spherical**	**PE Pellets (LDPE)**	high	*65-100% of pellets*
8		2	0.91	Spherical	PE Pellets (LDPE)	high	*65-100%*
9		5	0.91	Spherical	PE Pellets (LDPE)	high	*65-100%*
10		1	0.94	**Spherical**	**PE Pellets (HDPE)**	high	*65-100%*
11		2	0.94	Spherical	PE Pellets (HDPE)	high	*65-100%*

12		5	0.94	Spherical	PE Pellets (HDPE)	high	*65-100%*
13		1	1.0	Spherical	PE Pellets (HDPE)	high	*65-100%*
14		2	1.0	Spherical	PE Pellets (HDPE)	high	*65-100%*
15		5	1.0	Spherical	PE Pellets (HDPE)	high	*65-100%*
16		1	0.85	**Spherical**	**PP Pellets**	medium	*27-29% of pellets*
17		2	0.85	Spherical	PP Pellets	medium	*27-29%*
18		5	0.85	Spherical	PP Pellets	medium	*27-29%*
19		1	0.92	Spherical	PP Pellets	medium	*27-29%*
20		2	0.92	Spherical	PP Pellets	medium	*27-29%*
21		5	0.92	Spherical	PP Pellets	medium	*27-29%*
22		1	1.05	**Spherical**	**PS Pellets**	low	*0-25% of pelets*
23		2	1.05	Spherical	PS Pellets	low	*0-25%*
24		5	1.09	Spherical	PS Pellets	low	*0-25%*
25		1	1.09	Spherical	PS Pellets	low	*0-25%*
26		2	1.09	Spherical	PS Pellets	low	*0-25%*
27		5	1.09	Spherical	PS Pellets	low	*0-25%*
28	**Fragments**	1	0.91	**Sheet**	**Fragments PE (LDPE)**	high	*52-93% of fragments*
29		2	0.91	Sheet	Fragments PE (LDPE)	high	*52-93%*
30		5	0.91	Sheet	Fragments PE (LDPE)	medium	*52-93%*
31		1	0.94	**Sheet**	**Fragments PE (HDPE)**	high	*52-93%*
32		2	0.94	Sheet	Fragments PE (HDPE)	high	*52-93%*
33		5	0.94	Sheet	Fragments PE (HDPE)	medium	*52-93%*
34		1	0.97	Sheet	Fragments PE (HDPE)	high	*52-93%*
35		2	0.97	Sheet	Fragments PE (HDPE)	high	*52-93%*
36		5	0.97	Sheet	Fragments PE (HDPE)	medium	*52-93%*
37		1	1.00	Sheet	Fragments PE (HDPE)	high	*52-93%*
38		2	1.00	Sheet	Fragments PE (HDPE)	high	*52-93%*
39		5	1.00	Sheet	Fragments PE (HDPE)	medium	*52-93%*
40		1	0.91	**Cuboid**	**Fragments PE (LDPE)**	high	*52-93% of fragments*

41	2	0.91	Cuboid	Fragments PE (LDPE)	high	*52-93%*
42	5	0.91	Cuboid	Fragments PE (LDPE)	medium	*52-93%*
43	1	0.94	**Cuboid**	**Fragments PE (HDPE)**	high	*52-93%*
44	2	0.94	Cuboid	Fragments PE (HDPE)	high	*52-93%*
45	5	0.94	Cuboid	Fragments PE (HDPE)	medium	*52-93%*
46	1	0.97	Cuboid	Fragments PE (HDPE)	high	*52-93%*
47	2	0.97	Cuboid	Fragments PE (HDPE)	high	*52-93%*
48	5	0.97	Cuboid	Fragments PE (HDPE)	medium	*52-93%*
49	1	1.00	Cuboid	Fragments PE (HDPE)	high	*52-93%*
50	2	1.00	Cuboid	Fragments PE (HDPE)	high	*52-93%*
51	5	1.00	Cuboid	Fragments PE (HDPE)	medium	*52-93%*
52	1	1.05	**Sheet**	**Fragments PS**	low	*0-5% of fragments*
53	2	1.05	Sheet	Fragments PS	low	*0-5%*
54	5	1.05	Sheet	Fragments PS	low	*0-5%*
55	1	1.08	Sheet	Fragments PS	low	*0-5%*
56	2	1.08	Sheet	Fragments PS	low	*0-5%*
57	5	1.08	Sheet	Fragments PS	low	*0-5%*
58	1	1.05	Cuboid	Fragments PS	low	*0-5%*
59	2	1.05	Cuboid	Fragments PS	low	*0-5%*
60	5	1.05	Cuboid	Fragments PS	low	*0-5%*
61	1	1.08	Cuboid	Fragments PS	low	*0-5%*
62	2	1.08	Cuboid	Fragments PS	low	*0-5%*
63	5	1.08	Cuboid	Fragments PS	low	*0-5%*
64	1	0.85	**Cuboid**	**Fragments PP**	medium	*5-20% of fragments*
65	2	0.85	Cuboid	Fragments PP	medium	*5-20%*
66	5	0.85	Cuboid	Fragments PP	medium	*5-20%*
67	1	0.92	Cuboid	Fragments PP	medium	*5-20%*
68	2	0.92	Cuboid	Fragments PP	medium	*5-20%*
69	5	0.92	Cuboid	Fragments PP	medium	*5-20%*

70		1	1.30	**Sheet**	**Fragments PVC**	low	*2-5% of fragments (mainly 1-2mm)*
71		2	1.30	Sheet	Fragments PVC	low	*2-5% of fragments (mainly 1-2mm)*
72		5	1.30	Sheet	Fragments PVC	low	*2-5% of fragments*
73		1	1.40	**Sheet**	**Fragments PET**	low	*0-5%*
74		2	1.40	Sheet	Fragments PET	low	*0-5%*
75		5	1.40	Sheet	Fragments PET	low	*0-5%*
76	**Fibers**	1	1.14	**elongated**	**Fibers PA**	medium	*6-50% of fibers*
77		2	1.14	elongated	Fibers PA	medium	*6-50% of fibers*
78		5	1.14	elongated	Fibers PA	low	*6-50% of fibers*
79		1	0.85	**elongated**	**Fibers iPP-EPR**	medium	*26-53% of fibers*
80		2	0.85	elongated	Fibers iPP-EPR	medium	*26-53% of fibers*
81		5	0.85	elongated	Fibers iPP-EPR	low	*26-53% of fibers*
82		1	0.90	elongated	Fibers iPP-EPR	medium	*26-53% of fibers*
83		2	0.90	elongated	Fibers iPP-EPR	medium	*26-53% of fibers*
84		5	0.90	elongated	Fibers iPP-EPR	low	*26-53% of fibers*
85		1	1.40	**elongated**	**Fibers PET (Polyester)**	medium	*20% of fibers*
86		2	1.40	elongated	Fibers PET (Polyester)	medium	*20% fibers*
87		5	1.40	elongated	Fibers PET (Polyester)	low	*20% fibers*
88		1	0.91	**elongated**	**Fibers PP**	low	*0-9% of fibers*
89		2	0.91	elongated	Fibers PP	low	*0-9% fibers*
90		5	0.91	elongated	Fibers PP	low	*0-9% fibers*

B Some numerical aspects wrt the realistic modelling with WAQ

While running the calculations we encountered a number of numerical issues. Not all of these have actually been investigated to the full. Instead we have used workarounds.

The OSR-NSC model contains an intake/outlet combination: near the Maasvlakte the Eon power station takes in cooling water and releases it again somewhere else. From previous projects we know that such an intake may cause numerical problems. No problems occurred with the tracer calculation we did to get a feeling for the model, but they did occur with the plastics calculations. One hypothesis is that this is due to an interaction between the processes (falling most probably, as this concentrates the material in the lower layers) and flow towards the intake. Whatever the underlying cause, this problem disappeared by eliminating the discharge (from the water quality calculation only!).

As the Eon intake/outlet points are far from the area of interest and moreover located in a semi-enclosed region, this has no noticeable influence on the results.

A more serious problem was the mild instability that resulted from the very large falling/rising velocities. The numerical integration method is supposed to be robust against this type of transport phenomena (the vertical transport component is treated via an implicit scheme), but there is apparently still a limit to that. As can be seen from the table for some types of microplastics the falling/rising velocity is so large, that a particle travels the full depth (roughly 8 m) in 1/10th or even 1/20th of a day.

To avoid this instability, we limited the effect of the falling/rising velocity to three times the grid cell thickness per time step of 1 hour, that is, roughly, 72 m/day.[3] Even so, some calculations still show the instability.

The instability occurs in a coastal area near the Haringvliet and spreads out quickly (Figure B.1). In the upper panel the onset is seen as the small dark blue patch at 2 February, and a day later (the lower panel) the very high concentrations resulting from the instability have spread over a much larger area.

[3] *The actual limitation was that the falling/rising velocity should not exceed three times the layer thickness divided by the timestep. For a depth of 8 m, with 8 layers, this means a maximum velocity of 72 m/day.*

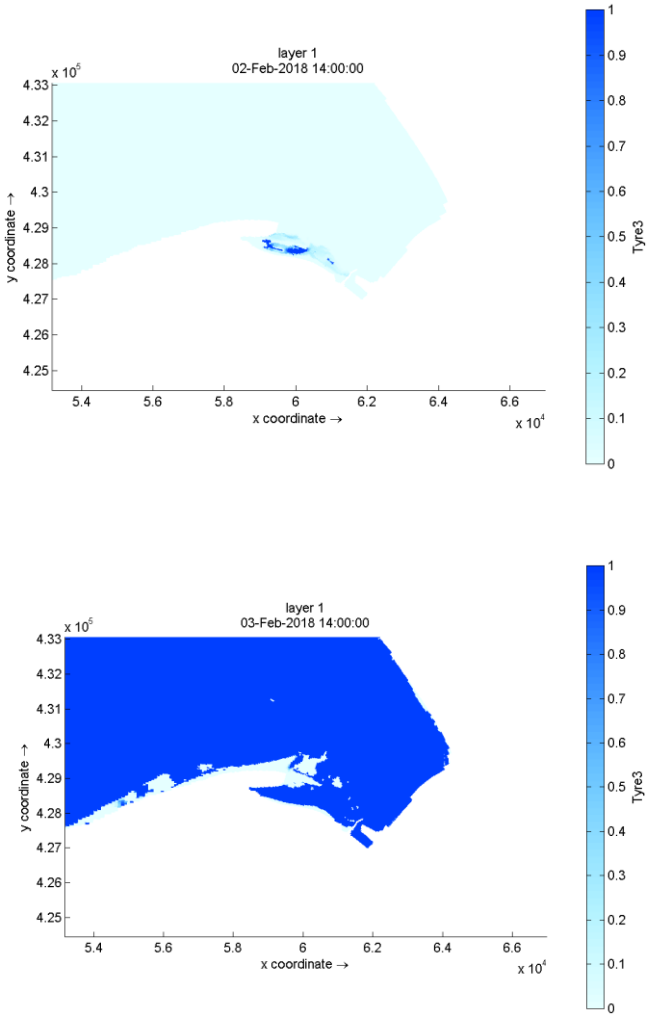

Figure B.1 Concentration of plastics of type 3 at 2 February (top panel) and 3 February (lower panel)

In the reporting we have left out the fractions for which this occurred. As these are all fractions for which the falling/rising velocity is very large, the expectation is that the corresponding material will be found mostly near the bottom or the surface and that it does not matter whether the falling/rising velocity is 200 or 300 m/day as a consequence.